School of Medicine
Department of Pediatrics

TRACHEOBRONCHIAL INNERVATION IS DEFICIENT IN INFANTS AND RATS WITH CONGENITAL DIAPHRAGMATIC HERNIA AND IT IS RESCUED BY RETINOIC ACID AND AMNIOTIC FLUID STEM CELLS

PhD Dissertation

Ms. Federica Pederiva

Thesis supervisor

Prof. Dr. Juan Antonio Tovar

Madrid, 2012

Facultad de Medicína
Departamento de Pediatría

LA INERVACIÓN TRAQUEOBRONQUIAL ES DEFICIENTE EN RECIÉN NACIDOS Y EN RATAS CON HERNIA DIAFRAGMÁTICA CONGÉNITA Y PUEDE SER RESCATADA CON ÁCIDO RETINOICO Y CON CÉLULAS MADRE AMNIÓTICAS

Memoria para optar al grado de doctor de la licenciada

Federica Pederiva

Director de tesis

Prof. Dr. Juan Antonio Tovar

Madrid, 2012

Summary

Congenital diaphragmatic hernia (CDH) still causes high mortality in newborns because of severe respiratory failure secondary to pulmonary hypoplasia. In addition, the ensuing chronic pulmonary disease continues to be the most significant source of morbidity in survivors. Pulmonary hypoplasia and lung injury caused by mechanical ventilation have been recognized as the major determinants of respiratory morbidity. However, pulmonary symptoms are also experienced by patients with mild to moderate lung hypoplasia, suggesting that other causes might be involved. Autonomic nerves control tracheobronchial smooth muscle whose contractility modulates lung growth and regulates airway patency. We therefore hypothesized that impaired trachebronchial innervation might interfere with lung development and contribute to induce long-term bronchopulmonary symptoms.

Using the nitrofen experimental rat model of CDH, we studied the tracheobronchial innervation and we were able to demonstrate that it was deficient in embryos and fetuses with CDH. We investigated the development of the tracheobronchial innervation, pointing out that it was delayed in embryos and fetuses with CDH and that the neural deficiency was partially compensated by an increase of the supporting glial tissue. In an attempt to translate these findings to the human condition as a partial explanation for chronic lung disease of survivors, we looked for the same lesions in infants with CDH and could confirm their presence.

We then undertook to demonstrate that prenatal interventions could improve the above-mentioned deficiencies and demonstrated in cultured hypoplastic rat lungs that both the deficient bronchial innervation and the poor tracheobronchial peristalsis could be rescued by the addition of retinoic acid.

Finally, we explored *in vitro,* in cultured lung explants, and *in vivo,* using intra-amniotic injection, the possible beneficial effects of amniotic fluid stem cells on hypoplastic lungs and demonstrated the viability of this approach.

La hernia diafragmática congénita sigue causando una elevada mortalidad en recién nacidos debido a la insuficiencia respiratoria grave secundaria a hipoplasia pulmonar. Las secuelas respiratorias crónicas siguen siendo la fuente más significativa de morbilidad entre los supervivientes. La hipoplasia pulmonar y el daño pulmonar causado por la ventilación mecánica son las principales causas de morbilidad respiratoria. Sin embargo también hay sintomatología respiratoria en pacientes con hipoplasia pulmonar moderada o leve, sugiriendo que podrían estar involucradas otras causas. La inervación autónoma regula el músculo liso traqueobronquial cuyo peristaltismo modula el crecimiento pulmonar y regula la permeabilidad del las vías aereas. Por estas razones pusimos a prueba la hipótesis de que alteraciones de la inervación traqueobronquial podrían interferir con el desarrollo pulmonar y contribuir a inducir secuelas respiratorias a largo plazo.

Utilizando el modelo experimental de hernia diafragmática congénita obtenido a través de la administratión de nitrofen a la rata, estudiamos la inervación traqueobronquial y demonstramos que estaba alterada en embriones y fetos con hernia diafragmática congénita. Investigamos el desarrollo de la inervación traqueobronquial y demonstramos que estaba retrasado en embriones y fetos con hernia diafragmática congénita y que el defecto de la inervación estaba parcialmente compensado por un aumento del tejido glial de soporte. En un intento de trasladar estos hallazgos a la clínica para explicar parcialmente la patología respiratoria crónica de los supervivientes, investigamos la presencia de las mismas alteraciones en recién nacidos con hernia diafragmática congénita y pudimos confirmarla.

A continuación, intentamos demonstrar que ciertas intervenciones prenatales pueden mejorar las deficiencias antes mencionadas y pudimos confirmar en cultivos de pulmones de rata que tanto las alteraciones de la inervación bronquial como la deficiencia de la peristalsis traqueobronquial pueden ser rescatadas por la adición de ácido retionoico.

Finalmente analizamos *in vitro*, en cultivos de explantes de pulmón, e *in vivo*, mediante la inyección intra-amniótica, los posibles efectos beneficiosos de células

madre de origen amniótico sobre la hipoplasia pulmonar y demostramos la viabilidad de este enfoque.

Index

Index of abbreviations

AChe: acetylcholinesterase

AECs-II: alveolar epithelial cells type II

AFS: amniotic fluid-derived stem (cells)

ASM: airway smooth muscle

BCA: bicinchoninic acid

CDH: congenital diaphragmatic hernia

cDNA: complementary DNA

CO_2: carbon dioxide

CT: cycle threshold

DEPC: diethylpyrocarbonate

D-MEM or DMEM: Dulbecco's Modified Eagle Medium

D-MEM/F12: Dulbecco's Modified Eagle Medium: Nutrient Mixture F-12

DNA: deoxyribonucleic acid

dNTPs: deoxynucleotide triphosphates

DTT: dithiothreitol

E0, E9.5, E13, E15, E18 and E21: gestational day 0, 9.5, 13, 15, 18 and 21

EDNRB: endothelin receptor type B

FBS: fetal bovine serum

FGF10: fibroblast growth factor 10

GER: gastroesophageal reflux

GFP: green fluorescent protein

GDNF: glial derived neurotrophic factor

h: hours

HBSS: Hank's buffer saline

ICC: cells of Cajal

IgG: immunoglobulin G

IU: international unit

kD or kDa: kilodalton

L: litre

MEM: minimum essential medium

mg: milligram

min: minutes

mL or ml: milliliter

mol: mole

mm^2: square millimeter

mmol: millimole

mRNA: messenger ribonucleic acid

n: number

NF: neurofilament

ng: nanogram

NGFR: nerve growth factor receptor

nm: nanometer

$p75^{NTR}$: low affinity neurotrophin receptor

PBS: phosphate buffered saline

PC: personal computer

PCR: polymerase chain reaction

PGP 9.5: protein gene product 9.5

PVDF: polyvinylidene fluoride

RA: retinoic acid

RALDH 2: retinaldehyde dehydrogenase type 2

RBL: rat basophilic leukemia

RBP: retinol binding protein

RET: REarranged during Transfection

RNA: ribonucleic acid

RT-PCR: real time polymerase chain reaction

S100B: S100 calcium binding protein B

SD: standard deviation

SDS: sodium dodecyl sulfate

SOD: superoxide dismutase

Sox10: SRY (sex determining region Y)-box 10

STRA6: stimulated by retinoic acid gene 6 homolog

Taq: *thermus aquaticus*

TGFβ1: transforming growth factor beta 1

TTF-1: thyroid transcription factor-1

VEFGα: vascular endothelial growth factor α

vs: versus

µg: microgram

µl: microliter

µm: micrometer

μm^2: square micrometer

µM: micromole

Introduction

1. CONGENITAL DIAPHRAGMATIC HERNIA

Congenital diaphragmatic hernia (CDH) is a malformation characterized by a posterolateral defect of the diaphragm, that allows herniation of abdominal viscera into the thoracic cavity. Left-sided hernia occurs in approximately 80% of cases, in which the entire gastrointestinal tract, the left lobe of the liver, the spleen and the kidneys can go up into the thorax. In right-sided hernias (20% of the cases), only the liver and a portion of the intestine tend to herniate. Bilateral hernias are uncommon and usually fatal. CDH occurs in 1 in every 2500 live births [1].

Mortality has traditionally been difficult to determine because of the "hidden mortality", which refers to infants with the congenital malformation who die *in utero* or shortly after birth, prior to transfer to a surgical center. The Northern Region Congenital Abnormalities Survey database recorded in the UK between 1991 and 2001 a mortality of 62%, that was unaffected by the introduction of new therapies [2]. A population-based study from Western Australia indicated that only 61% of infants with CDH are live born and nearly 33% of pregnancies were electively terminated, mostly (71%) because of the presence of another major anomaly [3].

Mortality after live birth is generally reported to range from 40-62%, and some authors argue that the true mortality of CDH has not changed with introduction of new therapies [4, 5]. The presence of associated anomalies has consistently been associated with decreased survival; other predictors of poor outcome are prenatal diagnosis, prematurity, low birth weight and early pneumothorax.

Over the past twenty years, pulmonary hypertension and pulmonary hypoplasia have been recognized as the two cornerstones of the pathophysiology of this malformation. CDH is characterized by a variable degree of pulmonary hypoplasia with bronchi of reduced size and branching associated with a decrease in cross-sectional area of the pulmonary vasculature and alterations of the surfactant system [6]. The number of normal bronchi is reduced in the ipsilateral lung and to a lesser degree in the contralateral one [7, 8]. The lungs have a reduced surface of alveolar-capillary membrane for gas exchange, which may be further decreased by surfactant dysfunction. In

addition to parenchymal disease, increased muscularization of the intraacinar pulmonary arteries appears to occur. Pulmonary capillary blood flow is decreased because of the small cross-sectional area of the pulmonary vascular bed, and flow may be further decreased by abnormal pulmonary vasoconstriction [9].

2. LONG TERM PULMONARY MORBIDITY

With improvements in neonatal intensive care and surgical management, an increased proportion of infants with severe forms of CDH survives. As a consequence, a higher rate of long-term sequelae and chronic morbidity have been described in these patients. Among others, pulmonary morbidity and gastroesophageal reflux (GER) are the most frequent contributors to overall morbidity in survivors of CDH, although the underlying mechanisms have not yet been fully understood. The structural abnormalities of distal airways associated with lung hypoplasia and barotrauma due to mechanical ventilation have been advocated as possible causes of the pulmonary sequelae. Due to their reduced pulmonary reserve, CDH survivors tend to suffer more severely from viral respiratory infections in their first year of life, also when the degree of pulmonary hypoplasia was described as mild to moderate [10]. After this period, most patients are able to lead normal o near-normal lives without significant respiratory morbidity, including participation in regular physical activity [11-13]. However, some children still require oxygen supplementation at two years of age [14]. Some of them experience recurrent bronchitis and fail to thrive [15]. Pulmonary function studies generally revealed mild to moderate airway obstruction with a tendency towards hyperinflation and a decreased inspiratory muscle strength. It has been hypothesized that the reduced lung tissue and the consequent alveolar distension may result in early airway closure as found in the aging emphysematous lung, which could be an additional risk factor in the development of chronic obstructive disease on the longer term [16, 17]. However, patients with normal lung function and restrictive pattern of changes have also been described [11, 12, 18]. Lung volumes were mostly found to be normal or near-normal and diffusion capacity was shown to be within normal limits [11,

[18, 19]. Although patients surviving CDH do not have many respiratory symptoms in their school year, the majority of them have some degree of obstructive and/or restrictive airway disease when carefully examined [20]. Lung morphology studies after CDH repair describe a striking increase in alveolar size, especially on the side of the former defect [21]. This indicates some degree of distension of the parenchyma to fill the hemithorax after repair and suggests that compensatory alveolar multiplication, if occurring at all, fails to normalize alveolar numbers [16]. There is a high prevalence of airway hyperresponsiveness in CDH survivors [11, 18]. In contrast to patients with bronchial asthma, CDH survivors tend to respond positively to pharmacological challenges like methacholine but not to metabisulfite, suggesting that their bronchial hyperresponsiveness might arise from an altered airway geometry [12]. As most neonates with CDH require complex pre- and postoperative intensive care, often including prolonged artificial ventilation, some of the observed residual defects might rather stem from this mechanical ventilation and oxygen toxicity than the malformation itself. A study compared the long-term outcome of CDH survivors with that of patients without CDH, who had undergone comparable intensive care and mechanical ventilation as newborns [18]. Mild airway obstruction was found in both groups with more peripheral airway obstruction in CDH patients than in controls. Thus, the authors suggested that both residual lung hypoplasia and neonatal intensive care are important determinants of persistent lung function abnormalities in CDH survivors.

3. EMBRYOLOGY OF THE TRACHEOBRONCHIAL TREE

The mammalian lung develops as a ventral outgrowth of the endodermal foregut, the respiratory diverticulum or lung bud, that begins to grow ventrocaudally through the surrounding splanchnic mesenchyme. The septation of the respiratory and digestive tracts occur differently in rat and human embryos. In rats, at 11.5 days of gestation two paired endodermal buds grow out of the primitive foregut and, as they elongate, the primitive foregut splits into two tubes, the dorsal esophagus and the ventral trachea [22]. In human, however, the trachea is first separated from the esophagus by

the laryngotracheal groove, which extends ventrally from the floor to the pharynx, then progresses anteriorly to divide the foregut dorsally into the esophagus and ventrally into the trachea. After elongation of the tracheal outgrowth, during the 3rd - 4th week of gestation, the caudal end of the laryngotracheal groove undergoes a first bifurcation, splitting into right and left primary bronchial buds, that are the rudiments of the two lungs [23, 24]. Between the 5th and the 28th week of gestation they continue to elongate and branch until the entire respiratory tree is formed. The mesenchyme that surrounds the developing trachea and bronchi gives origin to the bronchial musculature, the cartilaginous rings and the pulmonary connective tissue. The right lung of the rat is made up of four major lobes, the cranial, the medial, the accessory and the caudal, whereas the left lung consists of only one small lobe [22, 24]. In human, the right lung has three lobes, the upper, the middle and the lower, whereas the left lung is composed of two lobes, the upper and the lower.

Four histological stages can be distinguished during human lung development (table 1): pseudoglandular, canalicular, saccular and alveolar. The pseudoglandular stage takes place between the 6th and the 16th weeks of gestation. The bronchial tree is formed by the repeated dichotomous branching of the developing epithelium into the surrounding mesenchyme. The branching is complete at 16 generations by the 16th week of gestation in humans. After this stage, further growth occurs only by elongation and widening of existing airways. In the canalicular phase, between the 16th and the 28th week of gestation, each terminal bronchiole divides into two or more respiratory bronchioles and the respiratory vasculature begins to develop. From 28th week of gestation until term, during the saccular stage, the respiratory bronchioles subdivide to produce terminal sacs, the primitive alveoli, that continue to be produced until childhood. In the same period, the differentiation of type I and type II pneumocytes takes place. Finally, around the 36th week of gestation, in the alveolar phase, there is a huge multiplication of the alveoli establishing an extensive surface area. At birth, human neonates have entered the alveolar stage of development. Over 85% of alveoli are formed after birth by a process of air space septation. During early development, lung surface area increases because of the increase of the number of

alveoli; during later development stages, there is an expansion of the airspace of the lung. The increase in number and surface area of the alveoli begins to level off between the ages of 2 to 4 years. The timing in which alveolization is considered complete in humans ranges from 2 to 8 years. In contrast, rats are born during the saccular stage and reach the alveolar stage at 4 days of life. Most of the lung development is complete within the 2nd week after birth. Furthermore, the rat lung continues to proliferate at a slow rate throughout its life [25, 26].

TABLE 1.

The table illustrates the stages of lung development in human and rat lung in gestation days [25].

SPECIES	GLANDULAR	CANALICULAR	SACCULAR	ALVEOLAR
HUMAN	42-112	112-196	196-252	252-childhood
RAT	13-18	19-20	21-birth	Postnatal days 7-21

4. INNERVATION OF THE TRACHEOBRONCHIAL TREE

The respiratory tract is regulated by autonomic nerves, that control the smooth muscle tone, the submucosal gland secretion, the epithelial cell function, the bronchial vascular tone and the tracheobronchial reflexes. Shortly after separating from the foregut, the developing tubules are surrounded by smooth muscle and ensheathed in a network of newly forming nervous tissue. Two large nerve trunks lying in the adventitial surface of the airway wall run along the bronchial tree and give rise to a network of bundles with fine varicose fibers covering the airway smooth muscle from

the trachea to the growing tips of the airways and some nerves penetrate the smooth muscle layer. The maturation of the nerve trunks and the ganglia occurs centrifugally in the bronchial tree [27]. Because the neural crest cells that will populate the gut are already present in the foregut at the time when the lung buds emerge, it had been postulated that these cells migrated into the lung as it was forming. The tracheobronchial cells' positive staining with $p75^{NTR}$ antibody [27], a neural crest-derived cell marker, supported this theory, which was demonstrated unequivocally in 2005 by A. J. Burns and J. M. Delalande. Using the quail-chick grafting technique, they showed that vagal neural crest cells, that express the transcription factor Sox10 and receptor components of the RET and EDNRB signaling pathways, migrate from the foregut into the developing lung buds, where they accumulate to form interconnected ganglia containing neurons and glial cells [28]. The same results were later confirmed using the embryonic mouse lung [29]. The enteric neural crest cells are dependent on glial derived neurotrophic factor (GDNF) [30]. In the same way as for the gut, GDNF and other ligands of the same family are likely to be important in guidance, differentiation and survival of pulmonary neurons [31].

5. AIRWAY SMOOTH MUSCLE AND ITS RELATIONSHIP TO LUNG INNERVATION

Both neural tissue and airway smooth muscle (ASM) are an integral part of the branching epithelial tubules from the onset of the lung development. Smooth muscle forms a layer of cells which encircles the epithelial tubules to their growing tips, an arrangement whereby the ASM tone would have the potential to produce narrowing and relaxation [27]. Some authors first observed spontaneous narrowing of the airways in freshly excised human and pig lung [32-34] from the first trimester onward and in lung explants from fetal guinea pig, fetal mouse [35] and chick embryos. It became later clear that shortly after differentiation, the smooth muscle was able to respond strongly to agonists such as acetylcholine and histamine as well as to electrical field stimulation. The airway narrowing in response to neural stimulation was blocked by atropine and tetrodotoxin, indicating that functional cholinergic nerves were involved [33].

Spontaneous intermittent narrowing of the bronchi has been observed both *in vivo* and *in vitro* [36]. The spontaneous contractions moved the lung liquid backward and forward along the airway lumen. The fluid pressure and the stress forces acting on the walls of the bronchial tree have been suggested to provide the mechanical stimulus for lung growth. When lung liquid is drained and hence the pressure is decreased, the lung becomes hypoplastic [37]; in contrast, tracheal occlusion increases the pressure and enhances lung growth [38]. It has been observed that spontaneous contractions of the airways are unaffected by either atropine or tetrodotoxin [36]. The first finding indicates that neural activity is not essential, the latter shows that endogenous Ach is not involved. In addition, this rhythmic mechanical activity ceases in the presence of calcium antagonists. The authors concluded that spontaneous contractions are therefore of likely myogenic origin [36]. Hence, since it seems unlikely at this early stage that impulses from the central nervous system come down the vagus, it has been supposed that the role fulfilled by neural tissue in early gestation is not neurotransmission, but rather secretion of trophic factors for the smooth muscle that indirectly contributes to lung development [33, 36, 39, 40]. The nerves secrete trophic factors that influence growth and survival of the smooth muscle. In turn, the target tissue may provide a feedback by secreting neurotrophin, that helps nerves to survive and may influence the phenotypic expression of the neurotransmitters secreted during development [31, 33]. Positive immunostaining for neurotransmitters, like choline acetyltransferase [41], calcitonin gene-related peptide [42], nitric oxid synthase, vasoactive intestinal peptide and substance P, can be seen in the varicosities of the nerve fibers lying on smooth muscle cells later in gestation, by the end of pseudoglandular and during canalicular stages [40, 43]. The same authors [36, 40, 43] proposed the idea that the spontaneous contractions produce a rhythmic mechanical stimulus across the airway wall and the adjacent parenchyma that contributes to normal airway differentiation and branching by inducing expression of growth factors. Neurotrophic factors, like neurturin, a member of GDNF-family, and GDNF, have been isolated in airway smooth muscle cells or in the associated mesenchymal cells [31, 44, 45]. The picture that emerges is that airway smooth muscle and neural tissue are an Integral part of the lung from the

onset of its development. They exist in a dynamic relationship throughout gestation and persist as an integral part of the airways into postnatal life [40].

6. IN VITRO LUNG CULTURE

In the freshly isolated bronchial tree of fetal pigs and rabbits, spontaneous contractions were observed in proximal and distal airways. The onset of rhythmic contractions was rapid and they continued for more than one minute before weakening and disappearing to start again at a different part of the bronchial tree [32]. Likewise, in fetal lung explants in culture weak and infrequent spontaneous activities were observed after twenty four hours. By two days, strong waves of narrowing were observed along the main lobar bronchi and collaterals extending to the terminal sacs [36]. At the first moment of the contraction the liquid is pushed equally in both directions, but as the wave of contraction begins to move distally, most of the liquid follows this direction rather than moving proximally. The walls of the terminal buds comprise a single layer of undifferentiated epithelial cells, so they are likely to be more compliant than the airways and able to accommodate the minute volume of liquid moved. Upon relaxation of the airway wall after the spontaneous contraction, the liquid moves back and the terminal buds return to their normal volume. For most contractions, the time between each one was long enough to allow a complete flow back [36]. The frequency and the strength of the contractions were strongly temperature-dependant.[35]

Embryonic lung explants can undergo branching morphogenesis in culture. This *in vitro* lung culture model [31, 36, 46] has proved to be an useful tool to investigate lung development and has the advantage of allowing easy changes of lung environment by modifying the composition of the medium. Using this model, it has been demonstrated that bronchial peristalsis is deficient in hypoplastic nitrofen-exposed lung explants [47].

7. THE RETINOID HYPOTHESIS

The etiology of CDH is poorly understood. The "retinoid hypothesis" proposes that abnormalities in retinoid signaling or related pathways, contribute to abnormal development of the diaphragm. This hypothesis was formulated on the basis of animal data showing an association between the occurrence of diaphragmatic hernia and vitamin A deficiency, loss of retinoid receptor expression and exposure to teratogens that interfere with the synthesis of retinoic acid [48]. CDH has also been recently linked with a human mutation in the retinol binding protein receptor, STRA6 [49, 50]. Retinoids are the family of molecules derived from vitamin A, whose source are the carotinoids from fruits and vegetables and the retinyl esters from animal meat. After absorption through the gut, retinyl esters are transported in chylomicrons to the liver for storage, where they are metabolized into retinol. Retinol bound to retinol-binding protein is transferred from the liver via blood to target cells. Within cells, retinol bound to cellular retinol-binding proteins is converted to retinal by retinol dehydrogenase followed by a further dehydrogenation to retinoic acid (RA). RA exerts its biological effects through binding the nuclear retinoic acid receptors and the nuclear retinoid X receptor [51-53].

Different studies reveal the role of a retinoid signaling pathway disruption in the pathogenesis of CDH [54-59]. Most of them have focused on the diaphragm and the reduction of the incidence of CDH after administration of vitamin A and its derivatives. However, other authors have demonstrated that antenatal administration of vitamin A and RA attenuates lung hypoplasia by interfering with early determinants of lung underdevelopment, suggesting that retinoids could also be implicated in the pathogenesis of lung hypoplasia [60-65].

8. STEM CELLS

Amniotic fluid-derived stem (AFS) cells are multipotent cells that can be isolated from human and rodent amniotic fluid and are able to differentiate into multiple lineages

including representatives of all three embryonic germ layers [66]. The same cells can also engraft in irradiated bone marrow and give rise to all hematopoietic lineages [67]. Remarkable results have been obtained in injured kidneys, heart and lungs [68-70]. Finally, they can functionally contribute to the regeneration of various tissues and organs when transplanted in models of disease. The latter have been explored both in models of diseases and during development. A basal level of engraftment without differentiation was demonstrated after administration of AFS cells in uninjured lung. In contrast, in presence of lung damage, not only a significantly stronger engraftment was registered, but also the cells differentiate in specialised pneumocytes contributing and supplementing endogenous lung repair mechanisms [71]. It was initially hypothesized that stem cells undid irreversible cellular damage and rebuilt injured or diseased tissue by differentiating into the phenotype of injured tissue, repopulating the diseased organ with healthy cells and hence improving the function. However, recent research suggests that stem cells may influence recovery from injury via paracrine factors that promote tissue repair [72].

Hypotheses

1. The long term pulmonary morbidity observed in survivors of CDH might be partially explained by abnormalities of tracheobronchial innervation.

2. Abnormal tracheobronchial innervation could explain hypoperistalsis observed in cultured hypoplastic lungs.

3. Agents able to rescue lung hypoplasia in culture, like RA, could act by improving bronchial innervation and peristalsis.

4. Pluripotent AFS cells might rescue growth and motility of hypoplastic lungs *in vitro* and *in vivo*.

Aims

1. To demonstrate abnormal tracheobronchial innervation in rat embryos and fetuses with CDH.

2. To examine the development of this innervation during fetal life to characterize the nature of the anomalies.

3. To examine bronchopulmonary innervation in infants with CDH in a search for similar anomalies.

4. To demonstrate that deficient tracheobronchial innervation could partially account for pulmonary hypoplasia in CDH.

5. To examine whether rescue of lung hypoplasia by RA *in vitro,* is accompanied by rescue of bronchial innervation and peristalsis.

6. To study if AFS cells could rescue growth and motility of hypoplastic lungs *in vitro* and *in vivo*.

Papers

PUBLISHED PAPERS

I. Pederiva F, Lopez RA, Martinez L, Tovar JA. **Tracheal innervation is abnormal in rats with experimental congenital diaphragmatic hernia.** J Pediatr Surg 2009;44:1159-64.

II. Pederiva F, Aras Lopez R, Martinez L, Tovar JA. **Abnormal development of tracheal innervation in rats with experimental diaphragmatic hernia.** Pediatr Surg Int 2008;24:1341-6.

III. Pederiva F, Lopez RA, Rodriguez JI, Martinez L, Tovar JA. **Bronchopulmonary innervation defects in infants and rats with congenital diaphragmatic hernia.** J Pediatr Surg 2010;45:360-5.

IV. Pederiva F, Martinez L, Tovar JA. **Retinoic Acid Rescues Deficient Airway Innervation and Peristalsis of Hypoplastic Rat Lung Explants.** Neonatology 2012;101:132-9.

SUBMITTED PAPER

V. Pederiva F, Ghionzoli M, Pierro A, De Coppi P and Tovar JA. **Amniotic Fluid Stem Cells Rescue Both *In Vitro* And *In Vivo* Growth, Innervation And Motility In Nitrofen-Exposed Hypoplastic Rat Lungs Through Paracrine Effects.** Cell Transplant

TRACHEAL INNERVATION IS ABNORMAL IN RATS WITH EXPERIMENTAL CONGENITAL DIAPHRAGMATIC HERNIA.

Pederiva F, Lopez RA, Martinez L, Tovar JA.

J Pediatr Surg 2009;44:1159-64.

Journal of Pediatric Surgery (2009) **44**, 1159–1164

ELSEVIER

Journal of Pediatric Surgery

www.elsevier.com/locate/jpedsurg

Tracheal innervation is abnormal in rats with experimental congenital diaphragmatic hernia☆,☆☆

Federica Pederiva, Rosa Aras Lopez, Leopoldo Martinez, Juan A. Tovar*

Department of Pediatric Surgery and Research Laboratory, Hospital Universitario La Paz, 28046 Madrid, Spain

Received 10 February 2009; accepted 17 February 2009

Key words:
Diaphragmatic hernia;
Intrinsic innervation;
Trachea;
Nitrofen;
Neural crest;
Lung

Abstract

Background: Tracheobronchial motility influences lung development. Lung hypoplasia and lung sequelae accompany congenital diaphragmatic hernia (CDH) in which the vagus nerves and esophageal innervation are abnormal. As the vagus supplies tracheal innervation, this study tested the hypothesis that it might also be abnormal in rats with CDH.

Material and Methods: Intrinsic ganglia were counted and measured in whole mount acetylcholinesterase-stained tracheas from CDH and control E21 fetal rats. The relative surfaces occupied by neural structures were measured in tracheal sections immunostained for $p75^{NTR}$ and PGP 9.5. PGP 9.5 protein and mRNA expression were determined. Mann-Whitney tests were used for comparisons between groups using $P < .05$ as significant.

Results: $p75^{NTR}$ staining showed the neural crest origin of tracheal innervation. Scarce neural structures and smaller ganglia were found in CDH fetuses. PGP 9.5 protein expression was decreased in CDH fetuses, whereas PGP 9.5 mRNA levels were increased in comparison with controls.

Conclusions: Decreased density of neural structures and size of intramural ganglia, reduced expression of neural tissue and PGP 9.5 protein, and increased levels of PGP 9.5 mRNA reveal deficient tracheal innervation in rats with CDH. If similar anomalies exist in the human condition, they could contribute to explaining the pathogenesis of lung hypoplasia and bronchopulmonary sequelae.

Long-term pulmonary morbidity occurs often in survivors of congenital diaphragmatic hernia (CDH) as sequelae of pulmonary hypoplasia and barotrauma owing to mechanical ventilation. However, other causes might account for these symptoms, as frequent respiratory tract infections, asthma, or airway obstruction occurs also in cases with only mild to moderate pulmonary hypoplasia [1-3]. Mesenchymal-epithelial interactions are known to play a significant role in lung morphogenesis [4,5], but, apparently, tracheobronchial peristalsis operated by smooth muscle participates as well [6,7]. Tracheobronchial innervation, concentrated mainly in

☆ Supported in part by FIS (06/0486 and 06/0447), FIHULP, and FMM Grants.

☆☆ FP is a research fellow of CAM (FPI-000760 grant).

Presented at the National Conference of the Section on Surgery of the American Academy of Pediatrics, Boston, USA, October 10-12, 2008.

* Corresponding author. Department of Pediatric Surgery, Hospital Universitario "La Paz," 28046 Madrid, Spain. Tel.: +34 91 727 70 19; fax: +34 91 727 70 33.

E-mail address: jatovar.hulp@salud.madrid.org (J.A. Tovar).

0022-3468/$ – see front matter © 2009 Elsevier Inc. All rights reserved.
doi:10.1016/j.jpedsurg.2009.02.040

the membranous posterior wall and distributed in adventitial and submucosal plexuses, is of vagal origin [8]. As vagus nerves and esophageal intrinsic innervation are abnormal in babies [9] and in rats with CDH [10], in the present study we undertook to test the hypothesis that tracheal innervation might be abnormal in rat fetuses with CDH.

1. Material and methods

Adult Sprague-Dawley female rats were mated overnight. Twelve hours later, the presence of spermatozoids in the vaginal smear was verified to determine gestational day 0 (E0). Pregnant rats were then randomly divided into 2 groups: animals in the experimental group received intragastrically 100 mg of nitrofen dissolved in 1 mL of olive oil on E9.5, whereas those in the control group received only the vehicle. On E21 (preterm), the rats were sedated with isofluorane and killed by intracardiac injection of potassium chloride. The fetuses were recovered by cesarean delivery and the diaphragm was carefully inspected for the presence of CDH. The animal care committee approved all the animal experiments (license number: 31-06).

1.1. Histochemistry

Whole mount preparations of CDH (n = 10) and control (n = 10) tracheas were fixed in 4% paraformaldehyde overnight and subsequently rinsed in phosphate buffered saline (PBS). The tracheas were slit along the ventral cartilaginous wall and histochemically stained for acetylcholinesterase (AChe) [11] (0.1 mol/L acetate buffer [pH 6.0], 6.5 mL; acetylthiocholine-iodide, 5.0 mg; 0.1 mol/L sodium citrate, 0.46 mL; 30 mmol/L copper sulfate, 1.0 mL; distilled water, 1.6 mL; 5 mmol/L potassium ferricyanide, 0.4 mL) for 1 hour at 37°C. The specimens were then mounted into a Glycergel medium (DAKO, Glostrup, Denmark) and covered by glass.

The intrinsic ganglia in the posterior membranous wall of the tracheas were counted and their surface measured with the assistance of an image analysis software (Image Pro-Plus, version 5.0, Media Cybernetics, Washington, DC). The total number of cartilaginous rings of each trachea was divided into 3 parts to assign the ganglia to the appropriate segment.

1.2. Immunohistochemistry

Cervico-thoracic blocks of CDH (n = 10) and control (n = 10) fetuses were fixed in 10% buffered formalin and then embedded in paraffin. Transverse 5-μm-thick sections perpendicular to the tracheal axis from the proximal and distal parts of the organ were prepared, mounted on glass slides, and allowed to dry. They were then deparaffinized, unmasked, and peroxidase blocked before applying the primary antibody. The slides were incubated with anti–low-affinity neurotrophin receptor $p75^{NTR}$ (1:100; rabbit polyclonal $p75^{NTR}$; Upstate, Lake Placid, NY) and anti-protein gene product 9.5 (1:200; rabbit polyclonal PGP 9.5; Dako Cytomation, Glostrup, Denmark) antibodies overnight at 4°C. Antibodies were labeled with the biotinylated streptavidin-biotin method and visualized with diaminobenzidine. Slides were then lightly counterstained with hematoxylin before being dehydrated, cleared, and mounted.

The total surface of the sectioned organ (excluding the mucosa) and the surface of submucosal and adventitial immunostained neural tissue (ganglia + fibers) were measured at both levels in 2 to 3 low-power fields with the assistance of the image processing software. The areas to be measured were contoured on the PC screen with the cursor and the resulting surface was integrated by the software. The proportion of the total surface occupied by immunostained neural tissue was determined.

1.3. Immunoblotting

For immunoblotting, the membranous walls of the tracheas from normal and nitrofen-exposed fetuses were pooled (5 or more) and homogenized in the lysis buffer (1 mmol/L sodium vanadate; 1% sodium dodecyl sulfate; 0.01 mol/L Tris-HCl, pH 7.4) with protease inhibitors. The protein content was assessed using a protein assay kit (BCA Protein Assay Kit, Pierce, Rockford, USA). The electrophoresis of 20 μg of total tracheal protein in an 18% sodium dodecyl sulfate–polyacrylamide gel was performed, and the separated proteins were electroblotted to a poly(vinylidene fluoride) membrane (Bio-Rad, Hercules, CA, USA). After blocking, the membrane was incubated overnight with anti-PGP 9.5 (1:6000; rabbit polyclonal PGP 9.5; Dako Cytomation) antibody at 4°C; it was then washed with Tween-Tris-NaCl buffer and incubated with a horseradish peroxidase–conjugated polyclonal antibody at 1:10,000 dilution for 1 hour at room temperature. The immunocomplexes were detected using an enhanced horseradish peroxidase/luminol chemiluminescence (ECL Advance, GE Healthcare, Little Chalfont Buckinghamshire, UK) and subjected to autoradiography. The immunoblot bands were quantified with the NIH Image V1.56 software. Superoxide dismutase (SOD) expression from the same membrane (polyclonal antibody anti-Cu/Zn SOD [1:2000]) was used to correct the PGP 9.5 expression.

1.4. Messenger RNA isolation and quantitative real-time reverse transcriptase–polymerase chain reaction

The membranous walls of the tracheas were pooled (5 or more) and frozen at −80°C. Total RNA was extracted using an RNA extraction kit (Qiagen, Hilden, Germany), according to the recommended protocol. The RNA strand (0.5 μg) was

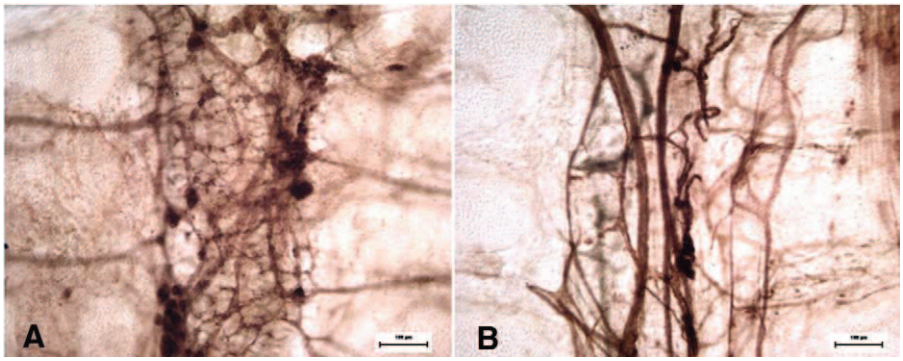

Fig. 1 Whole mount preparations of control (A) and CDH (B) tracheas stained for AChe. The cartilaginous rings are visible on each side of the posterior membranous wall. In controls, the nerve fibers are interconnected to form plexuses containing ganglia. These fibers run in the posterior membranous wall and send nerve bundles laterally between the cartilaginous rings (A). The neural network is clearly sparser in rats with CDH and the ganglia are smaller than in controls (B).

reverse transcribed into cDNA using a first strand cDNA synthesis kit for reverse transcriptase–polymerase chain reaction (RT-PCR; Roche, Manheim, Germany). Relative levels of gene expression were measured by RT-PCR, using LightCycler Fast Start DNA Master SYBR Green I kit (Roche, Spain) and the LightCycler detector. The values of PGP 9.5 were expressed after normalization by the levels of s26 ribosomal protein used as housekeeping. The specific primer sets used were as follows:

S26: Forward, 5′-AATTCGCTGCACGAACTGGC-3′; reverse, 5′-CAGCGCCAGCAGGTCTGAAT-3′
PGP 9.5: Forward, 5′-AGTGGCTCTCTGCAAAGCAG -3′; reverse, 5′-GGCAGTAGAACGCAAGAAGA -3′

1.5. Statistical methods

The results were expressed as percentages or as means ± SD, and both groups were compared by either 2-way ANOVA or nonparametric Mann-Whitney tests as appropriate with a threshold of significance at $P < .05$.

2. Results

2.1. Histochemistry

An AChe-positive neural network was present in both groups. In control tracheas, the nerve fibers were interconnected to form plexuses containing ganglia that ran in the membranous wall and sent nerve bundles laterally between the cartilaginous rings, as described in adult rat trachea [12]. The neural network was denser in the distal part of the trachea. In CDH tracheas, this network was sparser and the nerve trunks thinner than in control ones (Fig. 1).

The surface of the ganglia was significantly smaller in CDH fetuses at all levels as depicted in Table 1, whereas the number of ganglia was similar in both groups at both levels.

2.2. Immunohistochemistry

Tracheal neural cells stained positively for $p75^{NTR}$ in both groups, confirming their neural crest origin.

The relative surface of PGP 9.5–immunostained neural tissue (fibers + ganglia) over the total surface of the trachea was significantly reduced in the distal part of tracheas from CDH fetuses. Upon separate assessment of submucosal and adventitial peritracheal neural structures, it turned out that the difference was caused by a significant reduction of the amount of neural tissue in the peritracheal plexus as shown in Table 2.

2.3. Immunoblotting and quantitative real-time RT-PCR

The signals for PGP 9.5 were seen at approximately 20 to 25 kd, and the protein levels were significantly lower in the

Table 1 Surface of ganglia in whole mount preparations of the trachea (AChe staining)

	Control (n = 10)		CDH (n = 10)	
	Proximal	Distal	Proximal	Distal
Surface of ganglia (μm^2)	3579 ± 4154	4927 ± 5607	1688 ± 1896 *	3426 ± 3726 *

Values are shown as means ± SD.
* $P < .05$ vs control.

Table 2 Neural surface in transversal sections of the trachea

Marker	Surface measured	Control (n = 10)		CDH (n = 10)	
		Proximal	Distal	Proximal	Distal
PGP 9.5	Neural/overall surface (%)	1.19 ± 0.31	2.07 ± 0.94	1.03 ± 0.47	1.36 ± 0.51 *
	Peritracheal neural/overall surface (%)	0.61 ± 0.30	1.33 ± 0.57	0.55 ± 0.36	0.70 ± 0.35 *

Values are shown as means ± SD.
* $P < .05$ vs control.

tracheas from CDH fetuses compared to the control group (Fig. 2).

In contrast, PGP 9.5 mRNA expression was significantly increased in CDH tracheas in comparison with controls (Fig. 3).

3. Discussion

Survivors of CDH have long-term pulmonary morbidity owing to the pulmonary hypoplasia and barotrauma from mechanical ventilation. However, frequent respiratory tract infections, obstructive airway pattern, and increased reactive airway disease [1-3,13,14] were also seen in survivors with mild to moderate pulmonary hypoplasia, suggesting that other causes might be involved. Malformations of the tracheobronchial tree were described both in the experimental model of CDH [15] and in patients with CDH [16]. Abnormal motility of the tracheobronchial tree is also present in rats with experimental CDH [7].

The human lung develops as an endodermal foregut outgrowth destined to become the trachea; it elongates, invading the surrounding mesenchyme, and continues to branch until the bronchial tree is formed [17,18]. From the early stages of lung development, the airway smooth muscle covers the branching epithelial tubules destined to become the future bronchial tree and the smooth muscle layer is ensheathed in a network of nerves and ganglia [19-21]. It has been suggested that airway smooth muscle may function as a mechanical prerequisite for lung growth by generating a positive pressure in the liquid-filled tubules which is necessary for normal lung growth; the reduction of this pressure by draining of the liquid contents causes lung hypoplasia [22], whereas its increase by tracheal occlusion enhances lung growth [23,24]. Tracheobronchial innervation controls smooth muscle tension and also regulates secretion by the submucosal glands, epithelial cell function, bronchial vascular tone, and tracheobronchial reflexes [25,26]. As the airway smooth muscle has an important role in lung development, we speculated that an impaired control of the tracheobronchial motility might partially account for pulmonary hypoplasia.

The neural crest supplies tracheobronchial innervation through the vagus nerves [8,27]. These and the intrinsic esophageal innervation are deficient both in babies and in rat fetuses with CDH [10].

Staining with anti-p75^{NTR} antibody confirmed that tracheal neural cells are, like those of the gastrointestinal

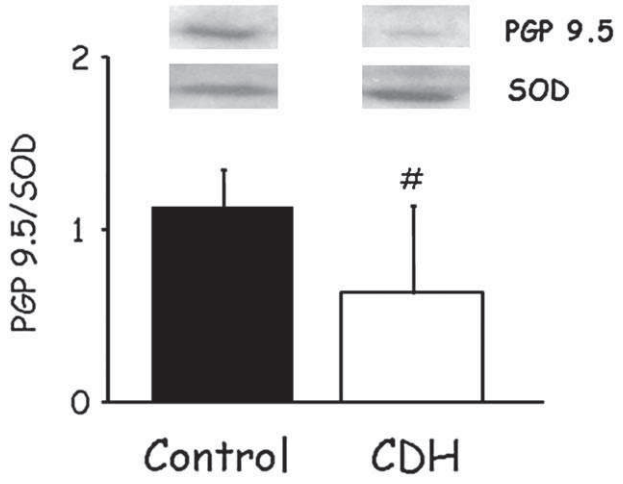

Fig. 2 PGP 9.5 protein level normalized to SOD in both groups (control + CDH). Anti–PGP 9.5 antibody hybridized with a single band between 20 and 25 kd. The expression of PGP 9.5 was significantly decreased in the CDH group ($^{\#}P < .05$ vs control).

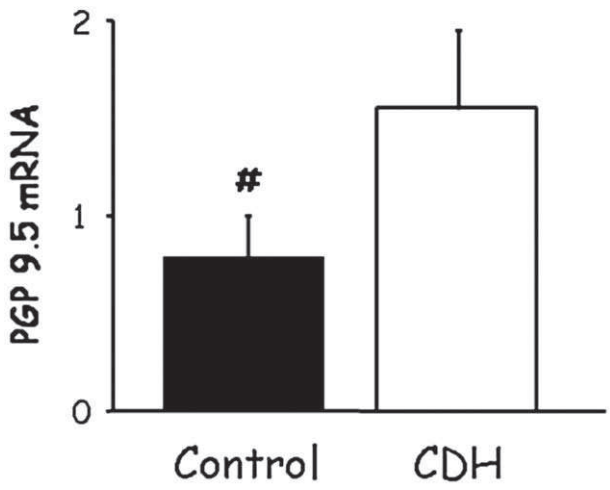

Fig. 3 PGP 9.5 mRNA expression level in each group of tracheas (control + CDH). The expression of PGP 9.5 was significantly increased in the CDH group ($^{\#}P < .05$ vs control).

tract, neural crest derived. The antiserum against PGP 9.5 has been used in immunostaining as a pan-neuronal marker of the peripheral nervous system, staining fibers, and ganglia. The ganglionic precursors can be distinguished with anti–PGP 9.5 since the early phase of development. The tracheal neural tissue was clearly deficient in CDH fetuses in terms of decreased surface of the ganglia (AChe) in the posterior wall and density of neural structures (PGP 9.5) in the peritracheal plexus of the distal half of the trachea. In addition, PGP 9.5–protein levels were decreased in the tracheas of fetuses with CDH. In contrast, PGP 9.5–mRNA expression was increased in them.

PGP 9.5 is a ubiquitin carboxyl-terminal hydrolase isozyme L1 [28] and is expressed in neurons and nerve fibers at all levels of the central and peripheral nervous system and in neuroendocrine tissue [29]. Ubiquitin is involved in protein degradation and the hydrolases regenerate ubiquitin from ubiquitin/protein complexes targeted for degradation. Different studies demonstrated both in rat [30] and in mouse [31] that there is a parallel distribution of PGP 9.5 protein and PGP 9.5 mRNA, although the correlation is not quantitatively absolute. PGP 9.5 is present in both motor and sensory neuronal precursors during their development and also in the differentiated neurons, suggesting a significant role for the ubiquitin hydrolases throughout the differentiation of these cells.

In our study, the PGP 9.5 mRNA transcripts were increased in the tracheas of fetuses with CDH in comparison with the controls, suggesting that posttranslational events occur in the development of CDH tracheas and may play a role in the impairment of the expression.

The present study is the first to demonstrate deficient tracheal innervation in the experimental model of CDH. The motor counterparts of these deficits are being currently investigated. If similar anomalies are present in babies with CDH, they might participate in the pathogenesis of lung hypoplasia and/or bronchopulmonary sequelae. Unfortunately, tracheal innervation could not be examined in babies with CDH because the standard techniques of neonatal autopsies do not allow appropriate harvesting of tracheal material for studies of this nature. Prospective collection of specimens suitable for complete studies of tracheal innervation is highly desirable.

References

[1] Trachsel D, Selvadurai H, Bohn D, et al. Long-term pulmonary morbidity in survivors of congenital diaphragmatic hernia. Pediatr Pulmonol 2005;39:433-9.

[2] Muratore CS, Kharasch V, Lund DP, et al. Pulmonary morbidity in 100 survivors of congenital diaphragmatic hernia monitored in a multidisciplinary clinic. J Pediatr Surg 2001;36: 133-40.

[3] Kamata S, Usui N, Kamiyama M, et al. Long-term follow-up of patients with high-risk congenital diaphragmatic hernia. J Pediatr Surg 2005;40:1833-8.

[4] Slavkin HC, Snead ML, Zeichner-David M, et al. Concepts of epithelial-mesenchymal interactions during development: tooth and lung organogenesis. J Cell Biochem 1984;26:117-25.

[5] Warburton D, Zhao J, Berberich MA, et al. Molecular embryology of the lung: then, now, and in the future. Am J Physiol 1999;276: L697-704.

[6] Jesudason EC. Small lungs and suspect smooth muscle: congenital diaphragmatic hernia and the smooth muscle hypothesis. J Pediatr Surg 2006;41:431-5.

[7] Jesudason EC, Smith NP, Connell MG, et al. Peristalsis of airway smooth muscle is developmentally regulated and uncoupled from hypoplastic lung growth. Am J Physiol Lung Cell Mol Physiol 2006; 291:L559-65.

[8] Burns AJ, Delalande JM. Neural crest cell origin for intrinsic ganglia of the developing chicken lung. Dev Biol 2005;277:63-79.

[9] Pederiva F, Rodriguez JI, Ruiz-Bravo El, et al. Abnormal intrinsic esophageal innervation in congenital diaphragmatic hernia. A likely cause of motor dysfunction. J Pediatr Surg 2009;44:496-9.

[10] Martinez L, Gonzalez-Reyes S, Burgos E, et al. The vagus and recurrent laryngeal nerves in experimental congenital diaphragmatic hernia. Pediatr Surg Int 2004;20:253-7.

[11] Karnovsky MJ, Roots L. A "direct-coloring" thiocholine method for cholinesterases. J Histochem Cytochem 1964;12:219-21.

[12] Kusindarta DL, Atoji Y, Yamamoto Y. Nerve plexuses in the trachea and extrapulmonary bronchi of the rat. Arch Histol Cytol 2004;67: 41-55.

[13] Ijsselstijn H, Tibboel D, Hop WJ, et al. Long-term pulmonary sequelae in children with congenital diaphragmatic hernia. Am J Respir Crit Care Med 1997;155:174-80.

[14] Vanamo K, Rintala R, Sovijarvi A, et al. Long-term pulmonary sequelae in survivors of congenital diaphragmatic defects. J Pediatr Surg 1996;31:1096-9.

[15] Xia H, Migliazza L, Diez-Pardo JA, et al. The tracheobronchial tree is abnormal in experimental congenital diaphragmatic hernia. Pediatr Surg Int 1999;15:184-7.

[16] Nose K, Kamata S, Sawai T, et al. Airway anomalies in patients with congenital diaphragmatic hernia. J Pediatr Surg 2000;35:1562-5.

[17] Spooner BS, Wessells NK. Mammalian lung development: interactions in primordium formation and bronchial morphogenesis. J Exp Zool 1970;175:445-54.

[18] Ten Have-Opbroek AA. The development of the lung in mammals: an analysis of concepts and findings. Am J Anat 1981;162:201-19.

[19] Weichselbaum M, Sparrow MP. A confocal microscopic study of the formation of ganglia in the airways of fetal pig lung. Am J Respir Cell Mol Biol 1999;21:607-20.

[20] Sparrow MP, Weichselbaum M, McCray PB. Development of the innervation and airway smooth muscle in human fetal lung. Am J Respir Cell Mol Biol 1999;20:550-60.

[21] Weichselbaum M, Everett AW, Sparrow MP. Mapping the innervation of the bronchial tree in fetal and postnatal pig lung using antibodies to PGP 9.5 and SV2. Am J Respir Cell Mol Biol 1996;15:703-10.

[22] Harding R, Hooper SB. Regulation of lung expansion and lung growth before birth. J Appl Physiol 1996;81:209-24.

[23] De Paepe ME, Johnson BD, Papadakis K, et al. Temporal pattern of accelerated lung growth after tracheal occlusion in the fetal rabbit. Am J Pathol 1998;152:179-90.

[24] Kitano Y, Flake AW, Quinn TM, et al. Lung growth induced by tracheal occlusion in the sheep is augmented by airway pressurization. J Pediatr Surg 2000;35:216-21.

[25] Barnes PJ. Neural control of human airways in health and disease. Am Rev Respir Dis 1986;134:1289-314.

[26] Coburn RF. Peripheral airway ganglia. Annu Rev Physiol 1987;49: 573-82.

[27] Tollet J, Everett AW, Sparrow MP. Spatial and temporal distribution of nerves, ganglia, and smooth muscle during the early pseudoglandular stage of fetal mouse lung development. Dev Dyn 2001;221: 48-60.

[28] Wilkinson KD, Lee KM, Deshpande S, et al. The neuron-specific protein PGP 9.5 is a ubiquitin carboxyl-terminal hydrolase. Science 1989;246:670-3.
[29] Wilson PO, Barber PC, Hamid QA, et al. The immunolocalization of protein gene product 9.5 using rabbit polyclonal and mouse monoclonal antibodies. Br J Exp Pathol 1988;69:91-104.
[30] Kajimoto Y, Hashimoto T, Shirai Y, et al. cDNA cloning and tissue distribution of a rat ubiquitin carboxyl-terminal hydrolase PGP9.5. J Biochem 1992;112:28-32.
[31] Schofield JN, Day IN, Thompson RJ, et al. PGP9.5, a ubiquitin C-terminal hydrolase; pattern of mRNA and protein expression during neural development in the mouse. Brain Res Dev Brain Res 1995;85:229-38.

ABNORMAL DEVELOPMENT OF TRACHEAL INNERVATION IN RATS WITH EXPERIMENTAL DIAPHRAGMATIC HERNIA.

Pederiva F, Aras Lopez R, Martinez L, Tovar JA.

Pediatr Surg Int 2008;24:1341-6.

Pediatr Surg Int (2008) 24:1341–1346
DOI 10.1007/s00383-008-2261-2

ORIGINAL ARTICLE

Abnormal development of tracheal innervation in rats with experimental diaphragmatic hernia

Federica Pederiva · Rosa Aras Lopez · Leopoldo Martinez · Juan A. Tovar

Published online: 28 October 2008

Abstract
Background We previously demonstrated that tracheobronchial innervation, originated from the vagus nerve and hence of neural crest origin, is deficient in rats with experimental congenital diaphragmatic hernia (CDH). The present study examines the development of this innervation during fetal life in an attempt to understand the nature of these deficiencies.
Materials and methods Pregnant rats were given either 100 mg nitrofen or vehicle on E9.5. Embryos were recovered on E15 and E18. Control and nitrofen/CDH pups ($n = 10$ each) were studied on each of these days and compared with our previous results on E21. Whole mount preparations of tracheas stained for anti-protein gene product 9.5 (PGP 9.5) and smooth muscle contractile α-actin were examined under confocal microscopy for the morphology of intrinsic neural network. Sections of tracheas were immunostained with anti-low-affinity neurotrophin receptor ($p75^{NTR}$), neural cell marker PGP 9.5, and anti-glial cell marker S100 antibodies. The proportions of sectional areas occupied by neural and glial structures were measured in the proximal and distal trachea. PGP 9.5 protein, and mRNA expressions were determined. Mann–Whitney tests with a threshold of significance of $P < 0.05$ were used for comparison.
Results Positive staining for $p75^{NTR}$ confirmed the neural crest origin of tracheal neural cells. The neural network appeared less organized on E15, and it was less dense on E18 in nitrofen-exposed embryos than in controls. The proportions of section surface occupied by neural elements were similar in both groups on E15, but that of glial tissue was significantly increased in nitrofen-exposed embryos. On E18, the relative neural surface was significantly reduced in CDH embryos in contrast with increased glial tissue surface. On E21 the proportion of neural tissue was reduced only in the distal trachea. The expression of PGP 9.5 protein was decreased in CDH fetuses on E18 and E21. In contrast, PGP 9.5 mRNA levels were increased in CDH fetuses on E18 and E21.
Conclusions The development of intrinsic innervation of the trachea in rats with CDH is abnormal with reduction of neural tissue accompanied by increase of glial tissue that could represent a response to neural damage. The significance of increased PGP 9.5 mRNA levels is unclear.

Keywords Diaphragmatic hernia · Intrinsic innervation · Trachea · Nitrofen · Neural crest · Lung $p75^{NTR}$ · PGP 9.5 · S100

Introduction

Long-term pulmonary morbidity occurs often in survivors of congenital diaphragmatic hernia (CDH) as sequela of pulmonary hypoplasia and barotrauma due to mechanical ventilation. Since tracheobronchial peristalsis plays a significant role in lung morphogenesis [1, 2], we hypothesized that abnormal tracheobronchial innervation might account in part for these symptoms. In our previous study on E21 (near-term) rats we found deficient tracheal neural tissue in

Presented at the 21st International Symposium on Pediatric Surgical Research, Leipzig, Germany, 2–4 October 2008.

F. Pederiva is a research fellow of the CAM (FPI-000760 Grant).

F. Pederiva · R. Aras Lopez · L. Martinez · J. A. Tovar (✉)
Department of Pediatric Surgery and Research Laboratory, Hospital Universitario La Paz, Paseo de la Castellana, 261, 28046 Madrid, Spain
e-mail: jatovar.hulp@salud.madrid.org

CDH fetuses in terms of decreased surface of ganglia and density of neural structures as well as abnormal expression of PGP 9.5 protein and levels of PGP 9.5 mRNA [3].

The present study addressed the development of tracheal innervation in the embryo–fetal period and tested the hypothesis that the abnormalities described in rat pups with CDH on E21 might be the result of either delayed development of innervation or of neural damage and repair.

Materials and methods

Adult Sprague–Dawley female rats were mated overnight. The finding of spermatozoids in the vaginal smear determined gestational day 0 (E0). Pregnant rats were then randomly divided into four groups: control E15, nitrofen E15, control E18 and CDH E18. Animals in the experimental group received intragastrically 100 mg of nitrofen dissolved in 1 ml of olive on E9.5, whereas those in the control group received only vehicle. On E15 and E18, the rats were sedated with isofluorane and killed by intracardiac injection of potassium-chloride. The embryos and fetuses were recovered and on E18 the diaphragm was inspected for the presence of CDH. On E15 all the embryos were used and randomly allocated to the different techniques. The Animal Care Committee approved all the animal experiments (license number: 31–06).

Immunohistochemistry

Whole mount preparations of all groups were fixed in 4% paraformaldehyde overnight and subsequently rinsed in phosphate buffered saline (PBS). Nonspecific binding was blocked by washing them in PBS with 1% bovine-serum albumin, before incubating the tracheas with the primary antibodies overnight. A rabbit polyclonal antibody against protein gene product 9.5 (PGP 9.5; 1:500; Dako Cytomation, Glostrup, Denmark) was used to stain the neural tissue, whereas the smooth muscle was identified with a mouse monoclonal anti-α-actin fluorochrome-labeled antibody (anti-actin, α-smooth muscle-Cy3^{TM} antibody; 1:1000: Sigma–Aldrich, St. Luis, MO). After washing with PBS, the samples were incubated at room temperature for 1 h with the fluorochrome-labeled anti-rabbit secondary antibody (Alexa Fluor® 488; 1:500; Molecular Probes, Eugene, OR). After further washing with PBS, the specimens were then mounted into glycerol on a glass slide. As a control the primary antibody was omitted with no staining above background as a result.

Fluorescent images of the nerves and smooth muscle in the double-stained whole mount preparations were obtained using a confocal laser scanning microscope (Leica TCS SP5) with LAS-AF software. The fluorescent markers were detected by a kripton/argon laser with excitation wavelengths of 488 nm for Alexa 488 and 561 nm for Cy3. The whole mounts were optically sectioned by scanning at increasing depths of focus in steps of 5 μm. After double staining, the green and the red images were captured separately, colorized and merged to show a composite nerve/smooth muscle image. The pattern of the neural network in the posterior membranous wall of the tracheas was compared between nitrofen/CDH and controls.

To measure the relative surface covered by neural tissue and glial cells, cervico-thoracic blocks of embryos and fetuses were fixed in 10% buffered formalin and then embedded in paraffin. Transversal 5 μm sections perpendicular to the tracheal axis from the proximal and distal parts of the organ were prepared, mounted on glass slides and allowed to dry. They were then deparaffinized, unmasked and peroxidase-blocked before applying the primary antibody. The slides were incubated with anti-low-affinity neurotrophin receptor p75^{NTR} (1:100; rabbit polyclonal p75^{NTR}; Upstate, Lake Placid, NY), anti-protein gene product 9.5 (1:200; rabbit polyclonal PGP 9.5; Dako Cytomation, Glostrup, Denmark) and anti-glial cell marker S100 (1:2000; rabbit polyclonal S100; Dako Cytomation, Glostrup, Denmark) antibodies overnight at 4°C. Antibodies were labeled with biotinylated streptavidin-biotin method and visualized with diaminobenzidine. Slides were then lightly counter-stained with hematoxylin before being dehydrated, cleared and mounted.

The total surface of the sectioned organ (excluding the mucosa) and the surface of immunostained neural (ganglia + fibers) and glial tissue were measured at both levels in 1–2 low-power fields with the assistance of image processing software (Image Pro-Plus^{TM}, version 5.0, Media Cybernetics, Washington, DC, USA). The areas to be measured were contoured on the PC screen with the cursor and the resulting surface was integrated by the software. The proportion of the total surface occupied by immunostained neural tissue and glial cells was determined.

Immunoblotting

Tracheas from the four groups were pooled (eight or more) and homogenized in lysis buffer (1 mmol/l sodium vanadate; 1% SDS; 0.01 mol/l Tris–HCl, pH 7.4) with protease inhibitors. The protein content was assessed using a protein assay kit (BCA Protein Assay Kit, Pierce). 20 μg of total tracheal protein was separated by 18% SDS-polyacrylamide gel electrophoresis and the separated proteins were electroblotted to a PVDF membrane (Bio-Rad). The membrane was blocked and then incubated overnight with anti-PGP 9.5 (1:6000; rabbit polyclonal PGP 9.5; Dako Cytomation, Glostrup, Denmark) antibody at 4°C; it was then rinsed in Tween-Tris–NaCl buffer and incubated with

a horseradish peroxidase-conjugated polyclonal antibody at 1:10000 dilution for 1 h at room temperature. The antigen–antibody complexes were detected using an enhanced horseradish peroxidase/luminol chemiluminescence kit (ECL advance GE Healthcare, UK) and subjected to autoradiography. The immunoblot bands were quantified with NIH Image V1.56 software. The normalization was done using super-oxide-dysmutase (SOD).

mRNA isolation and quantitative real time RT-PCR

The membranous walls of tracheas were pooled (eight or more) and frozen at −80°C. Total RNA was extracted using a RNA extraction kit (Qiagen, Spain), according to recommended protocol. The RNA strand (0.5 μg) was reverse-transcribed into cDNA using first strand cDNA synthesis kit for RT-PCR (Roche, Spain). Relative levels of gene expression were measured by RT-PCR, using Light-cycler Fast Start DNA Master SYBR Green I kit (Roche, Spain) and lighcycler detector. PGP 9.5 values were normalized to the levels of s26 ribosomal protein used as housekeeping. The specific primer sets used were as follows:

S26	PGP 9.5
Forward 5′-AATTCGCTGC ACGAACTGGC-3′	Forward 5′-AGTGGCTCTCTG CAAAGCAG-3′
Reverse 5′-CAGCGCCAGCA GGTCTGAAT-3′	Reverse 5′-GGCAGTAGAA CGCAAGAAGA-3′

Statistical methods

The results were expressed as percentages or as mean ± SD and both groups were compared by either two-way ANOVA or non-parametric Mann–Whitney tests as appropriate with a threshold of significance at $P < 0.05$.

Results

Immunohistochemistry

In both control groups (E15 and E18) the posterior membranous wall of the trachea contained smooth muscle ensheated in a plexus of nerve fibers with ganglia that sent nerve bundles laterally between the cartilaginous rings, as described in our previous study of the rat trachea on E21 [3].

On E15 the nerve fibers of the membranous wall of the tracheas were poorly interconnected in the nitrofen group (Fig. 1) whereas the neural network was better developed, although sparser, on E18 CDH (Fig. 2).

Tracheal neural cells stained positively for $p75^{NTR}$ in all groups, confirming their neural crest origin.

On E15, the relative surface of glial cells (immunostained for S100) over the total surface of the trachea was significantly increased in embryos exposed to nitrofen both at the proximal and distal levels (Table 1). In contrast, no differences were found comparing the relative surface of neural tissue (fibers + ganglia) immunostained for PGP 9.5 in nitrofen and control groups.

On E18, the proportion of section surface occupied by neural elements was significantly reduced in the tracheas from CDH fetuses (Fig. 3), while that of glial cells was significantly increased in the same group at both levels (Fig. 4), as shown in Table 2.

Immunoblotting and quantitative real time RT-PCR

The signals for PGP 9.5 were seen at approximately 20–25 kD. On E18, the protein levels were significantly

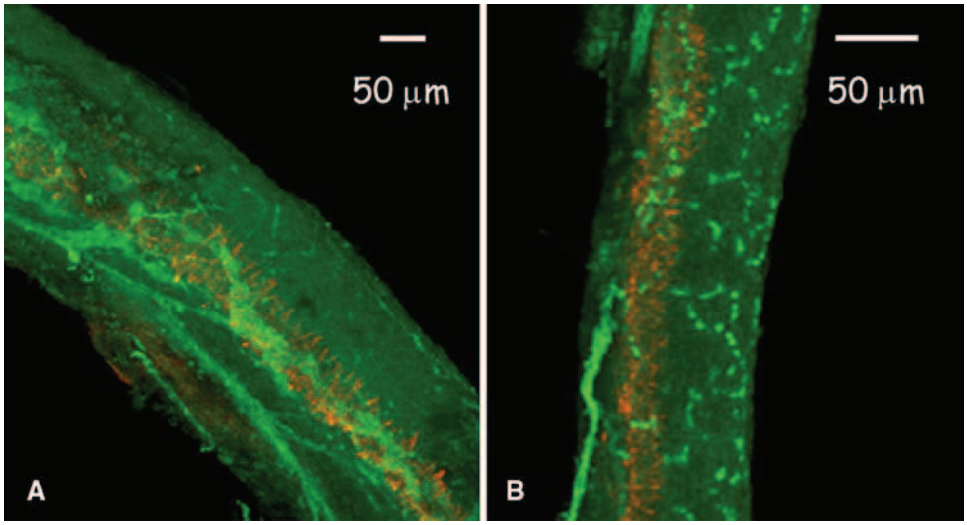

Fig. 1 Confocal projection of control (**a**) and nitrofen (**b**) tracheas of E15 embryos. Bundles of α-actin-positive muscle fibers (*red*) cover the posterior wall of the tracheas in both groups. In control embryos, PGP 9.5 immunoreactivity (*green*) reveals interconnected nerve fibers that form plexuses containing ganglia. These fibers are poorly interconnected in embryos exposed to nitrofen (**b**)

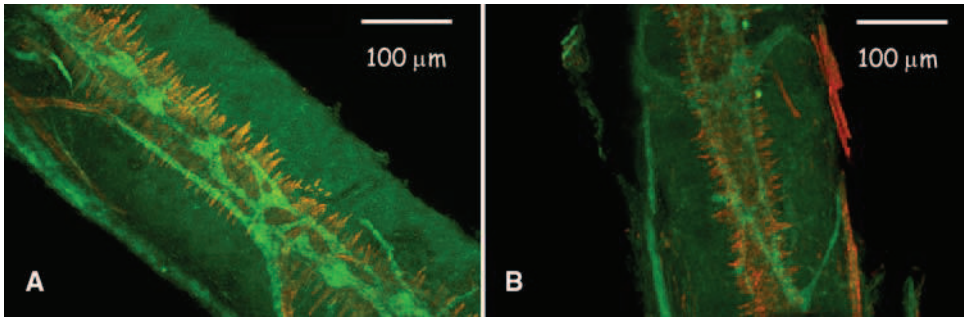

Fig. 2 Confocal projection of control (**a**) and nitrofen (**b**) tracheas of E18 fetuses. In both groups airway smooth muscle (*red*) covers the posterior wall of the trachea. In control fetuses, the fibers (*green*), running in the posterior wall, form dense plexuses with ganglia (**a**). The network is sparser in fetuses with CDH (**b**)

Table 1 Glial cell surface in transversal sections of the trachea on E15 (means ± SD)

Marker	Surface measured	Control ($n = 10$)		CDH ($n = 10$)	
		Proximal	Distal	Proximal	Distal
PGP 9.5	Neural/overall surface (%)	1.58 ± 1.11	2.48 ± 1.09	0.96 ± 1.01	1.91 ± 1.11
S 100	Glial cell/overall surface (%)	0.05 ± 0.06	0.09 ± 0.04	0.23 ± 0.12 *	0.20 ± 0.07 *

* $P < 0.05$ versus control

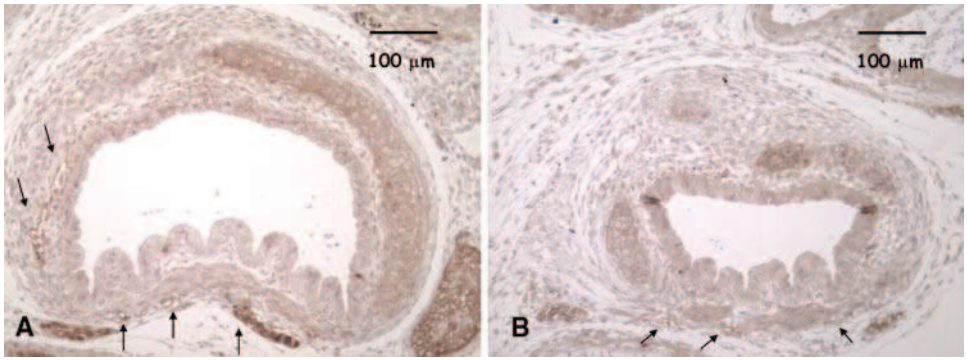

Fig. 3 Transversal sections of tracheas of control (**a**) and CDH (**b**) E18 fetuses immunostained for PGP 9.5. In control fetuses, a dense network of fibers (*arrows*) is present both in submucosal and peritracheal plexuses (**a**). In contrast, the neural network (*arrows*) is markly reduced in CDH fetuses (**b**). Notice the smaller size and the abnormal contour of the trachea in this group

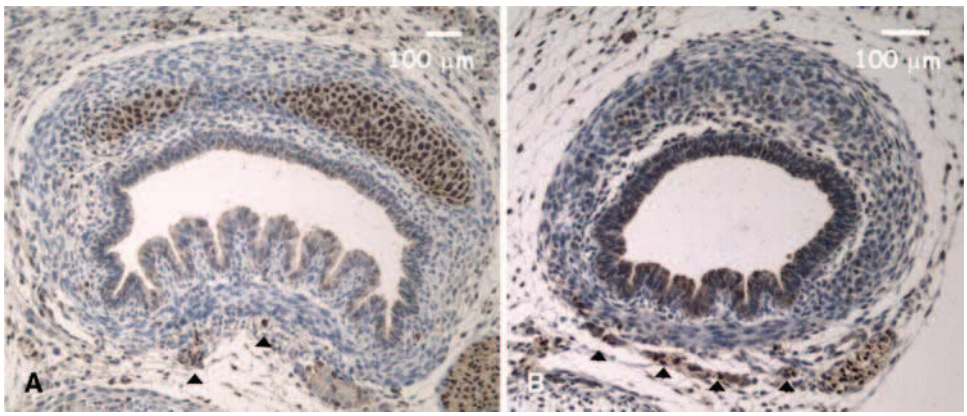

Fig. 4 Transversal sections of tracheas of control (**a**) and CDH (**b**) E18 fetuses immunostained for S100. In CDH trachea (**b**) glial tissue (*arrowheads*) is increased in comparison with the control group (**a**; *arrowheads*)

lower in the tracheas from CDH fetuses compared to control group (Fig. 5).

In contrast, PGP 9.5 mRNA expression was significantly increased in CDH tracheas in comparison with controls (Fig. 6).

On E15 the findings resembled those seen on E18 with lower PGP 9.5 protein levels and increased PGP 9.5 mRNA expression in nitrofen tracheas, but the differences were not significant.

Looking at the expression of the protein over the development, we found that PGP 9.5-protein levels increased significantly in control tracheas between E15 and E18 and tended to decrease between E18 and E21. In contrast, the protein expression did not change between

Table 2 Neural and glial cell surfaces in transversal sections of the trachea on E18 (mean ± SD)

Marker	Surface measured	Control ($n = 10$)		CDH ($n = 10$)	
		Proximal	Distal	Proximal	Distal
PGP 9.5	Neural/overall surface (%)	1.38 ± 0.53	3.11 ± 1.79	0.82 ± 0.63 *	1.41 ± 1.14 *
S 100	Glial cell/overall surface (%)	0.12 ± 0.06	0.15 ± 0.06	0.65 ± 0.27 *	0.96 ± 0.45 *

* $P < 0.05$ versus control

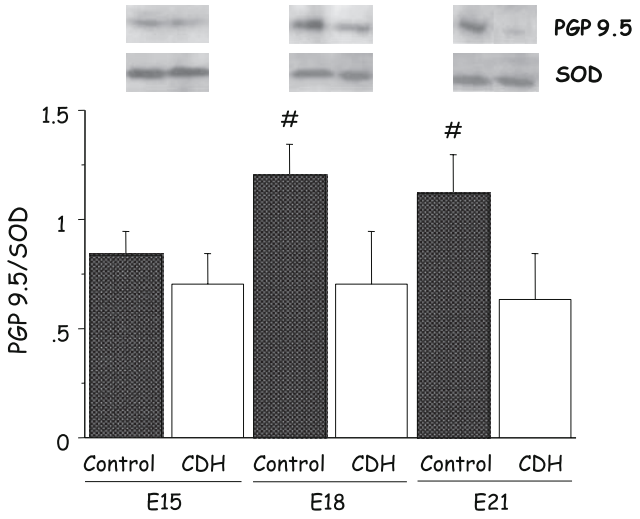

Fig. 5 PGP 9.5 protein level normalized to super-oxide-dysmutase (SOD) in all endpoints (E21 from our previous study [3]). Anti-PGP 9.5 antibody hybridized with a single band between 20 and 25 kD. The expression of PGP 9.5 is significantly decreased on E18 and E21 in CDH fetuses (#$P < 0.05$ vs. control). The reduction on E15 nitrofen-exposed embryos is not significant

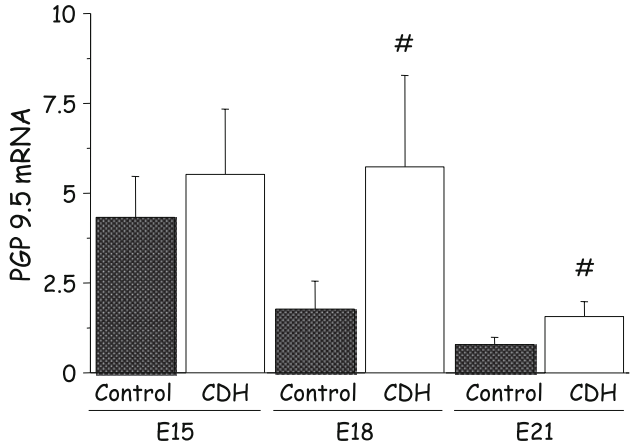

Fig. 6 PGP 9.5 mRNA expression level in all groups (E21 from our previous study [3]). It is significantly increased on E18 in fetuses with CDH (#$P < 0.05$ vs. control), whereas the difference on E15 is not significant

E15 and E18 in embryos and fetuses exposed to nitrofen and it was mildly reduced between E18 and E21. The PGP 9.5 mRNA expression was decreased over the development in the control groups; in contrast, there was a mild increment between E15 and E18 followed by a significant reduction over the last part of the gestation in nitrofen and CDH groups.

Discussion

Survivors of CDH have long-term pulmonary sequelae [4–6] mainly due to the pulmonary hypoplasia and barotrauma from mechanical ventilation but likely for other causes as well. Since the airway smooth muscle has an important role in lung development [1, 2], we speculated that impaired control of the tracheobronchial motility might account in part for pulmonary hypoplasia and that innervation of the airway smooth muscle, which has a crucial role in lung development [7, 8] could be abnormal in CDH. This muscle encircles the growing epithelial bronchi and provides tone to maintain the lung fluid at a positive pressure that stimulates lung growth by inducing growth factor production and cell proliferation [9–11]. The origin of this innervation is the neural crest which cells reach the developing trachebronchial tree from the vagus nerves [12]. The neural tissue ensheates the airways and sends bundles to the smooth muscle [13, 14].

In a previous study we described deficiencies of neural tissue in the tracheas of E21 (near-term) rats with CDH [3]: the density of neural tissue and the surface of ganglia were decreased as well as the expression of PGP 9.5 protein; in contrast, the levels of PGP 9.5 mRNA were increased. These findings suggested that delayed development and/or neural damage could account for deficient innervation.

In the present study we tested the first of these hypotheses by examining the development of tracheal neural tissue in control and nitrofen-exposed embryos and fetuses. PGP 9.5 is a ubiquitin carboxyl-terminal hydrolase isozyme L1 [15] expressed at all levels of the central and peripheral nervous system [16] in neurons and nerve fibers as well as in the neuronal precursors over the development, suggesting a role in the development and differentiation of these cells. With this staining we confirmed the patterns of innervation previously described in the upper airways of human [8] and normal mouse [7, 17] and showed that in

fetuses with CDH, the neural interconnections were poor in the tracheas on E15 and clearly sparser on E18 and E21.

PGP 9.5 protein levels increased significantly in control tracheas between E15 and E18 but remained unchanged in those from embryos and fetuses exposed to nitrofen. The PGP 9.5 mRNA expression progressively declined in controls during the period studied and it also did so in nitrofen-exposed fetuses but starting from higher levels.

This pattern is consistent with the hypothesis of a delayed development in animals with CDH in which tracheal innervation seems immature on E15, and deficient thereafter. On the other hand, increased PGP 9.5 mRNA transcripts in this group suggest post-translational events that could play a role in this impaired expression.

To test the hypothesis of a neural damage in the course of the development we used S100, a calcium-binding protein expressed in glial cells and also in Schwann cells [18, 19]. Its increased expression has been interpreted as a compensatory mechanism for defective neural tissue [20] and S100B mRNA levels have been used as a marker for brain injury [21, 22]. We found significantly increased population of glial cells in nitrofen-exposed embryos on E15 and in CDH fetuses on E18. This increment of glial tissue in CDH fetuses associated with scanty neural structures may be interpreted as a response to neural damage and compensation for the defective neuronal tissue.

The present study, which is the first to address the development of tracheal innervation in the experimental model of CDH, demonstrates that the deficits of tracheal innervation are the consequence of abnormal development in terms of delay and neural damage. Equivalent abnormalities in babies with CDH might contribute to the pathogenesis of lung hypoplasia and/or bronchopulmonary sequelae.

Acknowledgments This work was supported in part by FIS (06/0486 and 06/0447), FIHULP and FMM Grants.

References

1. Jesudason EC, Smith NP, Connell MG et al (2006) Peristalsis of airway smooth muscle is developmentally regulated and uncoupled from hypoplastic lung growth. Am J Physiol Lung Cell Mol Physiol 291:L559–L565
2. Jesudason EC (2006) Small lungs and suspect smooth muscle: congenital diaphragmatic hernia and the smooth muscle hypothesis. J Pediatr Surg 41:431–435
3. Pederiva F, Aras Lopez R, Martinez L, Tovar JA (2009) Tracheal innervation is abnormal in rats with experimental congenital diaphragmatic hernia. J Pediatr Surg (in press)
4. Trachsel D, Selvadurai H, Bohn D et al (2005) Long-term pulmonary morbidity in survivors of congenital diaphragmatic hernia. Pediatr Pulmonol 39:433–439
5. Muratore CS, Kharasch V, Lund DP et al (2001) Pulmonary morbidity in 100 survivors of congenital diaphragmatic hernia monitored in a multidisciplinary clinic. J Pediatr Surg 36:133–140
6. Kamata S, Usui N, Kamiyama M et al (2005) Long-term follow-up of patients with high-risk congenital diaphragmatic hernia. J Pediatr Surg 40:1833–1838
7. Tollet J, Everett AW, Sparrow MP (2001) Spatial and temporal distribution of nerves, ganglia, and smooth muscle during the early pseudoglandular stage of fetal mouse lung development. Dev Dyn 221:48–60
8. Sparrow MP, Weichselbaum M, McCray PB (1999) Development of the innervation and airway smooth muscle in human fetal lung. Am J Respir Cell Mol Biol 20:550–560
9. Sparrow MP, Warwick SP, Mitchell HW (1994) Foetal airway motor tone in prenatal lung development of the pig. Eur Respir J 7:1416–1424
10. Sparrow MP, Warwick SP, Everett AW (1995) Innervation and function of the distal airways in the developing bronchial tree of fetal pig lung. Am J Respir Cell Mol Biol 13:518–525
11. Cilley RE, Zgleszewski SE, Chinoy MR (2000) Fetal lung development: airway pressure enhances the expression of developmental genes. J Pediatr Surg 35:113–118 discussion 119
12. Burns AJ, Delalande JM (2005) Neural crest cell origin for intrinsic ganglia of the developing chicken lung. Dev Biol 277:63–79
13. Weichselbaum M, Everett AW, Sparrow MP (1996) Mapping the innervation of the bronchial tree in fetal and postnatal pig lung using antibodies to PGP 9.5 and SV2. Am J Respir Cell Mol Biol 15:703–710
14. Weichselbaum M, Sparrow MP (1999) A confocal microscopic study of the formation of ganglia in the airways of fetal pig lung. Am J Respir Cell Mol Biol 21:607–620
15. Wilkinson KD, Lee KM, Deshpande S et al (1989) The neuron-specific protein PGP 9.5 is a ubiquitin carboxyl-terminal hydrolase. Science 246:670–673
16. Wilson PO, Barber PC, Hamid QA et al (1988) The immunolocalization of protein gene product 9.5 using rabbit polyclonal and mouse monoclonal antibodies. Br J Exp Pathol 69:91–104
17. Tollet J, Everett AW, Sparrow MP (2002) Development of neural tissue and airway smooth muscle in fetal mouse lung explants: a role for glial-derived neurotrophic factor in lung innervation. Am J Respir Cell Mol Biol 26:420–429
18. Stefansson K, Wollmann RL, Moore BW (1982) Distribution of S-100 protein outside the central nervous system. Brain Res 234:309–317
19. Sheppard MN, Kurian SS, Henzen-Logmans SC et al (1983) Neurone-specific enolase and S-100: new markers for delineating the innervation of the respiratory tract in man and other mammals. Thorax 38:333–340
20. Boleken M, Demirbilek S, Kirimiloglu H et al (2007) Reduced neuronal innervation in the distal end of the proximal esophageal atretic segment in cases of esophageal atresia with distal tracheoesophageal fistula. World J Surg 31:1512–1517
21. Goncalves CA, Leite MC, Nardin P (2008) Biological and methodological features of the measurement of S100B, a putative marker of brain injury. Clin Biochem 41:755–763
22. Kochanek PM, Berger RP, Bayir H et al (2008) Biomarkers of primary and evolving damage in traumatic and ischemic brain injury: diagnosis, prognosis, probing mechanisms, and therapeutic decision making. Curr Opin Crit Care 14:135–141

BRONCHOPULMONARY INNERVATION DEFECTS IN INFANTS AND RATS WITH CONGENITAL DIAPHRAGMATIC HERNIA.

Pederiva F, Lopez RA, Rodriguez JI, Martinez L, Tovar JA.

J Pediatr Surg 2010;45:360-5.

Journal of Pediatric Surgery (2010) **45**, 360–365

ELSEVIER

Journal of Pediatric Surgery

www.elsevier.com/locate/jpedsurg

Bronchopulmonary innervation defects in infants and rats with congenital diaphragmatic hernia☆,☆☆

Federica Pederiva[a], Rosa Aras Lopez[a], Jose I. Rodriguez[b], Leopoldo Martinez[a], Juan A. Tovar[a,*]

[a]*Department of Pediatric Surgery and Research Laboratory, Hospital Universitario La Paz, 28046 Madrid, Spain*
[b]*Department of Pathology, Hospital Universitario La Paz, 28046 Madrid, Spain*

Received 21 October 2009; accepted 27 October 2009

Key words:
Diaphragmatic hernia;
Intrinsic innervation;
Nitrofen;
Neural crest;
Lung

Abstract

Introduction: Pulmonary morbidity in survivors of congenital diaphragmatic hernia (CDH) is caused by hypoplasia, barotraumas, or other reasons. We have previously shown deficient tracheal innervation in rats with CDH. Now we examine whether bronchopulmonary innervation is also abnormal in both infants and rats with CDH.

Material and Methods: Sections of E15, E18, and E21 rat lungs were immunostained for Protein gene product 9.5 and S100 antibodies. Similar immunostaining was performed on tissue from infants dying from CDH (n = 6) and other causes (n = 6) with Neurofilament, S100, and Rearranged during transfection antibodies. Nerve trunks/bronchus were counted, and the proportion of glial and RET-positive cells/bronchial surface was calculated. Glial cell-line derived neurotrophic factor protein and mRNA were measured in rat lungs.

Results: Nerve trunks/bronchus were decreased in infants and rat fetuses with CDH. In contrast, glial and RET-positive cells/bronchial surface were increased in infants and rats with CDH. Both lungs were equally affected. GDNF protein was high, whereas GDNF mRNA was decreased in preterm animals with CDH.

Conclusions: The lungs of infants and rats with CDH have decreased neural components compensated by increased supporting glial cells and persistence high expression of RET and GDNF protein. Because bronchopulmonary innervation controls airway smooth muscle, vessels, and glandular secretions, it is tempting to hypothesize that these deficiencies might play a role in respiratory morbidity in CDH.

Pulmonary hypoplasia persisting beyond infancy [1,2] and lung injury caused by mechanical ventilation [3] are major determinants of respiratory morbidity in survivors of congenital diaphragmatic hernia (CDH). These factors contribute to obstructive and restrictive pulmonary disease described in CDH survivors [3-5]. However, increased incidence of respiratory infections, bronchial obstruction, wheezing, asthma, and bronchial hyperreactivity has been found also in survivors with mild pulmonary hypoplasia [6],

Presented at the 56th Annual Meeting of the British Association of Paediatric Surgeons, Graz, Austria, June 18-20, 2009.

☆ Supported in part by Fondo de Investigación Sanitaria (06/0486 and 06/0447), Fundación de Investigación del Hospital Universitario La Paz, and Fundación Mutua Madrileña Grants.

☆☆ F.P. is a research fellow of Red SAMID of the Instituto de Salud Carlos III.

* Corresponding author. Tel.: +34 91 727 70 19; fax: +34 91 727 70 33.
E-mail address: jatovar.hulp@salud.madrid.org (J.A. Tovar).

0022-3468/$ – see front matter © 2010 Elsevier Inc. All rights reserved.
doi:10.1016/j.jpedsurg.2009.10.076

suggesting that other causes might be involved. We demonstrated previously that tracheal innervation is abnormal in rats with CDH [7,8] and concluded that, if similar anomalies were found in human CDH, this deficiency could play a role in chronic lung disease of survivors. We felt that the next step would be to examine bronchopulmonary innervation, and the current study tests the hypotheses that bronchopulmonary innervation might be abnormal in infants dying of CDH and also in rat fetuses with experimental CDH.

1. Materials and methods

Adult Sprague-Dawley female rats were mated overnight, and the presence of spermatozoids in the vaginal smear determined gestational day 0 (E0). Pregnant rats received intragastrically 100 mg of nitrofen dissolved in 1 mL of olive or only vehicle on E9.5. The embryos and fetuses were recovered by cesarean section on E15, E18, and E21. The diaphragm was inspected for the presence of CDH on E18 and E21, and only rats with the malformation were further processed. Because of size restrictions, all E15 embryos were processed. The Animal Care Committee approved the animal experiments (license number: 31-06). Paraffin blocks of the lungs from 6 newborns who had died of CDH and from 6 age-matched infants who died from other unrelated conditions were investigated following institutional research board approval. At least 3 bronchi of comparable size were examined in each lung both in infants and in rat fetuses at all endpoints.

1.1. Immunohistochemistry

Thoracic blocks of CDH (n = 10) and control (n = 10) embryos and fetuses of each endpoint were fixed in 10% buffered formalin and then embedded in paraffin. After the staining protocol previously described [7], the slides were incubated with anti–low-affinity neurotrophin receptor $p75^{NTR}$ (1:100; rabbit polyclonal $p75^{NTR}$; Upstate, Lake Placid, NY), antiprotein gene product 9.5 (1:200; rabbit polyclonal PGP 9.5; Dako Cytomation, Glostrup, Denmark), and antiglial cell marker S100 (1:800; rabbit polyclonal S100; Dako Cytomation) antibodies.

In a similar way, the human lung autopsy material was stained with antineurofilament (1:800; rabbit polyclonal NF; Dako Cytomation), antiglial cell marker S100 (1:600; rabbit polyclonal S100; Dako Cytomation), and anti-RET (1:200; rabbit polyclonal RET; Santa Cruz Biotechnology, Inc, Spain) antibodies.

Nerve trunks per bronchus, either stained by PGP 9.5 or NF, were counted. The proportion of glial supporting tissue (S100) and RET-positive cells over the bronchial section surface (excluding the mucosa) was calculated with the assistance of image processing software.

1.2. Immunoblotting

Both lungs from normal and nitrofen-exposed fetuses of each endpoint were pooled (3 or more) and underwent the procedures previously described [7] for immunoblotting, using a 15% sodium dodecyl sulfate polyacrylamide gel. The membrane was incubated with antiglial cell line–derived neurotrophic factor (1:10,000; rabbit polyclonal GDNF; BioVision, Mountain View, CA) antibody, and the results were normalized to superoxide dismutase (SOD; 1:2000; polyclonal antibody anti–Cu/Zn SOD).

1.3. mRNA isolation and quantitative real-time polymerase chain reaction

Total RNA from the lungs of 3 embryos and fetuses of each endpoint was isolated with a RNA extraction kit (Qiagen, Hilden, Germany, and Roche, Mannhein, Germany), and 1 μg was reverse transcribed into cDNA using first-strand cDNA synthesis kit for reverse transcriptase polymerase chain reaction (Roche, Spain). The specific sequences of forward and reverse primers (Bonsaitech, Spain) used were as follows; GDNF GTTATGGGATGTCGTGGCTG (forward) and CAGATAAACAAGCGGCGGCA (reverse). Each sample was run in duplicate, and the mean value was used to calculate mRNA expression. The quantity of GDNF in each sample was calculated comparing the CT values of each endpoint with E15 control, used as calibrator ($2^{-\Delta\Delta CT}$). The cycle threshold (CT) values of both calibrator and samples were normalized to the endogenous housekeeping gene 18s.

1.4. Statistical methods

The results were expressed as percentages or as means ± SD, and both groups were compared by either 2-way analysis of variance or nonparametric Mann-Whitney tests as appropriate, with a threshold of significance at $P < .05$.

2. Results

2.1. Immunohistochemistry

The neural crest origin of the lung neural cells was confirmed by the positive staining for $p75^{NTR}$ in all groups.

Peribronchial nerve trunks were significantly reduced in both lungs of infants with CDH (NF immunostaining; Fig. 1A) and of rat embryos exposed to nitrofen and fetuses with CDH (PGP 9.5 immunostaining; Fig. 2A) in comparison with controls. Ipsilateral and contralateral lungs were equally affected in both settings.

In contrast, the proportion of glial tissue surface over bronchial section surface was significantly increased both in infants with CDH (Figs. 1B and 3A [control] and B

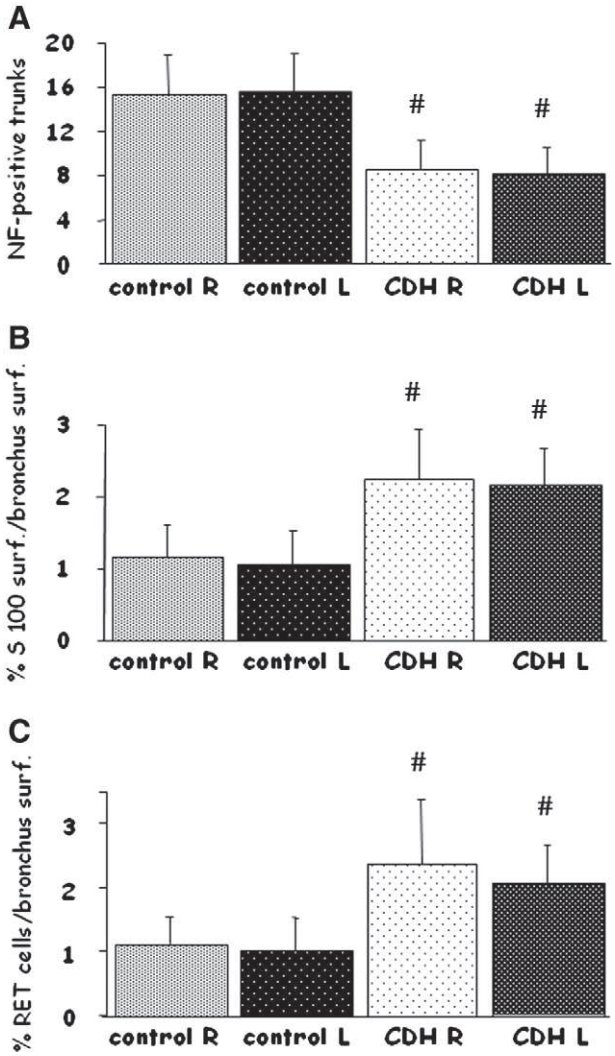

Fig. 1 A, The number of NF-positive nerve trunks per bronchus in human lungs is decreased in both lungs of infants with CDH (CDH R and L) in comparison with corresponding control lungs ($^{\#}P < .05$ versus control). B, The proportion of S100-stained glial tissue/bronchus section in human lungs is increased in both lungs (CDH R and L) of babies with CDH in comparison with controls ($^{\#}P < .05$ versus control). C, Proportion of RET-positive cells over bronchus section. It is increased in lungs of infants with CDH compared with controls ($^{\#}P < .05$ versus control).

[CDH]) and in rats exposed to nitrofen (Figs. 2B and 3C [control] and D [CDH]) without any difference between both lungs. The proportion of RET-positive cells over the bronchus surface was significantly increased in lungs of infants with CDH (Fig. 1C).

2.2. Immunoblotting and quantitative real-time reverse transcriptase polymerase chain reaction

The signals for GDNF were seen at 15 kD, and the protein levels remained persistently high in all endpoints in animals exposed to nitrofen (Fig. 4A).

GDNF mRNA transcripts that were increased on E15 were significantly decreased in E18 and E21 animals with CDH (Fig. 4B).

3. Discussion

Persistent lung hypoplasia with structural abnormalities in distal airways and barotrauma owing to neonatal intensive care treatment have been repeatedly considered as possible causes of long-term pulmonary sequelae in survivors of CDH [3-5,9]. However, these children are prone to develop pulmonary exacerbations secondary to viral respiratory infections, they experience wheezing and symptoms of airway hyperresponsiveness and asthma, and they have abnormalities in pulmonary function including obstructive, restrictive, or a combined ventilation impairment even when the pulmonary hypoplasia is mild to moderate [5,6,10,11]. This suggests that also other causes might contribute to pulmonary morbidity.

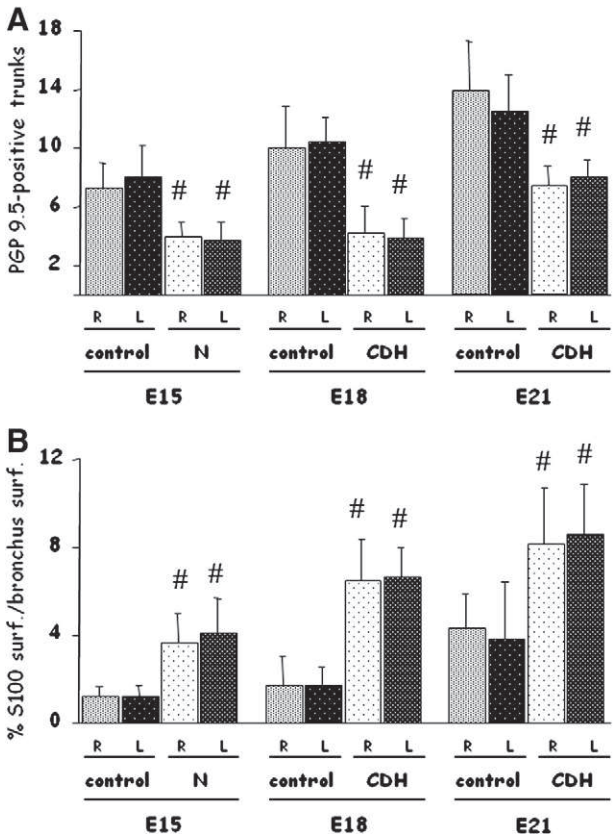

Fig. 2 A, The number of PGP 9.5–positive nerve trunks per bronchus in rat lungs is decreased ($^{\#}P < .05$ versus control) in both lungs of animals exposed to nitrofen (N R and L and CDH R and L) at all endpoints in comparison with control lungs ($^{\#}P < .05$ versus control). B, The proportion of S100-stained glial tissue/bronchus section in rat lungs is increased in both lungs of animals exposed to nitrofen (N R and L and CDH R and L) in comparison with control lungs ($^{\#}P < .05$ versus control).

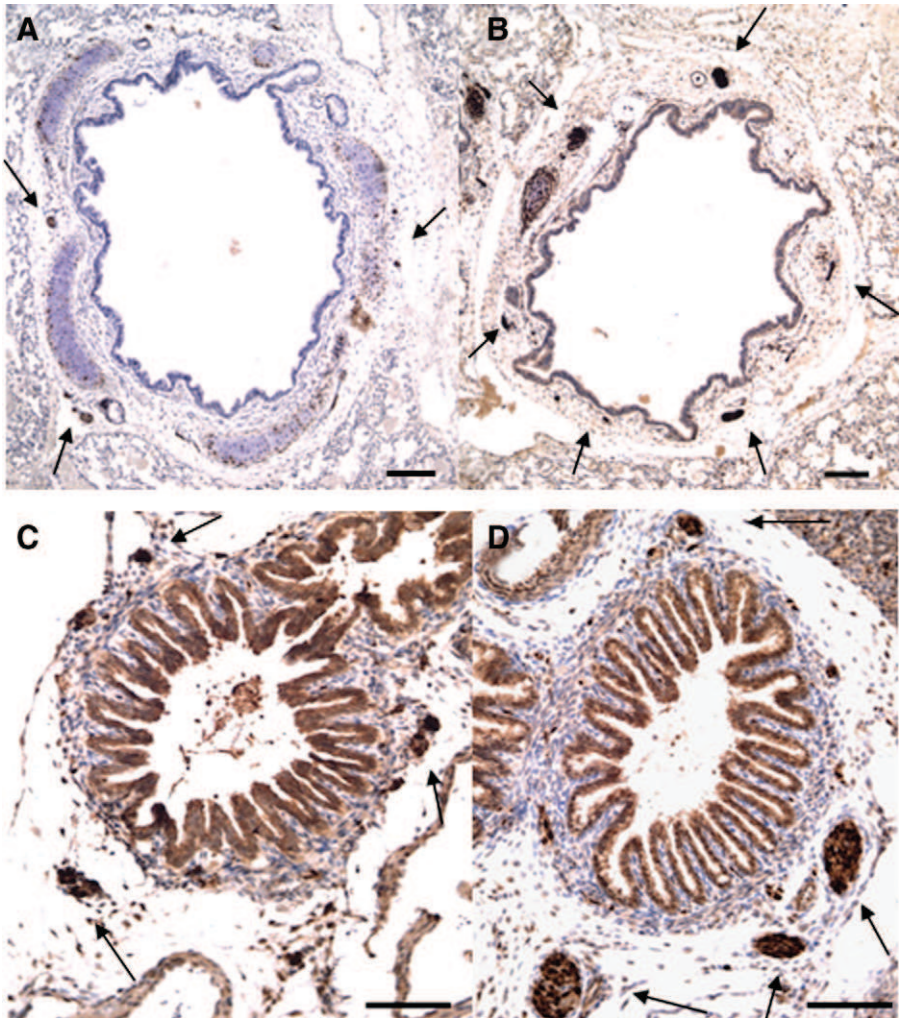

Fig. 3 Human: transversal section of human control (A) and CDH (B) lungs stained by S100 antibody. The amount of supporting glial cells (arrows) is clearly increased in lungs of infants with CDH. Scale bar = 100 μm. Rat: transversal sections of rat control (C) and CDH (D) lungs on E21 stained by S100 antibody. The proportion of supporting glial cells (arrows) is increased in bronchus of CDH fetuses, resembling the pattern depicted in CDH human lungs. Scale bar = 100 μm.

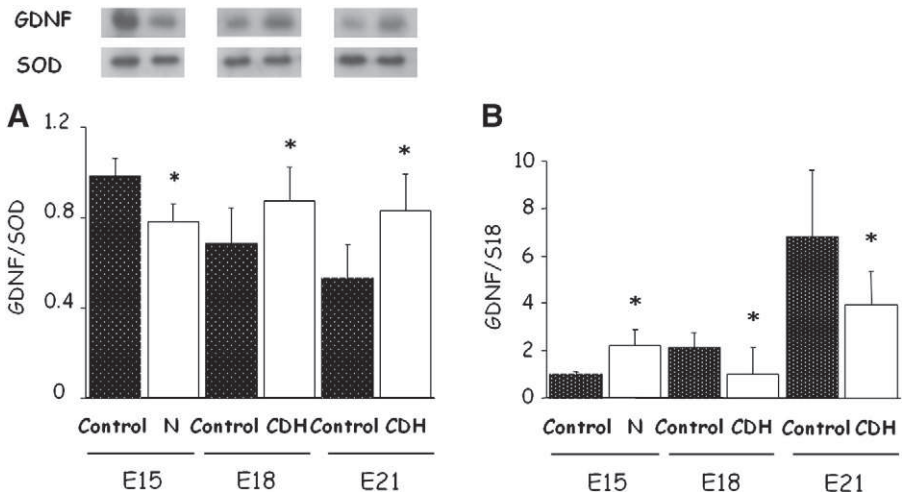

Fig. 4 A, The expression of GDNF protein (normalized to SOD) is decreased on E15 in embryos exposed to nitrofen, whereas it remains increased in CDH animals on E18 and E21 ($*P < .05$ versus control). B, The expression of GDNF mRNA is increased on E15 and decreased on E18 and E21 fetuses with CDH ($*P < .05$ versus control).

In previous studies [7,8], we found that tracheal neural tissue was deficient in animals exposed to nitrofen, probably because of delayed development, and, on the other hand, that the population of supporting glial cells was increased as a compensatory response to a neural damage. This led us to believe that also bronchopulmonary innervation might be abnormal in rats with CDH, and we investigated if a similar pattern could be found in infants with CDH. Some authors suggested that structural changes in distal airways could justify pulmonary symptoms without involvement of autonomic nerve abnormalities [3]. Because autonomic nerves control the bronchial smooth muscle tone and tracheobronchial reflexes in lower respiratory tract, we hypothesize that impaired innervation might contribute to explain the long-term pulmonary symptoms.

The neural crest origin of lung neural cells was elegantly demonstrated by using a quail-chick interspecies grafting [12] and confirmed also in our experiments by the positive staining to p75 antibody.

Abnormalities in bronchopulmonary innervation could be the consequence of delayed development with persistence of immature features and/or the result of neural damage. Moreover, a defective function of a neurotrophic factor may also play a role. To assess the first of these hypotheses, lung neural tissue was analyzed using the neural markers NF and PGP 9.5; the latter stains ganglionic precursors since the early phases of development [13], and for this reason, it was preferred for staining embryo-fetal rat material. The number of trunks per bronchus was significantly decreased after exposure to nitrofen on all endpoints selected. The findings in infants with CDH were quite similar, and the pattern in E21 rats resembled closely the human one. This pattern is consistent with the hypothesis of a delayed development and is similar to the one we previously described for tracheal innervation [7].

To test the hypothesis that a neural damage occurs, we used the S100 staining that unveils the supporting glial cells of pulmonary ganglia. The amount of these cells was clearly increased in animals exposed to nitrofen at all endpoints and also in the lungs of infants with CDH. Similar increases were interpreted as a compensation for deficient neural tissue [14]. The larger surface of S100 positive structures in lungs of animals and infants with CDH, in which the neural fibers are sparser, may be explained as a response to a neural damage. This finding resembled the pattern described in the trachea of rats with CDH [7].

We also studied the expression of RET, a receptor tyrosine kinase expressed by neural crest-derived cells during their migration and later required for maturation of the peripheral nervous system [15-17]. It has been demonstrated that RET expression is high in neural crest cells during migration and in neural crest-derived structures during embryogenesis, whereas it decreases in mature tissue [17]. The increased RET expression in lungs of infants with CDH in comparison with controls can be explained as a persistence of enteric neuron precursors in them, in contrast with controls in whom they were already differentiated. Unfortunately, for technical reasons, we were unable to analyze the expression of RET in rat lungs.

RET activation is responsive to the presence of GDNF, a molecule that guides the innervation in the developing lung, promoting survival, proliferation, and differentiation of enteric nervous system progenitors into neurons and glial cells [18,19]. In addition, GDNF acts as a chemoattractant of these progenitors being expressed by the mesenchyme before the entry of neural crest-derived cells [20,21], whereas the response of abovementioned cells to GDNF diminished in later stages of development [22,23]. The finding of persisting high levels of GDNF protein in preterm animals with CDH, like in earlier stages of development, is consistent with the hypothesis of a delayed development in which mechanisms of the immature period are maintained. In contrast, the GDNF mRNA is decreased in preterm rats with CDH and unable to compensate for the deficit of neural tissue found in the lungs of those animals.

In summary, our findings confirm that bronchopulmonary innervation is deficient in experimental and clinical CDH probably as a result of delayed development. This deficiency is compensated by a certain increase of the supporting glial tissue as an expression of repair of a damage of unknown mechanism. The fact that the lung ipsilateral and the contralateral to the hernia were equally affected further supports the concept of a primary developmental defect rather than the result of lung compression during development. The role of these anomalies that are, like other associated defects, of neural crest origin in chronic pulmonary disease of individuals with CDH remains to be determined.

References

[1] Hislop A, Reid L. Persistent hypoplasia of the lung after repair of congenital diaphragmatic hernia. Thorax 1976;31:450-5.
[2] Beals DA, Schloo BL, Vacanti JP, et al. Pulmonary growth and remodeling in infants with high-risk congenital diaphragmatic hernia. J Pediatr Surg 1992;27:997-1001.
[3] Ijsselstijn H, Tibboel D, Hop WJ, et al. Long-term pulmonary sequelae in children with congenital diaphragmatic hernia. Am J Respir Crit Care Med 1997;155:174-80.
[4] Marven SS, Smith CM, Claxton D, et al. Pulmonary function, exercise performance, and growth in survivors of congenital diaphragmatic hernia. Arch Dis Child 1998;78:137-42.
[5] Trachsel D, Selvadurai H, Bohn D, et al. Long-term pulmonary morbidity in survivors of congenital diaphragmatic hernia. Pediatr Pulmonol 2005;39:433-9.
[6] Wischermann A, Holschneider AM, Hubner U. Long-term follow-up of children with diaphragmatic hernia. Eur J Pediatr Surg 1995;5:13-8.
[7] Pederiva F, Aras Lopez R, Martinez L, et al. Abnormal development of tracheal innervation in rats with experimental diaphragmatic hernia. Pediatr Surg Int 2008;24:1341-6.
[8] Pederiva F, Aras Lopez R, Martinez L, et al. Tracheal innervation is abnormal in rats with experimental congenital diaphragmatic hernia. J Pediatr Surg 2009;44:1159-64.
[9] Muratore CS, Kharasch V, Lund DP, et al. Pulmonary morbidity in 100 survivors of congenital diaphragmatic hernia monitored in a multidisciplinary clinic. J Pediatr Surg 2001;36:133-40.

[10] Eber E. Adult outcome of congenital lower respiratory tract malformations. Swiss Med Wkly 2006;136:233-40.
[11] Kamata S, Usui N, Kamiyama M, et al. Long-term follow-up of patients with high-risk congenital diaphragmatic hernia. J Pediatr Surg 2005;40:1833-8.
[12] Burns AJ, Delalande JM. Neural crest cell origin for intrinsic ganglia of the developing chicken lung. Dev Biol 2005;277:63-79.
[13] Tollet J, Everett AW, Sparrow MP. Spatial and temporal distribution of nerves, ganglia, and smooth muscle during the early pseudoglandular stage of fetal mouse lung development. Dev Dyn 2001;221: 48-60.
[14] Boleken M, Demirbilek S, Kirimiloglu H, et al. Reduced neuronal innervation in the distal end of the proximal esophageal atretic segment in cases of esophageal atresia with distal tracheoesophageal fistula. World J Surg 2007;31:1512-7.
[15] Manie S, Santoro M, Fusco A, et al. The RET receptor: function in development and dysfunction in congenital malformation. Trends Genet 2001;17:580-9.
[16] Sebald M, Friedlich P, Burns C, et al. Risk of need for extracorporeal membrane oxygenation support in neonates with congenital diaphragmatic hernia treated with inhaled nitric oxide. J Perinatol 2004;24: 143-6.
[17] Pachnis V, Mankoo B, Costantini F. Expression of the c-ret proto-oncogene during mouse embryogenesis. Development 1993;119:1005-17.
[18] Trupp M, Ryden M, Jornvall H, et al. Peripheral expression and biological activities of GDNF, a new neurotrophic factor for avian and mammalian peripheral neurons. J Cell Biol 1995;130:137-48.
[19] Yamamoto M, Sobue G, Yamamoto K, et al. Expression of mRNAs for neurotrophic factors (NGF, BDNF, NT-3, and GDNF) and their receptors (p75NGFR, trkA, trkB, and trkC) in the adult human peripheral nervous system and nonneural tissues. Neurochem Res 1996;21:929-38.
[20] Natarajan D, Marcos-Gutierrez C, Pachnis V, et al. Requirement of signalling by receptor tyrosine kinase RET for the directed migration of enteric nervous system progenitor cells during mammalian embryogenesis. Development 2002;129:5151-60.
[21] Young HM, Hearn CJ, Farlie PG, et al. GDNF is a chemoattractant for enteric neural cells. Dev Biol 2001;229:503-16.
[22] Taraviras S, Marcos-Gutierrez CV, Durbec P, et al. Signalling by the RET receptor tyrosine kinase and its role in the development of the mammalian enteric nervous system. Development 1999;126:2785-97.
[23] Yu T, Scully S, Yu Y, et al. Expression of GDNF family receptor components during development: implications in the mechanisms of interaction. J Neurosci 1998;18:4684-96.

RETINOIC ACID RESCUES DEFICIENT AIRWAY INNERVATION AND PERISTALSIS OF HYPOPLASTIC RAT LUNG EXPLANTS.

Pederiva F, Martinez L, Tovar JA.

Neonatology 2012;101:132-9.

Original Paper

Neonatology

Neonatology 2012;101:132–139
DOI: 10.1159/000329613

Received: December 23, 2010
Accepted after revision: May 22, 2011
Published online: September 23, 2011

Retinoic Acid Rescues Deficient Airway Innervation and Peristalsis of Hypoplastic Rat Lung Explants

Federica Pederiva Leopoldo Martinez Juan A. Tovar

Department of Pediatric Surgery and Research Laboratory, Hospital Universitario La Paz, Madrid, Spain

Key Words
Diaphragmatic hernia · Intrinsic innervation · Nitrofen · Peristalsis · Lung hypoplasia · Retinoic acid

Abstract
Background: Bronchial peristalsis modulates lung growth and is deficient in hypoplastic nitrofen-exposed rat lung explants. Retinoic acid (RA) rescues lung hypoplasia. This study examines whether decreased bronchial innervation contributes to this developmental deficiency and if RA is able to recover bronchial innervation and motility. ***Material and Methods:*** After IRB approval, pregnant rats received either 100 mg nitrofen or vehicle on gestational day 9.5 (E9.5). Embryonic lung primordia harvested on E13 were cultured for 72 h and RA was added daily to the medium when appropriate. Lung growth was assessed by counting the number of terminal buds and measuring explant surface, total DNA and protein in control, control + RA, nitrofen and nitrofen + RA groups. Peristaltic contractions were recorded for 10 min under an inverted microscope. Lung explants stained for anti-protein gene product 9.5 (PGP 9.5) and smooth muscle α-actin were examined under a confocal microscope for depicting the specific relationship between neural and smooth muscle cells. PGP 9.5 and smooth muscle α-actin levels were quantified by Western blot analysis for assessing the neural and muscle cell expressions. Comparisons between groups were made with non-parametric tests. ***Results:*** The number of terminal buds, the explants' surface and the DNA and protein contents were significantly decreased in nitrofen-exposed lungs in comparison with controls. In contrast, these measurements were normal in explants exposed to both nitrofen and RA. Bronchial peristalsis (contractions/min) was significantly decreased in nitrofen-exposed lungs in comparison with controls; in contrast, in nitrofen + RA lungs it was similar to controls. In all study groups, the airways were surrounded by smooth muscle and ensheathed in a plexus of nerve fibers containing ganglia. PGP 9.5 protein levels were decreased in nitrofen-exposed lungs, but they normalized when RA was added. No differences were found in α-actin protein levels. Explants exposed only to RA were similar to control. ***Conclusions:*** Lung growth, bronchial innervation and peristalsis are decreased in nitrofen-exposed lung explants and are rescued by RA. If deficient airway innervation contributing to dysmotility and pulmonary hypoplasia can be pharmacologically rescued, new relatively simple prenatal interventions could be envisioned.

KARGER

Fax +41 61 306 12 34
E-Mail karger@karger.ch
www.karger.com

1661–7800/12/1012–0132$38.00/0

Accessible online at:
www.karger.com/neo

Prof. Dr. Juan A. Tovar
Department of Pediatric Surgery, Hospital Universitario La Paz
Paseo de la Castellana, 261
ES–28046 Madrid (Spain)
Tel. +34 91 727 70 19, E-Mail jatovar.hulp@salud.madrid.org

Introduction

Neural tissue and smooth muscle appear early in the developing fetal lung. As confocal microscopic studies have shown [1], the epithelial tubules are surrounded by smooth muscle and ensheathed in a network of newly-forming nerve plexus from embryogenesis onward and this spatial and temporal association persists into postnatal life. From early phases of lung development, the smooth muscle is functionally mature contracting in response to agonists such as acetylcholine and histamine, and to electric field stimulation. The latter response is blocked by atropine and tetrodotoxin, meaning that the airway smooth muscle is innervated by functional cholinergic nerves [2]. Moreover, spontaneous phasic contractions have been described in freshly excised first-trimester human [3] and pig lung [2], and in cultures of lung explants from fetal mouse [4]. Thus, there is evidence of strong neurogenic control of fetal airway smooth muscle.

It has been suggested that prenatal smooth muscle peristalsis has a pivotal role in modulating lung growth [5]. These phasic spontaneous contractions, different from the tonic smooth muscle activity in postnatal life [6], produce in the highly compliant developing lung a rhythmic mechanical stimulus that contributes to a normal airway branching and differentiation.

Bronchial peristalsis is deficient in hypoplastic nitrofen-exposed rat lung explants [5]. Moreover, we have demonstrated that tracheobronchial innervation is abnormal both in rat fetuses and newborns with CDH and lung hypoplasia [7–9].

Given these observations, we first postulated that abnormalities in bronchial innervation might contribute to explain the pulmonary developmental deficiency. The close relationship between innervation and lung growth led us to hypothesize that agents able to rescue lung hypoplasia in these animals, like retinoic acid (RA) that has been shown to have beneficial effects on CDH lungs [10–12], may also positively influence bronchial innervation and peristalsis.

Material and Methods

Adult Sprague-Dawley female rats were mated overnight. The finding of spermatozoids in the vaginal smear was considered as a mark of gestational day 0 (E0). Pregnant rats were then randomly divided into two groups. The animals in the experimental group intragastrically received 100 mg nitrofen dissolved in olive oil on E9.5 to induce fetal lung hypoplasia, whereas those in the control group received only vehicle. On E13, the rats were sedated with isoflurane and killed by intracardiac injection of potassium chloride. The embryos were recovered and the lung primordia were dissected free in Hank's buffer saline under a dissecting microscope. The Animal Care Committee approved all the animal experiments (license No. 32-06).

Organ Culture

Control and nitrofen-exposed lung explants were cultured on translucent polyester membrane transwell-clear inserts (Corning, Madrid, Spain) for 72 h at 37°C in 5% CO_2. Culture medium (DMEM/F12; Gibco, Barcelona, Spain) with 10% fetal bovine serum (Gibco), 100 IU/ml penicillin and 100 μg/ml streptomycin (Gibco) was changed every 24 h. Exogenous RA 1 μM (all-*trans*-retinoic acid; Sigma, Madrid, Spain) was diluted in ethanol and added daily to the culture medium at a final concentration of 0.4% [10]. The lungs were divided into four study groups: control (n = 20), nitrofen (n = 20), control + RA (n = 20), and nitrofen + RA (n = 20).

Lung Morphometry

Cultured lungs were photographed daily on an inverted microscope. The digitalized images of the last culture day were analyzed with the assistance of Image Pro-Plus™ version 5.0 processing software (Media Cybernetics, Washington, D.C., USA). The outline of the lung explant was contoured on the PC screen with the cursor and the resulting surface was integrated by the software. In the same images the terminal lung buds were counted on each explant.

Motility

At 72 h of culture, airway peristaltic contractions were recorded for 10 min under an inverted microscope with LAS-AF software (TCS SP5; Leica, Barcelona, Spain) and their frequency was expressed as number per minute.

Quantification of DNA and Protein Content

After 72 h of culture, the lung explants were snap-frozen and stored at –80°C. In half of them, DNA was extracted using QIAamp DNA Micro Kit (Qiagen, Barcelona, Spain) and the total DNA content was measured with a spectrophotometer. The remaining explants were homogenized in cell disruption buffer (Protein Isolation System Paris™; Ambion, Madrid, Spain) and the protein content was assessed using a BCA protein assay kit (Pierce, Madrid, Spain). Each value is the average of three measurements.

Immunohistochemistry

After detaching the cultured lungs from the membranes, they were fixed in 4% paraformaldehyde overnight and subsequently rinsed in phosphate-buffered saline (PBS). Non-specific binding was blocked by washing them in PBS with 1% bovine serum albumin, before incubating them with the primary antibodies overnight. A rabbit polyclonal antibody against protein gene product 9.5 (PGP 9.5; 1:500; Dako Cytomation, Glostrup, Denmark) was used to stain the neural tissue, whereas the smooth muscle was identified with a mouse monoclonal anti-α-actin fluorochrome-labeled antibody (anti-actin, α-smooth muscle-Cy3™ antibody; 1:1,000; Sigma-Aldrich, St. Louis, Mo., USA). After being washed with PBS, the samples were incubated at room temperature for 1 h with the fluorochrome-labeled anti-rabbit secondary anti-

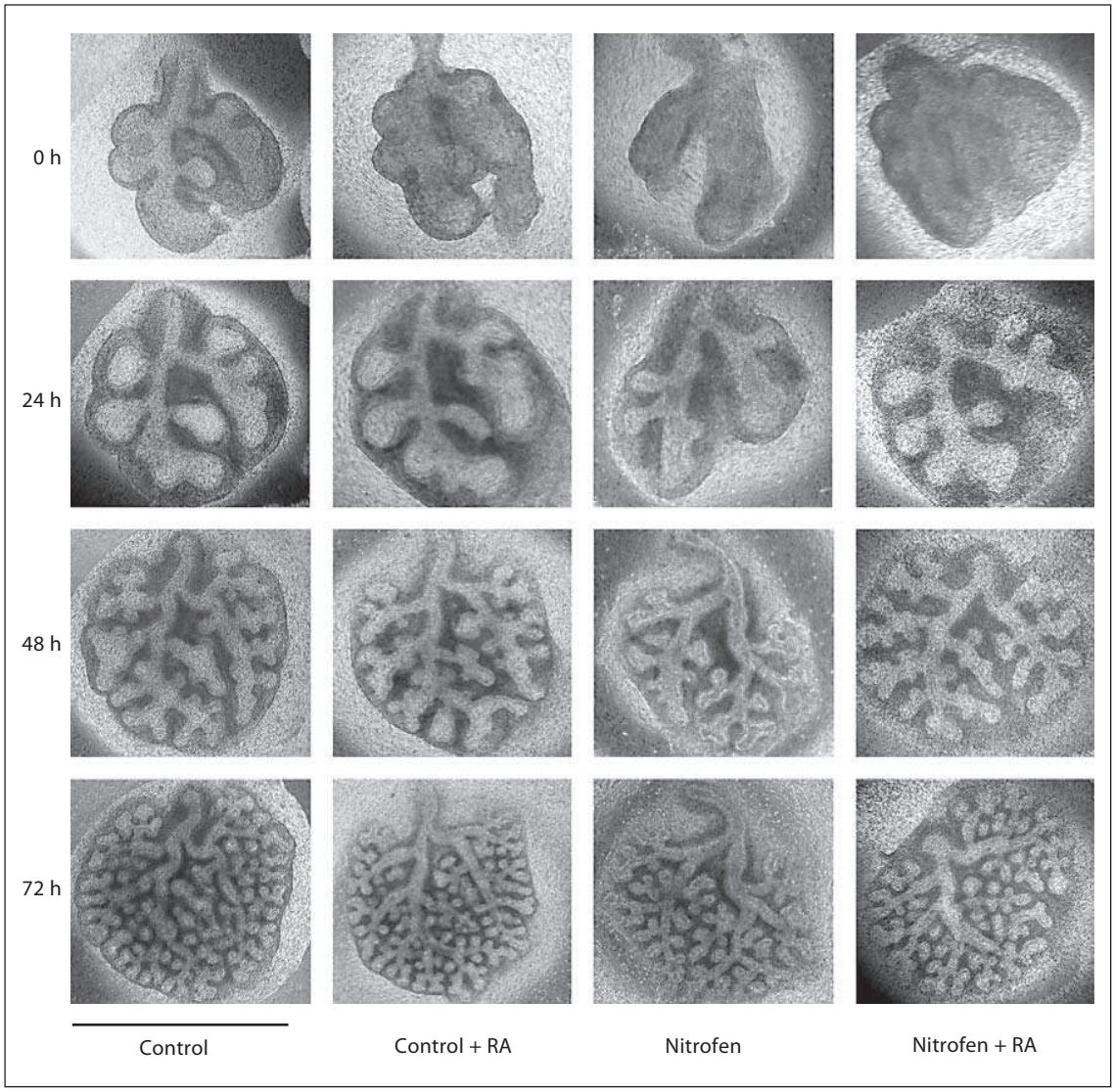

Fig. 1. Photographs of embryonic lung explants taken at the beginning of the culture and at 24, 48 and 72 h. RA rescued growth of nitrofen-exposed lung explant (fourth column). Control explant was not affected by retinoic acid (second column). Scale bar: 1 mm.

body (Alexa Fluor® 488; 1:500; Molecular Probes, Eugene, Oreg., USA). After further washing with PBS, the specimens were then mounted into glycerol on a glass slide. As a control, the primary antibody was omitted with no staining above background as the expected result.

Confocal Microscopy

Fluorescent images of the nerves and smooth muscle in the double-stained whole-mount preparations were obtained using a confocal laser scanning microscope with LAS-AF software (TCS SP5; Leica). The fluorescent markers were detected by a krypton/argon laser with excitation wavelengths of 488 nm for Alexa 488 and 561 nm for Cy3. The whole mounts were optically sectioned by scanning at increasing depths of focus in steps of 5 μm. After double staining, the green and the red images were captured separately, colorized and merged to show a composite nerve/smooth muscle image. The specific staining of neural structures by anti-PGP 9.5 antibody and of smooth muscle by anti-α-actin was assessed in each lung explant of the four study groups.

Immunoblotting

To quantify the levels of PGP 9.5 and α-actin proteins, six lungs from each group were pooled and homogenized in cell disruption buffer (Protein Isolation System Paris, Ambion). The protein content was assessed using a BCA protein assay kit (Pierce). Western blotting was performed with 18% SDS-polyacrylamide

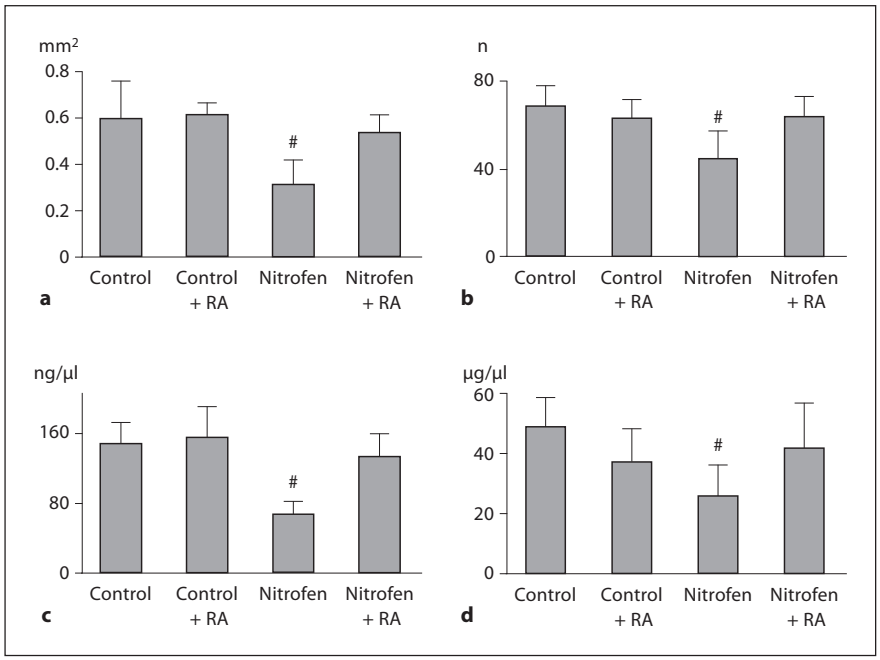

Fig. 2. Growth parameters analyzed in lung explants after 72 h of culture. The lung surface (**a**), the number of terminal buds (**b**), the total DNA content (**c**) and the protein content (**d**) were decreased in nitrofen-exposed lungs and restored to control values by RA. # $p < 0.05$ vs. control.

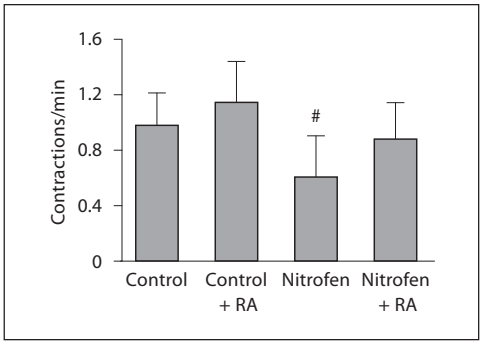

Fig. 3. Number of contractions per minute in control, control + RA, nitrofen and nitrofen + RA lung explants after 72 h of culture. The peristalsis was decreased in nitrofen-exposed explants and rescued by RA. # $p < 0.05$ vs. control. Three videos of airway peristalsis (control [E1], nitrofen [E2] and nitrofen + RA [E3] lung explants) from our work are viewable on the web (online suppl. videos 1–3, www.karger.com/doi/10.1159/000329613).

gel. Anti-PGP 9.5 (1:6,000; rabbit polyclonal PGP 9.5; Dako) and α-actin (1:6,000; mouse monoclonal α-actin; Sigma) antibodies were used and the values were normalized to superoxide dismutase (SOD).

Statistical Methods

The results were expressed as percentages or as means ± SD and the groups were compared by non-parametric Mann-Whitney tests with a threshold of significance at $p < 0.05$.

Results

As expected, the surface and the number of terminal buds of nitrofen-exposed lung explants were significantly decreased in comparison with the controls and the values were normal in those in which RA was added. In contrast, no changes were noticed when RA was added to control lungs (fig. 1, 2a, b).

In parallel, cell mass of the explants estimated by DNA and protein contents was significantly decreased in nitrofen-exposed explants when comparing them to the controls. Again, both parameters were normal if RA was added to the nitrofen-exposed explants and no changes were induced by this agent in controls (fig. 2c, d).

Bronchial peristalsis was significantly decreased in nitrofen-exposed explants in comparison with controls; in contrast, in nitrofen + RA lungs it was similar to controls. There was no difference between control and control + RA lungs (fig. 3).

In all study groups the epithelium of the airways was surrounded by smooth muscle fibers, arranged in a cylindrical pattern, that were in turn ensheathed in a plexus of nerve fibers containing ganglia. The neural plexus covering the airway wall gave rise to smaller bundles that grew into the layer of α-actin-positive cells. No gross change in the density of these structures could be seen in any of the groups (fig. 4).

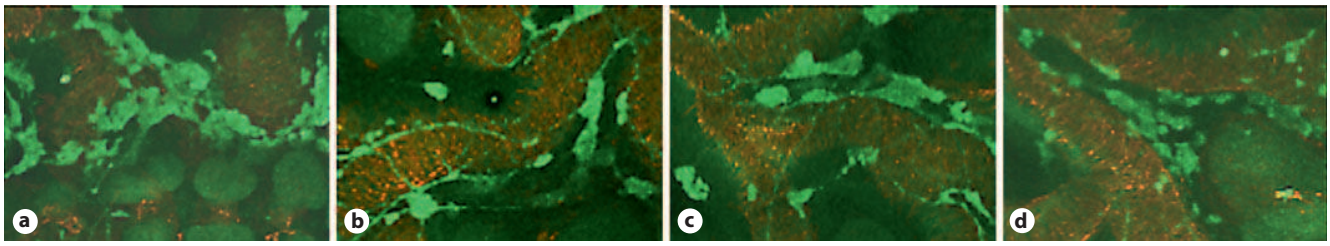

Fig. 4. Confocal projections of control (**a**), control + RA (**b**), nitrofen (**c**) and nitrofen + RA (**d**) lung explants after 72 h of culture. The α-actin-positive muscle cells (red; colors refer to the online version only) formed a cylindrical layer around the airway wall lying perpendicularly to its long axis. PGP 9.5-positive neural tissue (green) invested the epithelial tubules forming a network of ganglia interconnected by nerve trunks. Fine bundles descended toward the airway smooth muscle in all lungs.

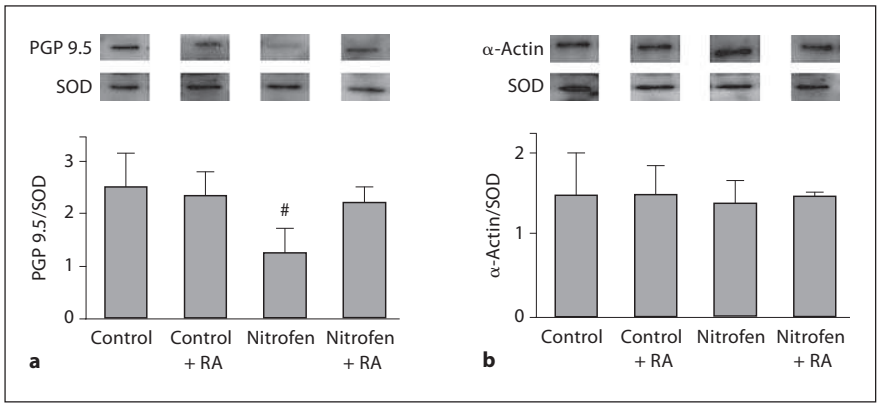

Fig. 5. a PGP 9.5 protein level normalized to SOD in all groups. The expression of PGP 9.5 was decreased in nitrofen-exposed explants. # $p < 0.05$ vs. control. The expression normalized adding RA. **b** α-Actin protein expression normalized to SOD. No differences were seen in the levels of the protein in the four study groups.

Immunoblotting

However, the PGP 9.5 protein signals seen at 20–25 kDa were significantly decreased only in the nitrofen-exposed explants that reverted to normal if RA was added (fig. 5a). As regards α-actin, the signals were seen at 40–45 kDa and no differences in the protein expression among groups could be found (fig. 5b).

Discussion

From early stages in gestation, the growing airways are surrounded by a layer of smooth muscle cells arranged cylindrically around the epithelial tubules, but also by a nerve plexus comprising nerve trunks and ganglia, with fine bundles innervating the smooth muscle [1]. Shortly after differentiation, the smooth muscle is able to respond strongly to agonists and to electrical field stimulation. At the same time, the airway narrowing in response to neural stimulation is blocked by atropine and tetrodotoxin, indicating that functional cholinergic nerves are present [2]. Moreover, spontaneous intermittent narrowing of the bronchi has been observed both in vivo and in vitro [4]. The spontaneous contractions moved the lung liquid backward and forward along the airway lumen generating a positive pressure in the tubules that is considered a mechanical prerequisite for lung growth. When lung liquid is drained and hence the pressure is decreased, the lung becomes hypoplastic; in contrast, tracheal occlusion increases the pressure and enhances lung growth. It has been observed that spontaneous contractions of the airways are unaffected by either atropine or tetrodotoxin [4]. The first finding indicates that neural activity is not essential, the latter shows that endogenous acetylcholine is not involved. In addition, this rhythmic mechanical activity ceases in the presence of calcium antagonists. The authors concluded that spontaneous contractions are therefore of likely myogenic origin [4]. Hence, it has been supposed that the role fulfilled by neural tissue in early gestation is not neurotransmission, but rather secretion of trophic factors for

the smooth muscle that indirectly contributes to lung development [1, 2, 4]. Positive immunostaining for neurotransmitters, like choline acetyltransferase, calcitonin gene-related peptide [13], nitric oxide synthase, vasoactive intestinal peptide and substance P, can be seen in the varicosities of the nerve fibers lying on smooth muscle cells later in gestation, by the end of pseudoglandular and during canalicular stage [1, 14]. The same authors [1, 4, 14] proposed the idea that the spontaneous contractions produce a rhythmic mechanical stimulus across the airway wall and the adjacent parenchyma that contributes to normal airway differentiation and branching by inducing expression of growth factors. Neurotrophic factors, like neurturin, a member of the GDNF family, and GDNF, have been isolated in airway smooth muscle cells or in the associated mesenchymal cells [15, 16].

The picture that emerges is that airway smooth muscle and neural tissue are an integral part of the lung from the onset of its development and that they exist in a dynamic relationship throughout gestation; hence, abnormalities in one part or in the other one might contribute to explain lung developmental deficiencies. The possible contribution of other excitatory mechanisms to airway peristalsis has been considered. Whereas the lung and the foregut have a common embryological origin [17], it has been supposed that spontaneous airway contractions resemble the gut peristalsis that requires c-kit-positive interstitial cells of Cajal (ICC) [18]. Hence, the presence of pacemaker cells in the lung was investigated by some authors, but the ICC were not found [19]. However, more recent research supports their involvement in tracheobronchial muscle contractility [20]. On the other hand, other authors have demonstrated that spontaneous peristalsis within the explanted esophagi was not ICC-dependent, as the contractile behavior persisted even when ICC were inhibited [21].

Congenital diaphragmatic hernia is a human malformation that causes high mortality in newborns because of severe respiratory failure secondary to pulmonary hypoplasia. This condition can be reproduced in rat pups by administrating the herbicide nitrofen (2,4-dichlorophenyl-*p*-nitrophenyl ether) to pregnant rats; lung hypoplasia can be found in all pups and congenital diaphragmatic hernia in most of them. An in vitro lung culture model [4, 15] has proved to be a useful tool to investigate lung development and has the advantage that lung's environment can be modified by altering the composition of the medium. Using this model, it has been demonstrated that bronchial peristalsis is deficient in hypoplastic nitrofen-exposed lung explants [5].

Given the close relationship between smooth muscle and neural tissue during development, we first hypothesized that abnormalities in embryonic bronchial innervation might also contribute to lung hypoplasia. We previously demonstrated that tracheobronchial innervation is deficient in hypoplastic nitrofen-exposed rat lungs in terms of decrease of the neural components; moreover, the expression of the neurotrophic factor GDNF was impaired in the same lungs. The decrease of neural tissue was seen early (E15) and late (E21) in rat gestation and the final pattern resembled closely that of babies with CDH. On the other hand, the amount of S-100-positive supporting glial cells of pulmonary ganglia was increased in lungs of animals exposed to nitrofen both early and late in gestation and also in babies with CDH [7–9]. Recently, it was shown that innervation is required for epithelial progenitor cell function during organogenesis, because removal of the parasympathetic submandibular ganglion before the homonymous gland developed in mice, impaired its development reducing the number of epithelial buds by weakening the expression of progenitor cells. The same coordinated development of the peripheral nervous system and a branched epithelium organ is likely in the lung. Basal progenitor cells express the nerve growth factor receptor, whose function to date has not been clarified [22, 23].

In the present study, we could demonstrate that in the nitrofen-exposed lung explants in which the frequency of peristaltic waves was decreased, the levels of PGP 9.5 were decreased as well. PGP 9.5 is a pan-neuronal marker that unveils ganglionic precursors since early phases of development [15]. Its decrease might cause an impairment in the signaling between nerves and airway smooth muscle, contributing to the hypoplasia of the lung.

The second hypothesis was that agents able to rescue pulmonary hypoplasia, like RA [10–12], might also improve bronchial innervation and peristalsis.

Despite evidence linking retinoids with CDH dating back more than 50 years, it is only lately that they have been related to the pathogenesis of pulmonary hypoplasia associated with CDH [10, 11, 24, 25]. The plasma concentration of retinol and of retinol-binding protein has been found decreased in newborns with CDH in comparison with controls. Those values were independent of maternal retinol status that was similar to controls for some authors [26], while higher than controls for others [27]. These findings supported the idea that human CDH is linked to abnormal retinoid homeostasis. It has been demonstrated that exogenous RA is able to increase the size of hypoplastic lung explants [10, 24]. Moreover, RA

induces FGF-10 expression in the foregut region where the lung forms [28]. Thus, since FGF-10 governs the directional outgrowth of lung bud during branching morphogenesis [29], RA signaling may connect formation of the laryngotracheal groove with activation of FGF-10-dependent bronchial morphogenesis [30]. FGF-10 is produced by airway smooth muscle progenitors and is required for their entry into the smooth muscle cell lineage [31].

In our experiments, RA not only significantly increased lung growth in nitrofen-exposed lung explants, as previously demonstrated [10], but it restored the hypoplastic lungs to the size, the number of terminal buds and the DNA and protein content of the control lungs. The frequency of peristaltic waves, that was decreased in nitrofen-exposed lungs, normalized adding RA to the medium. The improvement of airway peristalsis obtained with RA was not related to smooth muscle hypertrophy, because the expression of smooth muscle-specific marker α-actin was not increased in RA-treated groups. On the other hand, the levels of the pan-neuronal protein PGP 9.5 decreased in nitrofen-exposed lung explants were restored by RA. RA signaling has been found to play a role in neurite outgrowth both in vitro and in vivo [32].

This study demonstrated for the first time that bronchial neural tissue is deficient in nitrofen-exposed lung explants and that it is rescued, together with airway peristalsis and lung growth, by RA, suggesting that not only smooth muscle and peristalsis, but also bronchial neural tissue might contribute to lung development.

Studies like the present one, based on teratogenic animal models of malformations, may be criticized because it is not known whether the anomalies found are due to the direct effects of the chemical used or to the malformation induced by it. However, since its first description, the nitrofen rat model of CDH has evolved into a well-established one that faithfully reproduces the phenotypic features of the human condition including skeletal [33], cardiovascular [34] and lung malformations [9] as well as anomalies of the esophageal innervation [35, 36] suitable for research into this particular condition. It is therefore likely that the findings of the present study could also be present in human CDH patients, opening a new possible field of prenatal intervention for fetuses with CDH and lung hypoplasia.

Acknowledgements

Supported in part by FIS (06/0486 and 06/0447), IdiPAZ and FMM Grants and by the Spanish Health Institute Carlos III (grant No. RD08/0072: Maternal, Child Health and Development Network).

References

1 Sparrow MP, Weichselbaum M, McCray PB: Development of the innervation and airway smooth muscle in human fetal lung. Am J Respir Cell Mol Biol 1999;20:550–560.
2 Sparrow MP, Warwick SP, Everett AW: Innervation and function of the distal airways in the developing bronchial tree of fetal pig lung. Am J Respir Cell Mol Biol 1995;13:518–525.
3 McCray PB Jr: Spontaneous contractility of human fetal airway smooth muscle. Am J Respir Cell Mol Biol 1993;8:573–580.
4 Schittny JC, Miserocchi G, Sparrow MP: Spontaneous peristaltic airway contractions propel lung liquid through the bronchial tree of intact and fetal lung explants. Am J Respir Cell Mol Biol 2000;23:11–18.
5 Jesudason EC, Smith NP, Connell MG, et al: Peristalsis of airway smooth muscle is developmentally regulated and uncoupled from hypoplastic lung growth. Am J Physiol Lung Cell Mol Physiol 2006;291:L559–L565.
6 Somlyo AP, Somlyo AV: Signal transduction and regulation in smooth muscle. Nature 1994;372:231–236.
7 Pederiva F, Lopez RA, Martinez L, et al: Tracheal innervation is abnormal in rats with experimental congenital diaphragmatic hernia. J Pediatr Surg 2009;44:1159–1164.
8 Pederiva F, Aras Lopez R, Martinez L, et al: Abnormal development of tracheal innervation in rats with experimental diaphragmatic hernia. Pediatr Surg Int 2008;24:1341–1346.
9 Pederiva F, Lopez RA, Rodriguez JI, et al: Bronchopulmonary innervation defects in infants and rats with congenital diaphragmatic hernia. J Pediatr Surg 2010;45:360–365.
10 Montedonico S, Nakazawa N, Puri P: Retinoic acid rescues lung hypoplasia in nitrofen-induced hypoplastic foetal rat lung explants. Pediatr Surg Int 2006;22:2–8.
11 Babiuk RP, Thebaud B, Greer JJ: Reductions in the incidence of nitrofen-induced diaphragmatic hernia by vitamin A and retinoic acid. Am J Physiol Lung Cell Mol Physiol 2004;286:L970–L973.
12 Thebaud B, Tibboel D, Rambaud C, et al: Vitamin A decreases the incidence and severity of nitrofen-induced congenital diaphragmatic hernia in rats. Am J Physiol 1999;277:L423–L429.
13 Cadieux A, Springall DR, Mulderry PK, et al: Occurrence, distribution and ontogeny of CGRP immunoreactivity in the rat lower respiratory tract: effect of capsaicin treatment and surgical denervations. Neuroscience 1986;19:605–627.
14 Sparrow MP, Lamb JP: Ontogeny of airway smooth muscle: structure, innervation, myogenesis and function in the fetal lung. Respir Physiol Neurobiol 2003;137:361–372.
15 Tollet J, Everett AW, Sparrow MP: Development of neural tissue and airway smooth muscle in fetal mouse lung explants: a role for glial-derived neurotrophic factor in lung innervation. Am J Respir Cell Mol Biol 2002;26:420–429.

16 Widenfalk J, Nosrat C, Tomac A, et al: Neurturin and glial cell line-derived neurotrophic factor receptor-β (GDNFR-β), novel proteins related to GDNF and GDNFR-α with specific cellular patterns of expression suggesting roles in the developing and adult nervous system and in peripheral organs. J Neurosci 1997;17:8506–8519.
17 Spooner BS, Wessells NK: Mammalian lung development: interactions in primordium formation and bronchial morphogenesis. J Exp Zool 1970;175:445–454.
18 Huizinga JD, Robinson TL, Thomsen L: The search for the origin of rhythmicity in intestinal contraction; from tissue to single cells. Neurogastroenterol Motil 2000;12:3–9.
19 Jesudason EC, Smith NP, Connell MG, et al: Developing rat lung has a sided pacemaker region for morphogenesis-related airway peristalsis. Am J Respir Cell Mol Biol 2005; 32:118–127.
20 Shinkai T, Shinkai M, Pirker MA, et al: Spatial and temporal patterns of c-kit positive cells in embryonic lungs. Pediatr Surg Int 2011;27:181–185.
21 Rishniw M, Fisher PJ, Doran RM, et al: Striated myogenesis and peristalsis in the fetal murine esophagus occur without cell migration or interstitial cells of Cajal. Cells Tissues Organs 2009;189:410–419.
22 Knox SM, Lombaert IM, Reed X, et al: Parasympathetic innervation maintains epithelial progenitor cells during salivary organogenesis. Science 2010;329:1645–1647.
23 Rock JR, Hogan BL: Developmental biology. Branching takes nerve. Science 2010;329: 1610–1611.
24 Nakazawa N, Montedonico S, Takayasu H, et al: Disturbance of retinol transportation causes nitrofen-induced hypoplastic lung. J Pediatr Surg 2007;42:345–349.
25 Noble BR, Babiuk RP, Clugston RD, et al: Mechanisms of action of the congenital diaphragmatic hernia-inducing teratogen nitrofen. Am J Physiol Lung Cell Mol Physiol 2007;293:L1079–L1087.
26 Beurskens LW, Tibboel D, Lindemans J, et al: Retinol status of newborn infants is associated with congenital diaphragmatic hernia. Pediatrics 2010;126:712–720.
27 Major D, Cadenas M, Fournier L, et al: Retinol status of newborn infants with congenital diaphragmatic hernia. Pediatr Surg Int 1998;13:547–549.
28 Desai TJ, Malpel S, Flentke GR, et al: Retinoic acid selectively regulates Fgf10 expression and maintains cell identity in the prospective lung field of the developing foregut. Dev Biol 2004;273:402–415.
29 Bellusci S, Grindley J, Emoto H, et al: Fibroblast growth factor 10 and branching morphogenesis in the embryonic mouse lung. Development 1997;124:4867–4878.
30 Warburton D, Bellusci S, De Langhe S, et al: Molecular mechanisms of early lung specification and branching morphogenesis. Pediatr Res 2005;57:26R–37R.
31 Mailleux AA, Kelly R, Veltmaat JM, et al: Fgf10 expression identifies parabronchial smooth muscle cell progenitors and is required for their entry into the smooth muscle cell lineage. Development 2005;132:2157–2166.
32 So PL, Yip PK, Bunting S, et al: Interactions between retinoic acid, nerve growth factor and sonic hedgehog signalling pathways in neurite outgrowth. Dev Biol 2006;298:167–175.
33 Migliazza L, Xia H, Diez-Pardo JA, et al: Skeletal malformations associated with congenital diaphragmatic hernia: experimental and human studies. J Pediatr Surg 1999;34: 1624–1629.
34 Migliazza L, Otten C, Xia H, et al: Cardiovascular malformations in congenital diaphragmatic hernia: human and experimental studies. J Pediatr Surg 1999;34:1352–1358.
35 Pederiva F, Rodriguez JI, Ruiz-Bravo E, Martinez L, Tovar JA: Abnormal intrinsic esophageal innervation in congenital diaphragmatic hernia: a likely cause of motor dysfunction. J Paediatr Surg 2009;44:496–499.
36 Martinez L, Pederiva F, Martinez-Calonge W, et al: The myenteric plexus of the esophagus is abnormal in an experimental congenital diaphragmatic hernia model. Eur J Pediatr Surg 2009;19:163–167.

AMNIOTIC FLUID STEM CELLS RESCUE BOTH *IN VITRO* AND *IN VIVO* GROWTH, INNERVATION AND MOTILITY IN NITROFEN-EXPOSED HYPOPLASTIC RAT LUNGS THROUGH PARACRINE EFFECTS.

Pederiva F, Ghionzoli M, Pierro A, De Coppi P and Tovar JA.

Cell Transplant

Amniotic Fluid Stem Cells Rescue Both *In Vitro* And *In Vivo* Growth, Innervation And Motility In Nitrofen-Exposed Hypoplastic Rat Lungs Through Paracrine Effects.

Pederiva F[1], Ghionzoli M[2], Pierro A[2], De Coppi P[2*] and Tovar JA[1*]

Department of Pediatric Surgery and Research Laboratory ([1]),

Hospital Universitario La Paz, Madrid, Spain

Surgery Unit, UCL Institute of Child Health and Great Ormond Street Hospital for Children ([2]),

London, United Kingdom

[*] These authors equally contributed to the study

Supported in part by FIS (06/0486) and FMM Grants and by the Spanish Health Institute Carlos III (grant N. RD08/0072: Maternal, Child Health and Development Network) and De Coppi P. is supported by the Great Ormond Street Hospital Charity, London UK.

Address correspondence to:
Dr. Pederiva Federica
Department of Pediatric Surgery
Hospital Universitario "La Paz"
Paseo de la Castellana, 261, 28046, Madrid, Spain
E-mail: federica_pederiva@yahoo.it

ABSTRACT

Background: Lung hypoplasia can be prevented in vitro by retinoic acid (RA). Recent evidence suggests that amniotic fluid stem (AFS) cells may integrate injured lungs and influence their recovery. We tests the hypothesis that AFS cells might improve lung growth and motility by paracrine mechanisms.

Material and methods: Pregnant rats received either nitrofen or vehicle on E9.5. ***In vitro*** E13 embryonic lungs were cultured in presence of culture medium alone or with RA, basophils or AFS cells. ***In vivo*** GFP+rat-AFS-cells were transplanted in nitrofen-exposed rats on E10.5. E13 lung explants were cultured before analysis. The surface, the number of terminal buds and the frequency of bronchial contractions were assessed. PGP 9.5 and α-actin protein levels were measured. The lung explants transplanted with AFS cells were stained for α-actin, PGP9.5 and TTF-1. FGF10, VEGFα, and TGFβ1 levels secreted by the AFS cells in the culture medium were measured. Comparison between groups was made by Anova tests.

Results: ***In vitro*** The surface, the number of terminal buds and the bronchial peristalsis were increased in nitrofen+AFS-cells explants in comparison with nitrofen-exposed lungs. While nitrofen+RA lungs were similar to nitrofen+AFS ones, basophils did not normalize these measurements. PGP9.5 protein was decreased in nitrofen lungs, but after adding AFS cells, the value was similar to controls. No differences were found in the expression of α-actin. ***In vivo*** Surface, number of terminal buds and peristalsis were similar to control after injection of AFS cells in nitrofen-exposed rats. Colocalization with TTF-1-positive cells was found. The levels of FGF10 and VEGFα were increased in nitrofen+AFS-cells explants setting, while the levels of TGFβ1 were similar to controls.

Conclusions: Lung growth, bronchial motility and innervation are decreased in nitrofen explants and rescued by AFS cells both *in vitro* and *in vivo,* similarly to what observed before with RA. AFS cells beneficial effect was probably related to paracrine action of growth factors secretion.

Key Words: Diaphragmatic hernia, amniotic fluid stem cells, intrinsic innervation, Nitrofen, peristalsis, lung hypoplasia, retinoic acid.

INTRODUCTION

Severe pulmonary hypoplasia contributes significantly to the mortality and morbidity in newborns with congenital diaphragmatic hernia (CDH). Despite the improvements in neonatal resuscitation and intensive care, the mortality rate of CDH is still high and most of the newer treatment modalities have replaced mortality for a higher morbidity. Long-term pulmonary sequelae are frequently described in survivors of CDH and depend on the severity of lung hypoplasia and the degree of lung injury (16,21,30,33,40,42,43).

Since the first description of nitrofen-induced diaphragmatic hernia in rodents by Iritani (17), this experimental model has been extensively studied and has become a widely accepted model which closely replicates many features of the human condition (15,22). Different treatment modalities have been tried in the experimental model of CDH in an attempt to modulate prenatally the natural course of the malformation. Among those, retinoic acid (RA) has been demonstrated to prevent pulmonary hypoplasia *in vitro*, to stimulate alveologenesis and to accelerate alveolar cell proliferation in hypoplastic lungs (25-27,35). However, limitations on the clinical use of RA, which is known to be teratogenic (8,41), provide an opportunity to explore alternative procedures for the rescue of this devastating disease.

Stem cell-based therapies are promising new treatment approaches for a large number of diseases. Recently, it has been reported that amniotic fluid-derived stem (AFS) cells can be isolated from human and rodent amniotic fluid. AFS cells are broadly multipotent cells, able to differentiate into lineages belonging to all three embryonic germ layers (10). Moreover, they can also engraft in irradiated bone marrow and give rise to all hematopoietic lineages (13). Finally, they can functionally contribute to the regeneration of various tissues and organs when transplanted in models of disease. Remarkable results have been obtained in injured kidneys, heart and lungs (3,31,47). The latter have been explored both in models of diseases and during development and AFS cells have shown the potential not only to engraft and differentiate in specialised

pneumocytes but also to contribute and supplement endogenous lung repair mechanisms (7).

The aim of this study was to test the hypothesis that AFS cells could rescue lung growth and motility both *in vitro* and *in vivo* and to look further inside the mechanism of action of AFS cells.

MATERIAL AND METHODS

Adult Sprague-Dawley female rats (Harlan Laboratories, Barcelona, Spain) were mated overnight. The finding of spermatozoids in the vaginal smear was considered as a mark of gestational day 0 (E0). Pregnant rats were then randomly divided into two groups. The animals in the experimental group received intragastrically 100 mg of nitrofen dissolved in olive oil on E9.5 to induce fetal lung hypoplasia, whereas those in the control group received only vehicle.

In vitro On E13, the rats were sedated with isofluorane and killed by intracardiac injection of potassium-chloride. The embryos were recovered (**Figure 1**) and the lung primordia were dissected free in Hank's buffer saline (HBSS) under a dissecting microscope.

In vivo On E10.5 a laparotomy was performed and, after exposure of the uterus, $1x10^5$-10^6 GFP+ rat-AFS cells, previously trypsinized, were injected into amniotic fluid of nitrofen-exposed and control rats. On E13, as described above, the rats were sacrificed, the embryos recovered and the lung primordia were freed carefully from the heart and the esophagus (**Figure 1**).

The Animal Care committee approved all the animal experiments (license number: 32-06).

COLLECTION AND CHARACTERIZATION OF THE RAT AFS CELLS: samples of rat amniotic fluid were collected from transgenic GFP-positive pregnant Sprague-Dawley rats on E16 and GFP-rAFS cells were isolated and cultured, as prevoiusly described (4,10,13).

GFP-rAFS cells characterization was carried out with the following primary antibodies: anti-Oct 3/4 (mouse monoclonal, Santa Cruz Biotechnologies®, CA, 1:50), anti-CD45 (rabbit polyclonal, Abcam®, London, UK, 1:100), anti-CD34 (rabbit polyclonal, Abcam®, London, UK, 1:150), anti-pan cytokeratin (mouse monoclonal Abcam®, London, UK, 1:300), anti-vimentin (mouse monoclonal Abcam®, London, UK, 1:1000) and anti-alpha smooth muscle actin (αSMA mouse monoclonal Abcam®, London, UK, 1:100). Cover glass seeded with 2000 cells/cm^2 were rinsed in phosphate buffered saline (PBS) and fixed in 4% paraformaldehyde for 20 minutes. Cells were permeabilized with a 0.5% Triton X-100 solution, rinsed in PBS with 3% bovine-serum albumin to block nonspecific binding and incubated with primary antibodies for 1 hour at room temperature. After being washed with PBS, the samples were incubated at room temperature for 1 hour with the fluorochrome-labeled anti-mouse and anti-rabbit secondary antibodies (Alexa Fluor® 594; 1:150; Molecular Probes, Invitrogen, London, UK). After further washing with PBS, the specimens were then mounted into fluorescent medium with DAPI (1.5 μg/ml) on a polylysine slide (ThermoScientific, London, UK) and observed under epifluorescence microscope (ZEISS Axiophot).

Cell count were blindly evaluated for each stained slide over three low magnification fields (x10) and reported in the chart as percentage.

ORGAN CULTURE: ***In vitro*** The lung explants were divided into eight study groups: control (n=8), nitrofen (n=12), control + RA (n=8), nitrofen + RA (n=12), control + basophils (n=8), nitrofen + basophils (n=12), control + AFS cells (n=8), nitrofen + AFS cells (n=12).

Control and nitrofen-exposed lung explants were cultured on translucent membrane inserts (polyester membrane transwell-clear inserts, pore size: 3 μm, Corning, Madrid, Spain) for 72 hours at 37°C in 5% CO_2. Culture medium (D-MEM/F12, Gibco, Barcelona, Spain) with 10% fetal bovine serum (Gibco, Barcelona, Spain), 100 IU/ml penicillin and 100 μg/ml streptomycin (Gibco, Barcelona, Spain) was added until the lungs were lying on the air-medium surface and changed every 24 hours.

When lung explants were co-cultured in presence of RA, exogenous RA 1 µM (all-*trans*-retinoic acid, Sigma, Madrid, Spain) was diluted in ethanol and added daily to the culture medium at a final concentration of 0.4% (25).

When basophils needed to be added, the day before recovering the embryos, rat RBL 2H3 were trypsinized and 5000 cells/cm^2 were cultured on culture dishes (12 well culture dish, Corning, Madrid, Spain) in D-MEM medium (D-MEM/F12, Gibco, Barcelona, Spain) with 10% fetal bovine serum (Gibco, Barcelona, Spain), 100 IU/ml penicillin and 100 µg/ml streptomycin (Gibco, Barcelona, Spain).

When lung expants were co-cultured in presence of AFS cells, the day before harvesting the embryos, rat AFS cells were trypsinized and 5000 cells/cm^2 were cultured on culture dishes (12 well culture dish, Corning, Madrid, Spain) in α-MEM medium containing 15% ES-FBS, 1% glutamine, 1% penicillin/streptomycin (Gibco, Barcelona, Spain) supplemented with 18% Chang B and 2% Chang C (Irvine Scientific, Santa Ana, California) at 37°C with 5% CO_2 atmosphere (10). Before placing the inserts on the culture dishes, the medium was removed and replaced with D-MEM medium.

In vivo Control (n=8) and nitrofen-exposed (n=12) lung explants were cultured on translucent membrane inserts (polyester membrane transwell-clear inserts, Corning, Madrid, Spain) for 72 hours at 37°C in 5% CO_2. Culture medium (D-MEM/F12, Gibco, Barcelona, Spain) with 10% fetal bovine serum (Gibco, Barcelona, Spain), 100 IU/ml penicillin and 100 µg/ml streptomycin (Gibco, Barcelona, Spain) was added until the lungs were lying on the air-medium surface and changed every 24 hours.

LUNG MORPHOMETRY: Cultured lungs were photographed daily on an inverted microscope. The digitalised images of the last culture day were analysed with the assistance of image processing software (Image Pro-Plus™, version 5.0, Media Cybernetics, Washington, DC, USA). The outline of the lung explant was contoured on the PC screen with the cursor and the resulting surface was integrated by the software. In the same images the terminal lung buds were counted on each explant.

MOTILITY: At 72 hours of culture, airway peristaltic contractions were recorded for 10 minutes under an inverted microscope with LAS-AF software (Leica TCS SP5, Barcelona, Spain) and their frequency was expressed in number per minute.

IMMUNOBLOTTING: To quantify the levels of PGP 9.5 and α-actin proteins, five lungs from control, nitrofen, nitrofen + RA and nitrofen + AFS cells groups were pooled and homogenized in cell disruption buffer (Protein Isolation System Paris^{TM}, Ambion, Madrid, Spain). The protein content was assessed using a protein assay kit (BCA Protein Assay Kit, Pierce, Madrid, Spain). Western blotting was performed with 18% SDS-polyacrylamide gel. Anti-PGP 9.5 (1:6000; rabbit polyclonal PGP 9.5; Dako Cytomation, Glostrup, Denmark) and α-actin (1:6000; mouse monoclonal α-actin, Sigma, Madrid, Spain) antibodies were used and the values were normalized to SOD.

IMMUNOHISTOCHEMISTRY: After detaching the *in vivo* group nitrofen-exposed cultured lungs from the membranes, they were fixed in 4% paraformaldehyde overnight and subsequently rinsed in phosphate buffered saline (PBS). Nonspecific binding was blocked by washing them in PBS with 1% bovine-serum albumin, before incubating them with the primary antibodies overnight. To evaluate the AFS cells differentiation towards neuronal, muscle and epithelial lineage, three stainings were performed.

In the first, a mouse monoclonal antibody against protein gene product 9.5 (PGP 9.5; 1:500; Acris antibodies, Barcelona, Spain) was used to stain the neural tissue. In the second, smooth muscle was identified with a mouse monoclonal anti-α-actin fluorochrome-labeled antibody (anti-actin, α-smooth muscle-Cy3^{TM} antibody; 1:1000: Sigma-Aldrich, St. Luis, MO). In the third, the epithelial cells were stained with monoclonal mouse anti-thyroid transcription factor (TTF-1, Dako Cytomation, Glostrup, Denmark).

In all experiments, the anti-green fluorescent protein rabbit IgG fraction (anti-GFP, IgG; Molecular Probes, Eugene, Oregon) unveiled the injected AFS cells. After being washed with PBS, the samples were incubated at room temperature for 1 hour with

the fluorochrome-labeled anti-rabbit and anti-mouse secondary antibodies (Alexa Fluor® 488 and 568; 1:500; Molecular Probes, Eugene, Oregon). After further washing with PBS, the specimens were then mounted into glycerol on a glass slide. As a control, the primary antibody was omitted with no staining above background as the expected result.

CONFOCAL MICROSCOPY: Fluorescent images of the nerves, smooth muscle, epithelial cells and the injected AFS cells in the double-stained whole mount preparations were obtained using a confocal laser scanning microscope with LAS-AF software (Leica TCS SP5, Barcelona, Spain). The fluorescent markers were detected by a kripton/argon laser with excitation wavelenghts of 488 nm for Alexa 488, 568 nm for Alexa 568 and 561 nm for Cy3. The whole mounts were optically sectioned by scanning at increasing depths of focus in steps of 5 μm. After double staining, the green and the red images were captured separately, colorized and merged to show a composite image. The specific staining of neural structures by anti-PGP 9.5 antibody, of smooth muscle by anti-α-actin antibody and of epithelial cells by anti-TTF-1 antibody and the percentage of colocalization were assessed in each lung explant.

TOTAL RNA EXTRACTION AND RETROTRANSCRIPTION: Trypsinized AFS cells harvested from the culture setting of 8 control lungs co-cultured with AFS cells and 12 nitrofen-exposed explants co-cultured with AFS cells were suspended in sterile RNase free 1.5 ml microcentrifuge tubes and centrifuged for 1 minute to pellet the cells. After pouring off the supernatant, 1 ml of TRIzol Reagent (Life Technologies cat# 15596-026) was added to the tubes. Cells were lysed by thorough pipetting. The homogenate was then centrifuged at 12,000 x g for 10 minutes at 4°C. Homogenate was then transferred in a sterile microcentrifuge tube. The samples were incubated for 5 minutes at room temperature. 0.2 ml of Chloroform was added to each tube. Samples were shaken vigorously by hand for 15 seconds, incubated at room temperature for 5 minutes then centrifuged for 15 minutes at 12,000 x g at 4°C. The upper aqueous phase was transferred to a fresh tube. 0.5 ml of isopropyl alcohol was added to precipitate RNA. Samples were incubated at room temperature for 5 minutes and

centrifuged at 12,000 x g for 10 minutes at 4°C. Supernatant was discarded and pellet was washed with 1 ml 75% ethanol. The sample was mixed by vortexing and centrifuged at 7,500 x g for 5 minutes at 4°C. Supernatant was then removed and pellet left to air dry for 5-10 minutes. Pellet was dissolved in RNase free water or 0.5% SDS by passing the solution through a pipette tip and incubating for 10 minutes at 55-60°C. RNA concentration and purity of the sample were assessed by pipetting the diluted RNA sample in to a clean cuvette and absorbance was read at 260 nm and 280 nm. In order to determine the purity of the RNA sample, ratio of A260/A280 was calculated. We analyzed only samples with ratios ranging between 1.6 and 2, which represent a good RNA extraction. The first-strand cDNA was synthesized using 1 µg of total RNA in a total volume of 8 µl of DEPC water. After 1 µl of DNAse treatment, the mix was heated at 65°C for 10 min and 1 µl OligoDT plus 1 µl dNTPs mix 10 mM were added. The solution was then heated for 5 minutes at 65°C then cooled at 4°C, added 4 µl of First Strand Buffer x5, 2 µl 0.1 M DTT, 1 µl RNaseOUT™ and after a preheating at 42°C for 2 minutes, 1µl of Taq Polymerase (Invitrogen, London, UK) was added and left for 50 minutes at 42°C and then for 15 minutes at 70°C. Lastly 1 µl of RNAse H was added and the solution was incubated for 20 min at 37°C. The generated cDNA was diluted 1:5 in DEPC H2O and stored at −20°C.

PRIMER DESIGN AND REAL TIME PCR: Real-time PCR oligonucleotide primers (**Tab. 1**) were manually designed for each of the genes to assure maximal efficiency and sensitivity, according to the following parameters: primer length, melting temperature and avoidance of the formation of self and hetero-dimers, hairpins and self-complementarity. These properties were verified using two different internet-based interfaces: Primer-3 and Oligonucleotide Properties Calculator. When possible, "GC clamps" were placed at the 3'-end of each primer to minimize breathing between primer and template DNA, which can promote mispriming and decrease efficiency. Primers were designed such that amplicon sizes ranged between 50 and 250 bps. Melting curve analysis was always performed at the end of each PCR assay to control the specificity; definite reactions should result in a single melting peak corresponding to the PCR product being amplified. Real-time PCR was performed using the default

thermocycler program for all genes: 3 minutes of pre-incubation at 94°C followed by 50 cycles for 30 seconds at 94°C, 30 seconds at 60°C and 45 seconds at 72°C. Individual real-time PCR reactions were carried out in 30 µl volumes in a 96-well plate (Applied Biosystems™, London, UK) containing 8 µl DEPC water, 1 µl of sense and antisense primers (10 µM) and 15 µl SYBR Green with ROX ® plus 5 µl of sample. At the end of each reaction, cycle threshold (Ct) was manually set up at the level which reflected the best kinetic PCR parameters, and melting curves were acquired and analyzed.

We used a relative quantification method to measure gene expression by relating the PCR signal of the target transcript in a treatment group to control AFS cells of comparable passage number cultured for 72 hours at 37°C in 5% CO_2 in D-MEM/F12 medium with 10% fetal bovine serum, 100 IU/ml penicillin and 100 µg/ml streptomycin. In this work, the 2-ΔΔCt method of relative quantification was adapted to estimate copy numbers in our target genes. The ΔΔCt calculation for the relative quantification of target was used as follows: ΔΔCt = (Ct, target gene – Ct, β2 microglobulin)χ – (Ct, target gene – Ct, β2 microglobulin)y, where χ = unknown sample and y = AFS cells control. After validation of the method, results for each sample were expressed in N-fold changes in χ target gene copies, normalized to β2 microglobulin relative to the copy number of the target gene in AFS cells control, according to the following equation: amount of target = 2-ΔΔCt. A minimum of two experiments were carried out for each gene and sample. At each experiment, each individual sample was run in duplicate wells and the Ct of each well was recorded at the end of the reaction. The average and standard deviation (SD) of the three Cts were calculated and results for each sample were expressed as the N-fold copy number of a given gene relative to AFS cells control as expressed by calculating the geometric mean between the two experiments.

STATISTICAL METHODS: The results were expressed as percentages or as means±SD and the groups were compared by Anova tests with a threshold of significance at $p<0.05$. Tukey's range test was used as post-hoc test.

RESULTS

Thirty adult Sprague-Dawley pregnant rats were randomised to receive nitrofen or vehicle at E9.5. All animals survived to the procedure and were sacrificed at E13. Fetuses were collected and a total of 80 embryonic lungs were isolated under dissecting microscope and cultured in defined condition (see methods and **Fig. 1**). An additional culture set was dedicated to observe 20 lungs derived from control and nitrofen-exposed fetuses, which received, at E10.5, an *in utero* transplantation of AFS cells (**Fig. 1**). This procedure was however associated to a high mortality and only 15% of embryos survived. We continued the injections of AFS cells in utero until we obtained 20 lungs (12 nitrofen exposed lungs and 8 control lungs) to study. Similarly to the first group, animals were sacrificed at E13 and the harvested lungs underwent to *in vitro* culture for 72 hours.

GFP-rAFS cells expressed the marker Oct 3/4. CD34, CD45 and pan-cytokeratin were absent, while the mesenchymal cell marker vimentin and the smooth muscle marker αSMA were expressed in the cells (**Fig. 2**).

Embryonic lungs appeared dramatically different among the groups. In particular, as described before (25), embryonic lungs of fetuses which were exposed to nitrofen showed a marked hypoplasia, which appeared not influenced by basophils co-culture (**Fig. 3**). On the contrary, it appears that embryonic lungs which were exposed to nitrofen but cultured in presence of AFS cells or RA, did not differ from the ones derived from normal control animals (**Fig. 3A**). Remarkably this was also the case of the nitrofen-exposed lungs transplanted *in utero* with AFS at E10.5 and harvested at E13 (**Fig. 3A**).

To confirm this quality aspect, both lung surface and number of terminal buds were blindly measured. Similarly to what has been reported before (25), both surface (nitrofen 0.3 ± 0.12 mm^2 vs control 0.56 ± 0.17 mm^2, $p<0.005$; **Fig. 3B**) and number of terminal buds (nitrofen 41 ± 9 vs control 63 ± 8, $p<0.005$; **Fig. 3C**) were significantly decreased in nitrofen-exposed lung explants in comparison with the controls and the values did not normalize after being co-cultured with basophils

(surface: nitrofen + basophils 0.34 ± 0.19 mm^2 vs control 0.56 ± 0.17 mm^2, p<0.005; buds: nitrofen + basophils 36 ± 4 vs control 63 ± 8, p<0.005; **Fig. 3B and C**). In contrast, both parameters showed normalization in these lungs co-cultured in presence of AFS cells (surface: nitrofen + AFS cells 0.50 ± 0.08 mm^2 vs control 0.56 ± 0.17 mm^2, p=0.17; buds: nitrofen + AFS cells 60 ± 11 vs control 63 ± 8, p=0.42; **Fig. 3B and C**) or when RA (surface: nitrofen + RA 0.50 ± 0.07 mm^2 vs control 0.56 ± 0.17 mm^2, p=0.18; buds: nitrofen + RA 61 ± 6 vs control 63 ± 8, p=0.47) was added to the culture medium (**Fig. 3B and C**). The latter were confirmed also when AFS cells were transplanted *in utero* (surface: *in vivo* nitrofen + AFS cells 0.48 ± 0.08 mm^2 vs control 0.56 ± 0.17 mm^2, p=0.19; buds: *in vivo* nitrofen + AFS cells 56 ± 14 vs control 63 ± 8, p=0.17; **Fig. 3B and C**).

Importantly, no changes were noted when basophils, AFS cells or RA were added to control lungs (data not shown).

Among the various functional parameters which could be evaluated, peristalsis may play a pivotal role for the normal development of embryonic lungs (34). After video recording, samples were examined blindly and showed that rescue of normal development by AFS cells is also evident by the normalization of peristaltic movement. In fact, while bronchial peristalsis was significantly decreased in nitrofen-exposed explants in comparison with controls (nitrofen 0.5 ± 0.1 contractions/minute vs control 0.9 ± 0.1 contractions/minute, p<0.005; **Fig. 3D**), in nitrofen + AFS cells (0.9 ± 0.2 contractions/minute vs control 0.9 ± 0.1 contractions/minute, p=0.69; **Fig. 3D**) as well in nitrofen + RA (0.8 ± 0.2 contractions/minute vs control 0.9 ± 0.1 contractions/minute, p=0.77; **Fig. 3D**) lungs it was similar to normal controls. Interestingly, the presence of basophils did not influence the functional movement of the embryonic lungs, which remained impaired (nitrofen + basophils 0.6 ± 0.07 contractions/minute vs control 0.9 ± 0.1 contractions/minute, p<0.005; **Fig. 3D**). In contrast, the transplantation *in utero* of AFS cells resulted in the restoration of regular peristalsis in the nitrofen-exposed

lungs (**Fig. 3D**). Normal controls in medium did not differ from the exposed to RA or AFS cells (data not shown).

It has been suggested that both airway smooth muscle and neural tissue contribute to normal airway differentiation and branching from the early stages of development. To see whether the growth of neural tissue and smooth muscle were normal in lung explants, PGP 9.5 and α-actin protein levels were assessed. PGP 9.5 is a pan-neuronal protein that reveals neurons and their processes from the onset of lung development. The PGP 9.5 protein signals were seen at 20-25 kd. Similarly to what has been demonstrated before (29), the PGP 9.5 protein levels were significantly decreased in the nitrofen-exposed explants when compared to controls and the values did not normalize in presence of basophils (**Fig. 4A**). In contrast, PGP 9.5 expression was rescued to normal values when the nitrofen-exposed explants were co-cultured with AFS cells (**Fig. 4A**). This is similar to what is obtained when RA is administrated (**Fig. 4A**), as demonstrated before (29). Differently, α-actin did not differ among the groups (**Fig. 4B**).

When we analysed the nitrofen-exposed cultured lungs after *in utero* AFS cells transplantation, confocal microscopy revealed that GFP+ AFS cells were diffusely present on the bronchial tree, but, interestingly, they did not colocalize with α-actin- or PGP9.5-positive cells (**Fig. 5A and B**). In contrast, 50-70% of GFP+ AFS cells colocalized with TTF-1-positive cells (**Fig. 5C and D**). TTF-1 is a marker for alveolar epithelial cells type II (AECs-II) and it has been found to be essential for branching and for lung surfactant protein A and B production by the AECs-II. We postulated however that differentiation was not essential for the therapeutic effect since the lungs were rescued also when not exposed in direct contact to AFS cells. In this setting the AFS cells were lying attached on the bottom of the well and no GFP+cells were seen floating in the medium or on the membrane close to the lung explant. To evaluate whether the beneficial effect of stem cells could be mediated by paracrine mechanisms through secretion of growth factors (9) we evaluated the levels of three growth factors involved in lung morphogenesis in the culture medium

of nitrofen-exposed lungs co-cultured with AFS cells and compared to those of a control. FGF10, which has a pivotal role in modulating embryonic lung branching morphogenesis and cytodifferentiation, and VEGFα, which may play an important role in the angiogenesis, were significantly higher expressed in the medium of nitrofen-exposed lung explants co-cultured with AFS cells (**Fig. 6A and B**). In contrast, TGFβ1 mRNA expression, that is a negative regulator of lung epithelial proliferation and differentiation, was similar to controls (**Fig. 6C**).

DISCUSSION

Congenital diaphragmatic hernia is a malformation still causing mortality in newborns mainly because of severe respiratory failure secondary to pulmonary hypoplasia. This condition can be reproduced in pup rats by administrating the herbicide nitrofen (2,4-dichlorophenyl-*p*-nitrophenyl ether) to the pregnant mothers. In this model, lung hypoplasia is usually found in all pups and a diaphragmatic hernia in most of them (17). These lungs can be easily cultured *in* vitro and this has been very useful to investigate lung development, which can be generally influenced by altering the composition of the medium (18,34,38).

Using this setting, we have demonstrated for the first time that AFS cells are able to rescue both *in vitro* and *in vivo* hypoplastic nitrofen-exposed embryonic lungs. This is comparable to the rescue obtained when hypoplastic nitrofen-exposed embryonic lungs were cultured in presence of exogenous RA (25,27,28,35). The mechanism of action has not been fully elucidated, but it has been demonstrated that nitrofen inhibits RALDH 2, that catalyzes the final step in RA production (24). Therefore, the increase in lung branching morphogenesis in nitrofen-induced hypoplastic lungs exposed to exogenous RA is consistent with the hypothesis that the decrease of RALDH 2 activity can be partially countered by the increase of substrate (2).

In our experimental conditions, RA, which was used as positive control, restored indeed the hypoplastic lungs to the size and the number of terminal buds of the control lungs. The frequency of peristaltic waves, that was decreased in nitrofen-exposed lungs, normalized after adding RA to the medium. While interesting to

explore different pathways which could be involved in the hypoplastic lungs and their rescue, RA has the limitations of not being suitable to be used in the clinic (8,41) and alternative therapeutic options are needed.

It has been recently demonstrated that the pluripotent AFS cells (10) are able to integrate into developing as well as injured lung tissue, influencing its recovery from injury, and differentiate into lung epithelial lineages (7). In the present study, we found that hypoplastic nitrofen-exposed lung explants co-cultured with AFS cells were restored to the size and the number of terminal buds of the control lungs. Moreover, the frequency of peristaltic waves, that was decreased in nitrofen-exposed lungs, as expected (20), normalized after adding AFS cells to the medium. The improvement of airway peristalsis obtained with AFS cells as well as with RA was not related to smooth muscle hypertrophy (19,29), because the expression of smooth muscle-specific marker α-actin was not increased in AFS cells or RA treated groups. In contrast, the levels of PGP 9.5, a pan-neuronal marker that unveils ganglionic precursors since early phases of development (39), were decreased in nitrofen-exposed lungs and they normalized after adding the AFS cells or RA to the medium.

In order to mimic a possible therapeutic approach, we subsequently tested whether AFS cells could be therapeutic in nitrofen-exposed pregnant rats. Indeed lung growth and motility, evaluated after harvesting and culturing the embryonic lungs, could be rescued when AFS cells were injected in pregnant rats one day after the administration of the nitrofen. This could be observed in spite of a high rate of in uterus embryonal mortality, being the overall survival 15%. To determine whether AFS cells were able to differentiate into neural, muscle or epithelial lineages after integration, we analyzed the colocalization of GFP+ AFSC with PGP9.5+ or α-actin+ or TTF-1+ cells. We found that AFS cells colocalized with TTF-1+ cells.

Despite the minimal indication of engraftment, the main therapeutic effect produced by AFS cells seems mediated by paracrine mechanisms elicited through trophic mediators (5,9,14,32,36,37), as evident by the co-culture experiments. Among the

various factors which could be driving this effect, FGF-10, VEGFα and TGFβ1 were evaluated in this study. FGF-10 is essential for lung branching morphogenesis having a central role in inducing the spatial coordinates for patterning the epithelial tubules. TGFβ1 opposes these effects: its signaling is thought to prevent local budding and to maintain proximal airways in an unbranched form by suppressing epithelial cell proliferation and by promoting synthesis of extracellular matrix components around airways. VEGFα is a strong promoter of angiogenesis and its signaling is responsible for the differentiation of embryonic mesenchymal cells into endothelial cells; the interaction between the epithelium and mesenchyme contribute to lung neovascularisation that is crucial in normal lung development (6,11,23,45,46,48). Interestingly, we found that the levels of FGF-10 and VEGFα secreted by AFS cells were increased in comparison with controls when nitrofen-exposed lung explants were co-cultured with AFS cells. These findings were consistent with the demonstration that the temporospatial pattern of FGF-10 expression is severely disrupted in the presence of nitrofen-induced lung hypoplasia, whereas exogenous FGF-10 can rescue hypoplastic lungs in culture (1). This is also consistent with the fact that it has recently been shown that also RA has a major role in early lung morphogenesis by inducing FGF-10 expression within the mesoderm subjacent to the site of origin of the laryngotracheal groove (12). It is possible that AFS cells are capable to produce high levels of FGF-10 in response to the damaged lungs which they are exposed to (44).

In conclusion, we have demonstrated for the first time that AFS cells can rescue nitrofen-induced hypoplastic lungs in co-culture. It is possible that, as previously demonstrated in other model of disease, AFS cells might have a therapeutic role in CDH, particularly in babies with severe hypoplastic lungs. This effect could be also obtained during the gestation since AFS cells transplanted *in utero* in the same animal model produced similar effect.

REFERENCES

1. Acosta, J. M.; Thebaud, B.; Castillo, C.; Mailleux, A.; Tefft, D.; Wuenschell, C.; Anderson, K. D.; Bourbon, J.; Thiery, J. P.; Bellusci, S. and others. Novel mechanisms in murine nitrofen-induced pulmonary hypoplasia: FGF-10 rescue in culture. Am J Physiol Lung Cell Mol Physiol 281(1):L250-257; 2001.

2. Babiuk, R. P.; Thebaud, B.; Greer, J. J. Reductions in the incidence of nitrofen-induced diaphragmatic hernia by vitamin A and retinoic acid. Am J Physiol Lung Cell Mol Physiol 286(5):L970-973; 2004.

3. Bollini, S.; Cheung, K. K.; Riegler, J.; Dong, X.; Smart, N.; Ghionzoli, M.; Loukogeorgakis, S. P.; Maghsoudlou, P.; Dube, K. N.; Riley, P. R. and others. Amniotic Fluid Stem Cells Are Cardioprotective Following Acute Myocardial Infarction. Stem Cells Dev; 2011.

4. Bollini, S.; Pozzobon, M.; Nobles, M.; Riegler, J.; Dong, X.; Piccoli, M.; Chiavegato, A.; Price, A. N.; Ghionzoli, M.; Cheung, K. K. and others. In vitro and in vivo cardiomyogenic differentiation of amniotic fluid stem cells. Stem Cell Rev 7(2):364-380; 2011.

5. Caplan, A. I.; Dennis, J. E. Mesenchymal stem cells as trophic mediators. J Cell Biochem 98(5):1076-1084; 2006.

6. Cardoso, W. V. Molecular regulation of lung development. Annu Rev Physiol 63:471-494; 2001.

7. Carraro, G.; Perin, L.; Sedrakyan, S.; Giuliani, S.; Tiozzo, C.; Lee, J.; Turcatel, G.; De Langhe, S. P.; Driscoll, B.; Bellusci, S. and others. Human amniotic fluid stem cells can integrate and differentiate into epithelial lung lineages. Stem Cells 26(11):2902-2911; 2008.

8. Collins, M. D.; Mao, G. E. Teratology of retinoids. Annu Rev Pharmacol Toxicol 39:399-430; 1999.

9. Crisostomo, P. R.; Markel, T. A.; Wang, Y.; Meldrum, D. R. Surgically relevant aspects of stem cell paracrine effects. Surgery 143(5):577-581; 2008.

10. De Coppi, P.; Bartsch, G., Jr.; Siddiqui, M. M.; Xu, T.; Santos, C. C.; Perin, L.; Mostoslavsky, G.; Serre, A. C.; Snyder, E. Y.; Yoo, J. J. and others. Isolation of amniotic stem cell lines with potential for therapy. Nat Biotechnol 25(1):100-106; 2007.

11. Desai, T. J.; Cardoso, W. V. Growth factors in lung development and disease: friends or foe? Respir Res 3:2; 2002.

12. Desai, T. J.; Malpel, S.; Flentke, G. R.; Smith, S. M.; Cardoso, W. V. Retinoic acid selectively regulates Fgf10 expression and maintains cell identity in the prospective lung field of the developing foregut. Dev Biol 273(2):402-415; 2004.

13. Ditadi, A.; de Coppi, P.; Picone, O.; Gautreau, L.; Smati, R.; Six, E.; Bonhomme, D.; Ezine, S.; Frydman, R.; Cavazzana-Calvo, M. and others. Human and murine amniotic fluid c-Kit+Lin- cells display hematopoietic activity. Blood 113(17):3953-3960; 2009.

14. Gnecchi, M.; He, H.; Liang, O. D.; Melo, L. G.; Morello, F.; Mu, H.; Noiseux, N.; Zhang, L.; Pratt, R. E.; Ingwall, J. S. and others. Paracrine action accounts for marked protection of ischemic heart by Akt-modified mesenchymal stem cells. Nat Med 11(4):367-368; 2005.

15. Greer, J. J.; Allan, D. W.; Babiuk, R. P.; Lemke, R. P. Recent advances in understanding the pathogenesis of nitrofen-induced congenital diaphragmatic hernia. Pediatr Pulmonol 29(5):394-399; 2000.

16. Ijsselstijn, H.; Tibboel, D.; Hop, W. J.; Molenaar, J. C.; de Jongste, J. C. Long-term pulmonary sequelae in children with congenital diaphragmatic hernia. Am J Respir Crit Care Med 155(1):174-180; 1997.

17. Iritani, I. Experimental study on embryogenesis of congenital diaphragmatic hernia. Anat Embryol (Berl) 169(2):133-139; 1984.

18. Jesudason, E. C.; Connell, M. G.; Fernig, D. G.; Lloyd, D. A.; Losty, P. D. Early lung malformations in congenital diaphragmatic hernia. J Pediatr Surg 35(1):124-127; discussion 128; 2000.

19. Jesudason, E. C.; Smith, N. P.; Connell, M. G.; Spiller, D. G.; White, M. R.; Fernig, D. G.; Losty, P. D. Developing rat lung has a sided pacemaker region for morphogenesis-related airway peristalsis. Am J Respir Cell Mol Biol 32(2):118-127; 2005.

20. Jesudason, E. C.; Smith, N. P.; Connell, M. G.; Spiller, D. G.; White, M. R.; Fernig, D. G.; Losty, P. D. Peristalsis of airway smooth muscle is developmentally regulated and uncoupled from hypoplastic lung growth. Am J Physiol Lung Cell Mol Physiol 291(4):L559-565; 2006.

21. Kamata, S.; Usui, N.; Kamiyama, M.; Tazuke, Y.; Nose, K.; Sawai, T.; Fukuzawa, M. Long-term follow-up of patients with high-risk congenital diaphragmatic hernia. J Pediatr Surg 40(12):1833-1838; 2005.

22. Kluth, D.; Kangah, R.; Reich, P.; Tenbrinck, R.; Tibboel, D.; Lambrecht, W. Nitrofen-induced diaphragmatic hernias in rats: an animal model. J Pediatr Surg 25(8):850-854; 1990.

23. Maeda, S.; Suzuki, S.; Suzuki, T.; Endo, M.; Moriya, T.; Chida, M.; Kondo, T.; Sasano, H. Analysis of intrapulmonary vessels and epithelial-endothelial interactions in the human developing lung. Lab Invest 82(3):293-301; 2002.

24. Mey, J.; Babiuk, R. P.; Clugston, R.; Zhang, W.; Greer, J. J. Retinal dehydrogenase-2 is inhibited by compounds that induce congenital diaphragmatic hernias in rodents. Am J Pathol 162(2):673-679; 2003.

25. Montedonico, S.; Nakazawa, N.; Puri, P. Retinoic acid rescues lung hypoplasia in nitrofen-induced hypoplastic foetal rat lung explants. Pediatr Surg Int 22(1):2-8; 2006.

26. Montedonico, S.; Sugimoto, K.; Felle, P.; Bannigan, J.; Puri, P. Prenatal treatment with retinoic acid promotes pulmonary alveologenesis in the nitrofen model of congenital diaphragmatic hernia. J Pediatr Surg 43(3):500-507; 2008.

27. Nakazawa, N.; Montedonico, S.; Takayasu, H.; Paradisi, F.; Puri, P. Disturbance of retinol transportation causes nitrofen-induced hypoplastic lung. J Pediatr Surg 42(2):345-349; 2007.

28. Nakazawa, N.; Takayasu, H.; Montedonico, S.; Puri, P. Altered regulation of retinoic acid synthesis in nitrofen-induced hypoplastic lung. Pediatr Surg Int 23(5):391-396; 2007.

29. Pederiva, F.; Martinez, L.; Tovar, J. A. Retinoic acid rescues deficient airway innervation and peristalsis of hypoplastic rat lung explants. Neonatology in press; 2011.

30. Peetsold, M. G.; Heij, H. A.; Kneepkens, C. M.; Nagelkerke, A. F.; Huisman, J.; Gemke, R. J. The long-term follow-up of patients with a congenital diaphragmatic hernia: a broad spectrum of morbidity. Pediatr Surg Int 25(1):1-17; 2009.

31. Perin, L.; Da Sacco, S.; De Filippo, R. E. Regenerative medicine of the kidney. Adv Drug Deliv Rev 63(4-5):379-387; 2011.

32. Rabb, H. Paracrine and differentiation mechanisms underlying stem cell therapy for the damaged kidney. Am J Physiol Renal Physiol 289(1):F29-30; 2005.

33. Rocha, G. M.; Bianchi, R. F.; Severo, M.; Rodrigues, M. M.; Baptista, M. J.; Correia-Pinto, J.; Guimaraes, H. A. Congenital Diaphragmatic Hernia - The Neonatal Period (Part I). Eur J Pediatr Surg; 2008.

34. Schittny, J. C.; Miserocchi, G.; Sparrow, M. P. Spontaneous peristaltic airway contractions propel lung liquid through the bronchial tree of intact and fetal lung explants. Am J Respir Cell Mol Biol 23(1):11-18; 2000.

35. Sugimoto, K.; Takayasu, H.; Nakazawa, N.; Montedonico, S.; Puri, P. Prenatal treatment with retinoic acid accelerates type 1 alveolar cell proliferation of the hypoplastic lung in the nitrofen model of congenital diaphragmatic hernia. J Pediatr Surg 43(2):367-372; 2008.

36. Tang, Y. L.; Zhao, Q.; Qin, X.; Shen, L.; Cheng, L.; Ge, J.; Phillips, M. I. Paracrine action enhances the effects of autologous mesenchymal stem cell transplantation on vascular regeneration in rat model of myocardial infarction. Ann Thorac Surg 80(1):229-236; discussion 236-227; 2005.

37. Togel, F.; Weiss, K.; Yang, Y.; Hu, Z.; Zhang, P.; Westenfelder, C. Vasculotropic, paracrine actions of infused mesenchymal stem cells are important to the recovery from acute kidney injury. Am J Physiol Renal Physiol 292(5):F1626-1635; 2007.

38. Tollet, J.; Everett, A. W.; Sparrow, M. P. Development of neural tissue and airway smooth muscle in fetal mouse lung explants: a role for glial-derived neurotrophic factor in lung innervation. Am J Respir Cell Mol Biol 26(4):420-429; 2002.

39. Tollet, J.; Everett, A. W.; Sparrow, M. P. Spatial and temporal distribution of nerves, ganglia, and smooth muscle during the early pseudoglandular stage of fetal mouse lung development. Dev Dyn 221(1):48-60; 2001.

40. Trachsel, D.; Selvadurai, H.; Bohn, D.; Langer, J. C.; Coates, A. L. Long-term pulmonary morbidity in survivors of congenital diaphragmatic hernia. Pediatr Pulmonol 39(5):433-439; 2005.

41. Tzimas, G.; Nau, H. The role of metabolism and toxicokinetics in retinoid teratogenesis. Curr Pharm Des 7(9):803-831; 2001.

42. van den Hout, L.; Reiss, I.; Felix, J. F.; Hop, W. C.; Lally, P. A.; Lally, K. P.; Tibboel, D. Risk factors for chronic lung disease and mortality in newborns with congenital diaphragmatic hernia. Neonatology 98(4):370-380; 2010.

43. Vanamo, K.; Rintala, R.; Sovijarvi, A.; Jaaskelainen, J.; Turpeinen, M.; Lindahl, H.; Louhimo, I. Long-term pulmonary sequelae in survivors of congenital diaphragmatic defects. J Pediatr Surg 31(8):1096-1099; discussion 1099-1100; 1996.

44. Wang, M.; Crisostomo, P. R.; Herring, C.; Meldrum, K. K.; Meldrum, D. R. Human progenitor cells from bone marrow or adipose tissue produce VEGF,

HGF, and IGF-I in response to TNF by a p38 MAPK-dependent mechanism. Am J Physiol Regul Integr Comp Physiol 291(4):R880-884; 2006.

45. Warburton, D.; Bellusci, S. The molecular genetics of lung morphogenesis and injury repair. Paediatr Respir Rev 5 Suppl A:S283-287; 2004.

46. Warburton, D.; Bellusci, S.; De Langhe, S.; Del Moral, P. M.; Fleury, V.; Mailleux, A.; Tefft, D.; Unbekandt, M.; Wang, K.; Shi, W. Molecular mechanisms of early lung specification and branching morphogenesis. Pediatr Res 57(5 Pt 2):26R-37R; 2005.

47. Warburton, D.; Perin, L.; Defilippo, R.; Bellusci, S.; Shi, W.; Driscoll, B. Stem/progenitor cells in lung development, injury repair, and regeneration. Proc Am Thorac Soc 5(6):703-706; 2008.

48. Warburton, D.; Schwarz, M.; Tefft, D.; Flores-Delgado, G.; Anderson, K. D.; Cardoso, W. V. The molecular basis of lung morphogenesis. Mech Dev 92(1):55-81; 2000.

TABLE

Table 1

Primer template table

	Forward Primer	Reverse Primer
rB2M	5'-GGCACGATGGCTCGC-3'	5'-TCCCATTCTCCGGTGGAT-3'
rFGF10	5'-TCCGCTGGAGAAAGCTGTTC-3'	5'-GTTAATGGCTTTGACGGCAAC-3'
rVEGFa	5'-CTGCAAAAACACAGACTCGCGT-3'	5'-AGGACTGTTCTGTCGACGGTG-3'
rTGFb1	5'-GCTGAACCAAGGAGACGGAA-3'	5'-GAAGGGTCGGTTCATGTCATG-3'

LEGENDS FOR THE FIGURES

Figure 1

In the ***in vitro*** model, pregnant rats received intragastrically either nitrofen or vehicle on E9.5. On E13 the embryos were recovered and the lung primordia harvested.

In the ***in vivo*** model, pregnant rats received intragastrically either nitrofen or vehicle on E9.5. A laparotomy was performed on E10.5 and $1x10^5$-10^6 GFP+ rat-AFS cells were injected into the amniotic fluid of both groups. The embryos were recovered on E13 and the lung primordia were dissected free.

Figure 2

Immunophenotyping of GFP-rAFS cells. More than 90% of GFP-rAFS cells expressed vimentin (**d**), while Oct 3/4 (**a**) and αSMA (**f**) were expressed to a lesser extent. CD45 (**b**), CD34 (**c**) and pancitokeratin (**e**) were absent.

Figure 3

A. Photographs of embryonic lung explants taken at the beginning of the culture, at 24 h, 48 h and 72 h. Nitrofen-exposed embryonic lungs were markedly hypoplastic (second column) in comparison with controls and they were not influenced by their co-culture with basophils (fifth column). In contrast, AFSC rescued growth of nitrofen-exposed lung explants both when co-cultured with lungs (third column) and when injected in the amniotic fluid (sixth column). A similar effect was obtained by adding RA to the medium (fourth column). Scale bar: 0.5 mm.

Growth parameters (**B** and **C**) and peristalsis (**D**) analysed in lung explants after 72 hours of culture. The lung surface (**B**), the number of terminal bud (**C**) and the number of contractions per minute (**D**) were decreased in nitrofen-exposed lungs and restored to control values in presence of RA or AFS cells. This was also the case of the nitrofen-exposed lungs transplanted with AFS at E10.5. (# $p<0.05$ vs control)

The presence of basophils did not influence the growth or functional movement of the embryonic lungs, which remained impaired.

Figure 4

A. PGP9.5 protein level normalized to super-oxide-dysmutase (SOD) in Control, N, N+RA, N+AFSC groups. The expression of PGP 9.5 was decreased in nitrofen-exposed explants (# $p<0.05$ vs control). The expression normalized adding RA to the medium or co-culturing the nitrofen-exposed lungs with AFS cells. **B.** α-actin protein expression

normalized to SOD. No differences were seen in the levels of the protein in the four study groups.

Figure 5

Confocal projections of nitrofen-exposed lung cultured after *in utero* AFS cells transplantation. GFP+ AFS cells (green) were diffusely present on the bronchial tree, but they did not colocalized with α-actin- (**A**) or PGP9.5- (**B**) positive cells (red). 50-70% of GFP+ AFS cells colocalized with the alveolar epithelial TTF-1-(**C and D**) positive cells (red). Scale bar (**A**, **C**): 250 µm. Scale bar (**B**, **D**): 125 µm

Figure 6

FGF10 (**A**), VEGFα (**B**) and TGFβ1 (**C**) mRNA expression in the medium of nitrofen-exposed lung explants co-cultured with AFS cells compared with a control (AU: Arbitary Unit). While levels of FGF10 and VEGFα, which are respectively a promoter of branching morphogenesis and a promoter of vasculogenesis, had increased, the values of TGFβ1, a negative regulator of lung epithelial proliferation and differentiation, was similar to controls.

Figure 1

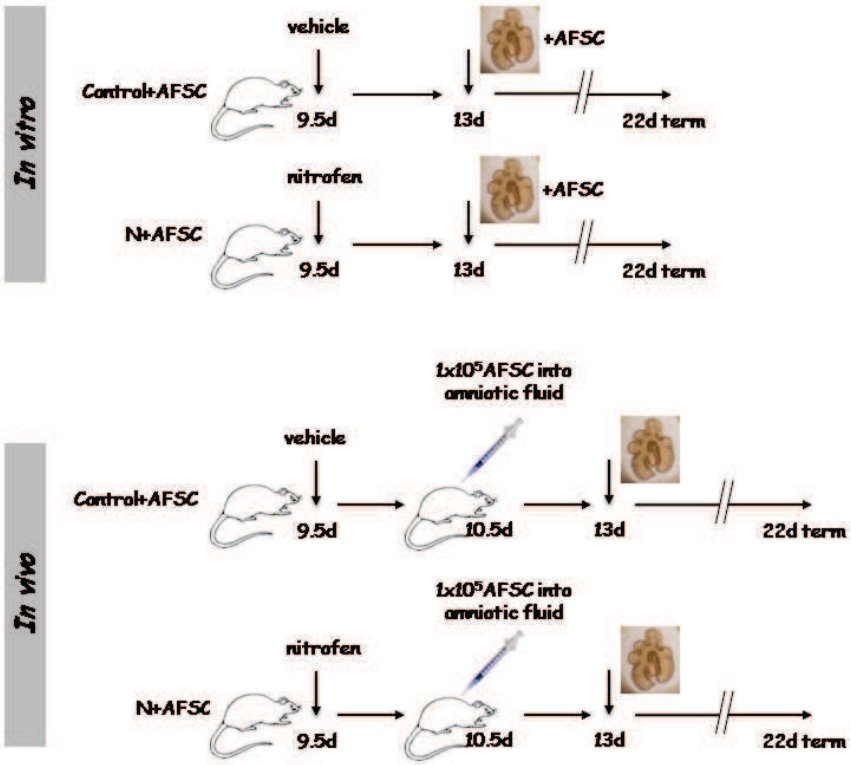
In vitro
vehicle
+AFSC
Control+AFSC
9.5d
13d
22d term
nitrofen
+AFSC
N+AFSC
9.5d
13d
22d term
In vivo
1x10⁵AFSC into amniotic fluid
vehicle
Control+AFSC
9.5d
10.5d
13d
22d term
1x10⁵AFSC into amniotic fluid
nitrofen
N+AFSC
9.5d
10.5d
13d
22d term

Figure 2

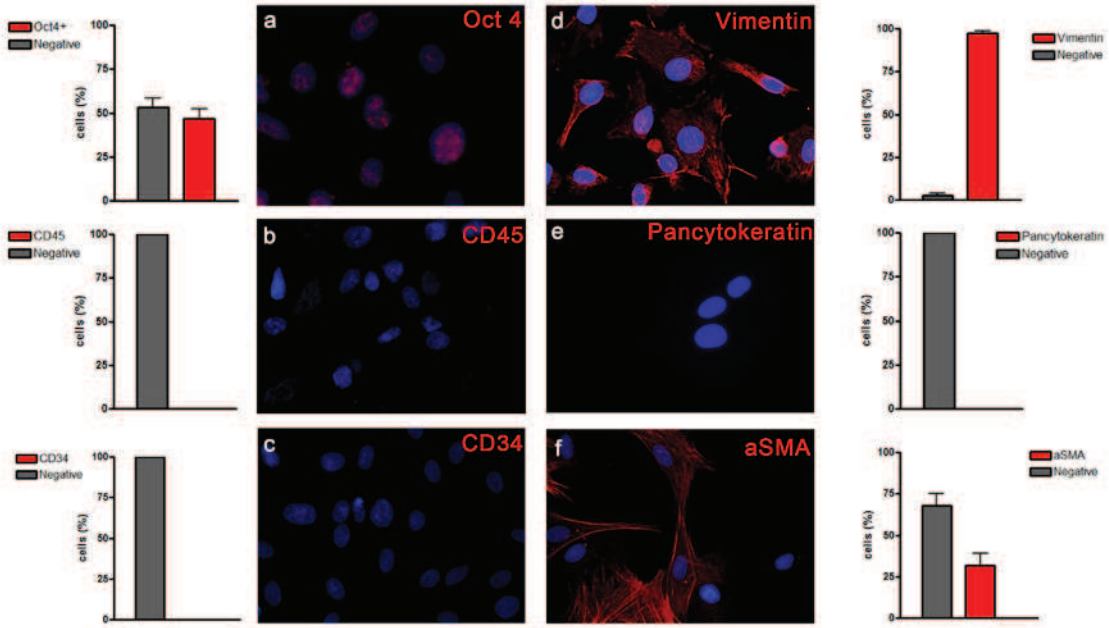
Oct4+
Negative
cells (%)
100
75
50
25
0
a
Oct 4
d
Vimentin
Vimentin
Negative
CD45
Negative
b
CD45
e
Pancytokeratin
Pancytokeratin
Negative
CD34
Negative
c
CD34
f
aSMA
aSMA
Negative

Figure 3

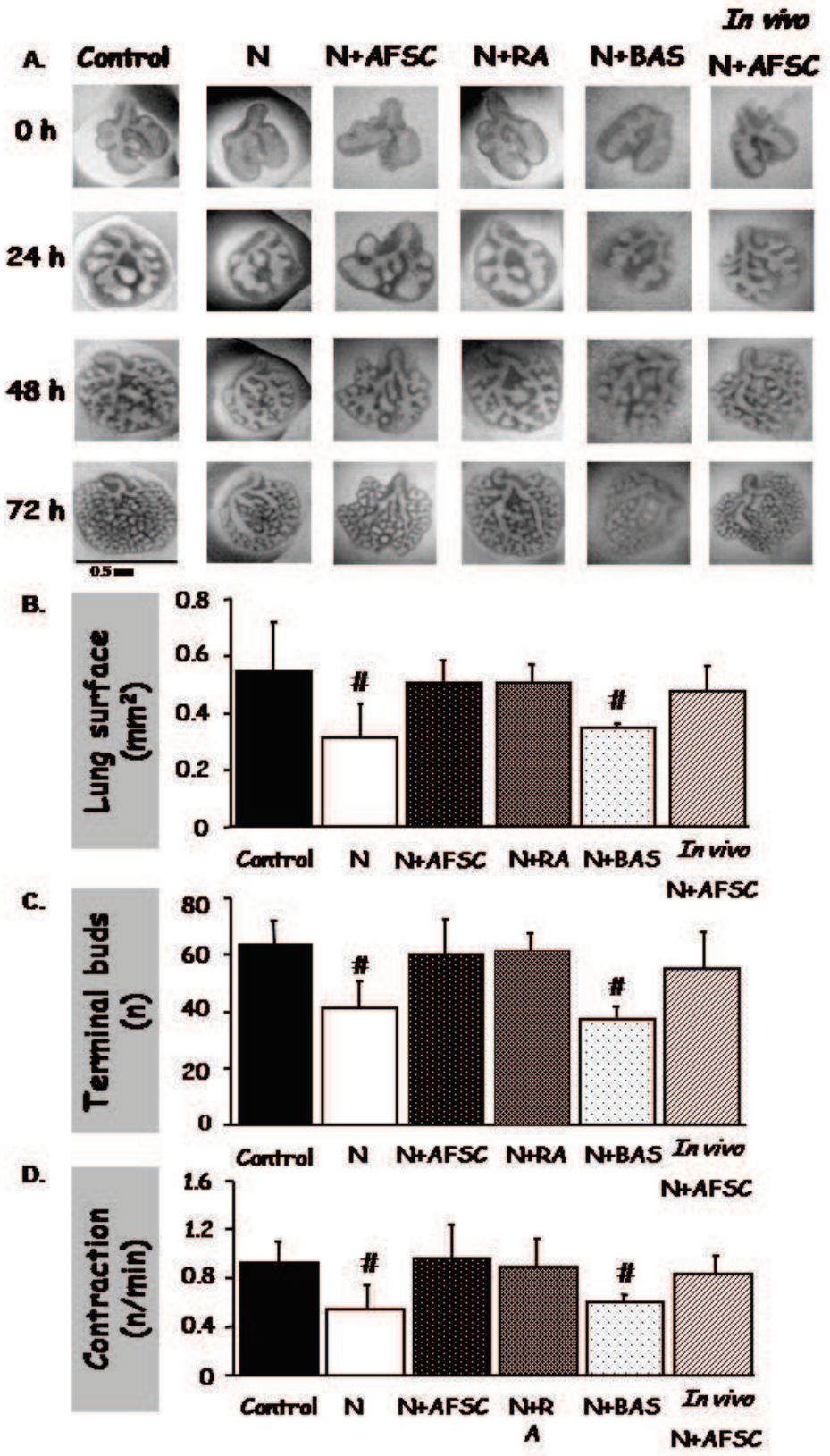
A.
Control
N
N+AFSC
N+RA
N+BAS
In vivo N+AFSC
0 h
24 h
48 h
72 h
0.5
B.
Lung surface (mm²)
0.8
0.6
0.4
0.2
0
#
Control
N
N+AFSC
N+RA
N+BAS
In vivo N+AFSC
C.
Terminal buds (n)
80
60
40
20
0
#
Control
N
N+AFSC
N+RA
N+BAS
In vivo N+AFSC
D.
Contraction (n/min)
1.6
1.2
0.8
0.4
0
#
Control
N
N+AFSC
N+RA
N+BAS
In vivo N+AFSC

Figure 4

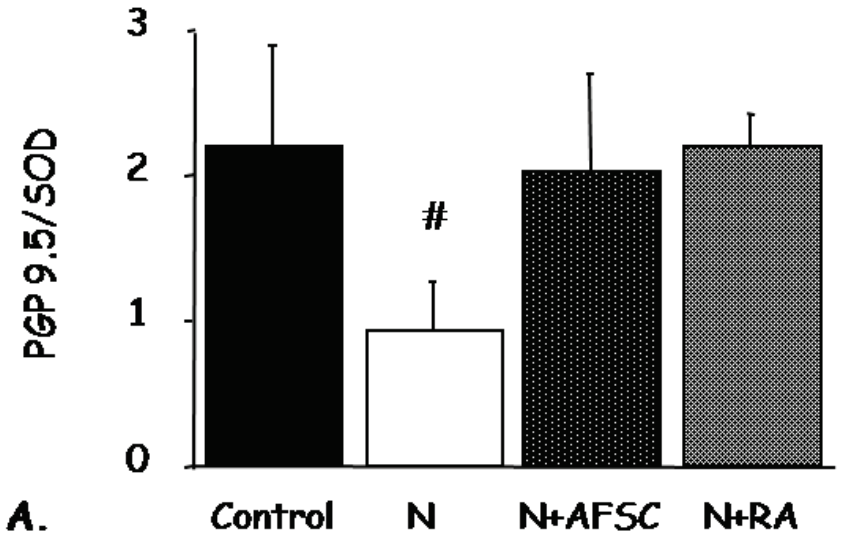
PGP 9.5/SOD
3
2
1
0
#
A.
Control
N
N+AFSC
N+RA

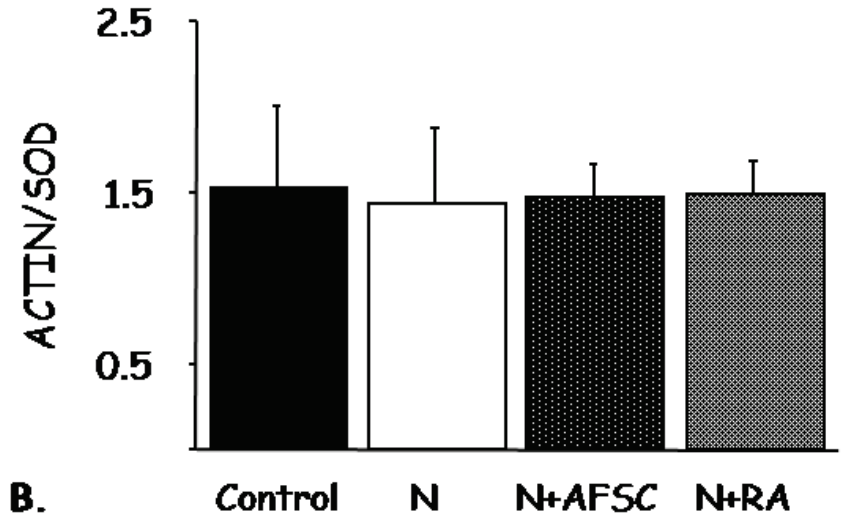
ACTIN/SOD
2.5
1.5
0.5
B.
Control
N
N+AFSC
N+RA

Figure 5

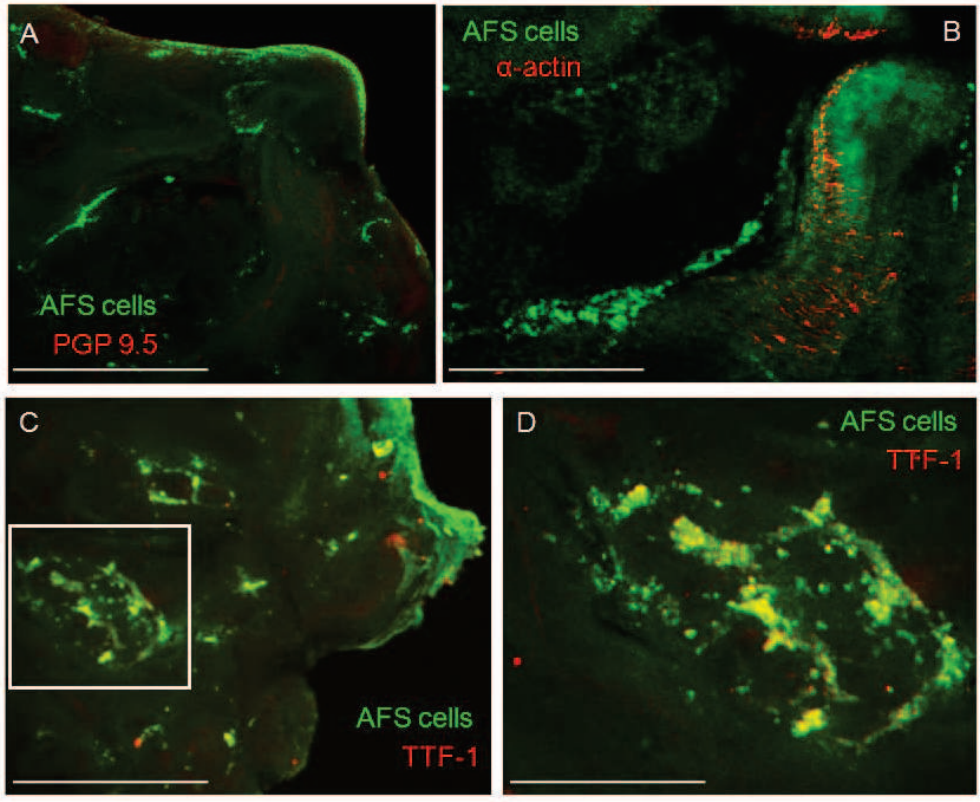
A
AFS cells
PGP 9.5
AFS cells
α-actin
B
C
AFS cells
TTF-1
D
AFS cells
TTF-1

Figure 6

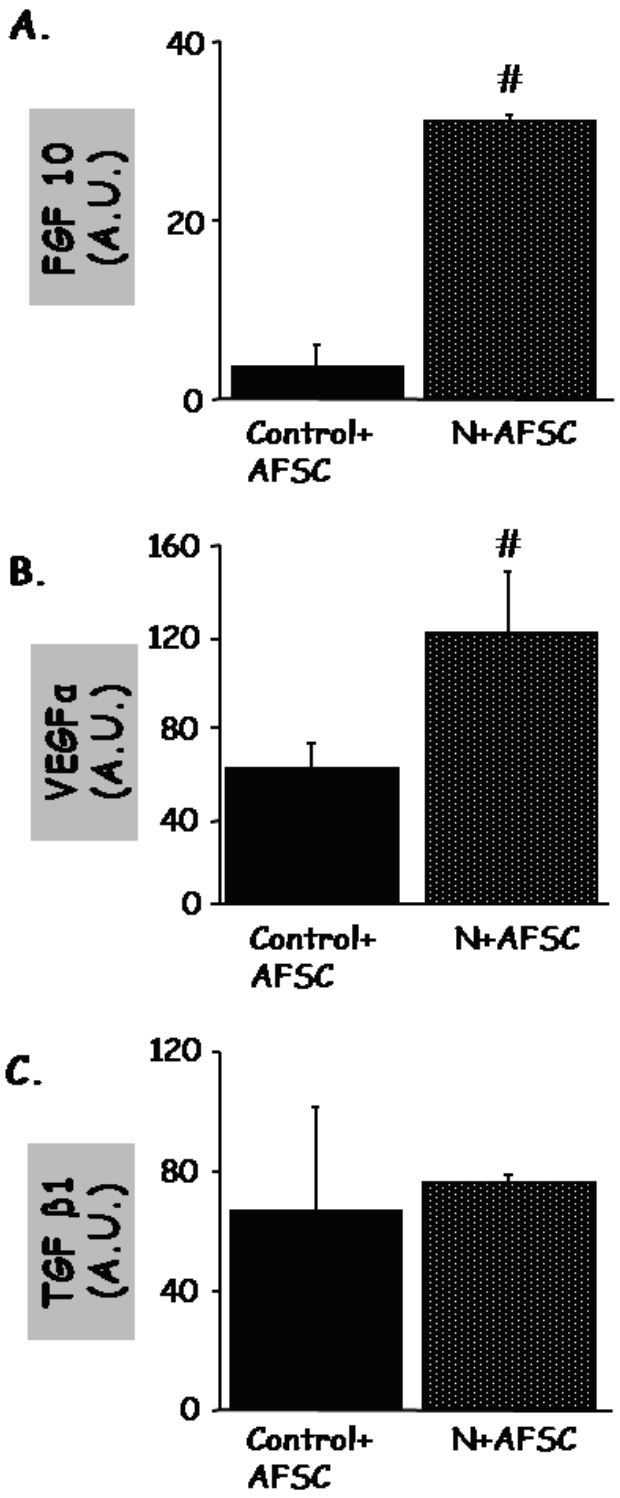
A.
FGF 10 (A.U.)
40
20
0
#
Control+ AFSC
N+AFSC
B.
VEGFα (A.U.)
160
120
80
40
0
#
Control+ AFSC
N+AFSC
C.
TGF β1 (A.U.)
120
80
40
0
Control+ AFSC
N+AFSC

Discussion

Congenital diaphragmatic hernia is a malformation that still causes high mortality in newborns mainly because of severe respiratory failure secondary to pulmonary hypoplasia. Unfortunately, most of the newer treatment modalities have replaced mortality for a higher morbidity. As a matter of fact, long-term pulmonary disease continues to be the most significant source of morbidity in survivors of CDH. Persistent lung hypoplasia with structural abnormalities in distal airways [97, 98] and barotrauma from neonatal intensive care treatment have been considered as possible causes of long-term pulmonary sequelae [12, 18, 19, 99]. However, these children are prone to develop exacerbations secondary to viral respiratory infections and suffer from obstructive, restrictive or a combined ventilation impairment even when the pulmonary hypoplasia is mild to moderate [10, 12, 13, 75, 100, 101]. This led us to believe that also other causes might contribute to pulmonary morbidity. Some authors suggested that structural changes in distal airways could justify pulmonary symptoms without involvement of autonomic nerve abnormalities [18]. Because autonomic nerves control the bronchial smooth muscle tone and the tracheobronchial reflexes in lower respiratory tract, we hypothesized that impaired innervation might contribute to explain the long-term pulmonary symptoms.

Congenital diaphragmatic hernia can be reproduced in rat pups by administrating the herbicide nitrofen (2,4-dichlorophenyl-p-nitrophenyl ether) to pregnant mothers. In this model, lung hypoplasia can be found in all pups and congenital diaphragmatic hernia in most of them. Since its first description by Iritani [76], the nitrofen rodent model of CDH has been extensively studied and has become a widely accepted tool which closely replicates many features of the human condition [77, 78].

Using this setting, we first confirmed the neural crest origin of tracheobronchial neural cells by the positive staining with p75 antibody. Then, we could depict an AChe-positive neural network in the tracheas of preterm fetuses with CDH and we compared them with the controls. As previously shown in adult rat trachea [102], the nerve fibers of control tracheas were interconnected to form plexuses containing ganglia and ran in the membranous wall sending nerve bundles laterally between the cartilaginous rings.

Interestingly, the neural network was sparser and the nerve trunks thinner in the tracheas of animals with CDH. Moreover, while the number of ganglia was similar in control tracheas and in the ones of pups with CDH, in the latter the surface of the ganglia was smaller. In addition, in the same tracheas PGP 9.5-protein levels were decreased, while PGP 9.5-mRNA expression was increased in comparison with controls. PGP 9.5 is a ubiquitin carboxyl-terminal hydrolase isozyme L1 [103] expressed over the development at all levels of the central and peripheral nervous system [104] in differentiated neurons and in nerve fibers as well as in neuronal precursors, leading to believe that it has a role in the development and differentiation of neuronal cells. PGP 9.5 protein and PGP 9.5 mRNA have been demonstrated to have a parallel distribution in rat tissues [105], suggesting that the increase of PGP 9.5 mRNA in our setting could be due to post-translational events occurring in the development of CDH trachea.

The deficiencies found in the tracheal innervation of near term CDH fetuses stimulated us to look further into the development of this innervation in the embryo-fetal period. Interestingly, we found that the pattern of innervation in embryos and fetuses with CDH was similar to the one depicted in CDH preterm pups, with poor neural interconnections and sparser nerve fibers. PGP 9.5 protein was decreased and PGP 9.5 mRNA was increased throughout development. The immaturity of the tracheal innervation early in embryo-fetal life and its deficiency thereafter seemed to confirm the hypothesis of a delayed development occurring in animals with CDH. At the same time, we described an increased population of S100-positive glial cells in embryos and fetuses with CDH. S100 is a calcium-binding protein expressed in glial and Schwann cells [106, 107], whose increased expression has been interpreted as a compensatory mechanism for defective neural tissue [108]. Hence, the increment of glial tissue in embryos and fetuses with CDH might be interpreted as either a response to neural damage or a compensation for the defective neuronal tissue.

After demonstrating that tracheal innervation was abnormal in rats with CDH, the next step was to examine bronchopulmonary innervation assuming that it could also be impaired. Since we felt that, if abnormalities of bronchopulmonary innervation were

found also in babies with CDH, they could play a role in chronic lung disease of survivors of CDH, we investigated if a similar pattern could be found also in infants dead of CDH. The number of trunks per bronchus was significantly decreased in embryos and fetuses with CDH. Surprisingly, the findings in infants with CDH were quite similar and the pattern in preterm rats closely resembled the human one. As previously described for tracheal innervation, these deficits in bronchopulmonary innervation were consistent with the hypothesis that the development in animals and infants with CDH was delayed. Also in this case, the neural deficiency was compensated by a certain increase of the supporting glial tissue. S100 staining, that unveils the supporting glial cells of pulmonary ganglia, revealed similar increases also in the lungs of infants with CDH. To further support the hypothesis of a delayed development of the innervation, we studied the expression of RET, a receptor tyrosine kinase expressed by neural crest-derived cells during their migration and later required for the peripheral nervous system maturation [109-111]. RET expression is high in neural crest cells during migration and in neural crest-derived structures during embryogenesis, whereas it decreases in mature tissue [111]. Hence, its increased expression in lungs of infants with CDH could be explained as a persistence of the enteric neuron precursors, while the same cells were already differentiated in the correspondent controls. Unfortunately, for technical reasons, we were unable to analyze the expression of RET in rat lungs. RET activation depends on the presence of GDNF, that pilots the innervation and the differentiation of the enteric nervous system progenitors in the developing lung [112, 113]. In addition, GDNF acts as chemoattractant of these progenitors and it is expressed by the mesenchyme before the entry of neural crest-derived cells [114, 115], whereas the response of the target cells to GDNF decreased in later stages of development [116, 117]. The persistent increase of GDNF protein in lungs of preterm animals with CDH, like in earlier stages of development, gave further support to the hypothesis of a delayed development of innervation in which characteristics of the immature period were maintained. At the same time, the decrease of GDNF mRNA in the lungs of animals with CDH failed to compensate the deficit of neural tissue. Importantly, the lungs ipsilateral and contralateral to the

hernia were equally affected, supporting the concept that lung hypoplasia associated to CDH is a primary developmental defect rather than the result of lung compression during embryogenesis.

Confocal microscopic studies [40] have shown that neural tissue and smooth muscle appear early in the developing fetal lung, being epithelial tubules surrounded by smooth muscle and ensheathed in a network of nerve plexus from embryogenesis onward, but, interestingly, this spatial and temporal association persists into postnatal life. Prenatal smooth muscle seems to have a pivotal role in modulating lung growth [47] and the mechanical stimulus generated by its spontaneous phasic contractions contribute to a normal airway branching and differentiation. Taking into consideration that bronchial peristalsis is deficient in hypoplastic nitrofen-exposed rat lung explants [47] and that the tracheobronchial innervation is impaired in rat fetuses with CDH and lung hypoplasia, as we could demonstrate, we postulated that abnormalities in bronchial innervation might contribute to the pulmonary developmental deficiency.

The lungs can be easily cultured *in* vitro and this has been very useful to investigate lung development, which can be influenced by altering the composition of the medium [31, 36]. Using this setting, we could demonstrate that in the nitrofen-exposed lung explants in which the frequency of peristaltic waves was decreased, the levels of PGP 9.5 were decreased as well. It has been observed that spontaneous contractions of the airways are unaffected by either atropine, indicating that neural activity is not essential, or tetrodotoxin, showing that endogenous Ach is not involved [36]. In addition, this rhythmic mechanical activity ceases in the presence of calcium antagonists. It has been concluded that spontaneous contractions are therefore of likely of myogenic origin [36]. Hence, it has been supposed that the role fulfilled by neural tissue in early gestation is not neurotransmission, but rather secretion of trophic factors for the smooth muscle that indirectly contributes to lung development [33, 36, 39, 40]. The same authors [36, 40, 43] proposed the idea that the spontaneous contractions produce a rhythmic mechanical stimulus across the airway wall and the adjacent parenchyma that contributes to normal airway differentiation and branching by inducing expression

of growth factors. Neurotrophic factors, like neurturin, a member of GDNF-family, and GDNF, have been isolated in airway smooth muscle cells or in the associated mesenchymal cells [31, 44, 45]. In this light, the decrease of neural structures, revealed by the reduced amount of PGP 9.5-positive cells, might cause an impairment of the signalling between nerves and airway smooth muscle, contributing to the hypoplasia of the lung. In addition, it has been shown recently that innervation is required for epithelial progenitor cell function during organogenesis, because removal of the parasympathetic submandibular ganglion before the homonymous gland developed in mice, impaired its development reducing the number of epithelial buds by weakening the expression of progenitor cells [118]. The same coordinated development of the peripheral nervous system and a branched epithelium organ is likely in the lung. Moreover, basal progenitor cells express the nerve growth factor receptor (NGFR), whose function to date has not been clarified [119-121].

Given these observations, we expected that agents like RA, that has been shown to have beneficial effects on CDH lungs in which it is able to rescue lung hypoplasia [48, 56, 57, 61, 122], may also positively influence bronchial innervation and peristalsis. Despite evidence linking retinoids with CDH dating back more than 50 years [54], only lately they have been related to the pathogenesis of pulmonary hypoplasia associated with CDH [56, 61, 63, 77, 123]. Plasma concentration of retinol and of retinol-binding protein (RBP) have been found decreased in newborns with CDH in comparison with controls. Those values were independent of maternal retinol status that was similar to controls for some authors [124], while higher than controls for others [125]. These findings supported the idea that human CDH is linked to abnormal retinoid homeostasis. It has been demonstrated that exogenous retinoic acid is able to increase the size of hypoplastic lung explants [61, 63-65]. Moreover, RA induces FGF10 expression in the foregut region where the lung forms [95]. Thus, since FGF10 governs the directional outgrowth of lung bud during branching morphogenesis [126], RA signaling may connect formation of the laryngo-tracheal groove with activation of FGF10-dependent bronchial morphogenesis [93]. FGF10 is produced by airway smooth muscle progenitors and is required for their entry into the smooth muscle cell lineage [127].

In our experiments, RA not only significantly increased lung growth in nitrofen-exposed lung explants, as previously demonstrated [61], but it restored the hypoplastic lungs to the size, the number of terminal buds and the DNA and protein content of the control lungs. The frequency of peristaltic waves, that was decreased in nitrofen-exposed lungs, normalized adding RA to the medium. The improvement of airway peristalsis obtained with RA was not related to smooth muscle hypertrophy, because the expression of smooth muscle-specific marker α-actin was not increased in RA treated groups. On the other hand, the levels of the pan-neuronal protein PGP 9.5, that was decreased in nitrofen-exposed lung explants, were restored by RA. RA signalling has been found to play a role in neurite outgrowth both *in vitro* and *in vivo* [128]. However, limitations for the clinical use of RA, which is known to be teratogenic [79, 80], invite to explore alternative procedures for the rescue of this devastating disease.

Stem cell-based therapies are becoming promising approaches for a large number of diseases. Recently, it has been reported that AFS cells can be isolated from human and rodent amniotic fluid. AFS cells are broadly multipotent cells, able to differentiate into lineages belonging to all three embryonic germ layers [66]. Moreover, they can also engraft in irradiated bone marrow and give rise to all hematopoietic lineages [67]. Finally, they can functionally contribute to the regeneration of various tissues and organs when transplanted into animal models of disease. Remarkable results have been obtained in injured kidneys, heart and lungs [68-70]. The latter have been explored both in models of diseases and during development and AFS cells have shown the potential not only to engraft and differentiate into specialised pneumocytes but also to contribute and supplement endogenous lung repair mechanisms [71].

We found that hypoplastic nitrofen-exposed lung explants co-cultured with AFS cells were restored to the size and number of terminal buds equivalent to those of control lungs. Moreover, the frequency of peristaltic waves, that was decreased in nitrofen-exposed lungs, normalized after adding AFS cells to the medium. The improvement of airway peristalsis obtained with AFS cells, similarly to what we found with RA, was not related to smooth muscle hypertrophy [82, 83], because the expression of smooth muscle-

specific marker α-actin was not increased in AFS cells treated group. In contrast, the levels of PGP 9.5 were decreased in nitrofen-exposed lungs and they normalized after adding the AFS cells to the medium.

In order to mimic a possible therapeutic approach potentially viable in the clinical setting, we subsequently tested whether AFS cells could be beneficial on the lungs of the fetuses when injected directly into the ambiotic fluid one day after the administration of nitrofen to pregnant rats. Indeed lung growth and motility, evaluated after harvesting and culturing the embryonic lungs, could be rescued when AFS cells were administered in this manner. This could be observed in spite of a high rate of *in utero* embryonal mortality, being the overall survival 15%. To determine whether AFS cells were able to differentiate into neural, muscle or epithelial lineages after integration, we analyzed the colocalization of GFP+ AFSC with PGP9.5+ or α-actin+ or TTF-1+ cells. We found that AFS cells colocalized with alveolar epithelial TTF-1+ cells.

Despite the minimal indication of engraftment, the main therapeutic effect produced by AFS cells seems mediated by paracrine mechanisms elicited through trophic mediators [72, 84-88], as evident by the co-culture experiments. Among the various factors that could be driving this effect, FGF10, VEGFα and TGFβ1 were evaluated in this study. FGF10 is essential for lung branching morphogenesis having a central role in inducing the spatial coordinates for patterning the epithelial tubules. TGFβ1 opposes these effects preventing local budding and maintaining proximal airways in an unbranched form by suppressing epithelial cell proliferation and by promoting synthesis of extracellular matrix components around airways. VEGFα is a strong promoter of angiogenesis and its signalling is responsible for the differentiation of embryonic mesenchymal cells into endothelial cells; the interaction between the epithelium and mesenchyme contribute to lung neovascularisation that is crucial in normal lung development [26, 89-93]. Interestingly, we found that the levels of FGF10 and VEGFα secreted by AFS cells were increased in comparison with controls when nitrofen-exposed lung explants were co-cultured with AFS cells. These findings were consistent with the demonstration that the temporo-spatial pattern of FGF10

expression is severely disrupted in the presence of nitrofen-induced lung hypoplasia, whereas exogenous FGF10 can rescue hypoplastic lungs in culture [94]. This is also consistent with the fact that it has recently been shown that also RA has a major role in early lung morphogenesis by inducing FGF10 expression within the mesoderm subjacent to the site of origin of the laryngotracheal groove [95]. It is likely that AFS cells are capable to produce high levels of FGF10 when they are in a damaged lungs setting [96].

Conclusions

1. Tracheal innervation of preterm rat fetuses with nitrofen-induced CDH is deficient in terms of decreased density of neural structures and surface of ganglia.

2. The deficits of tracheal innervation in rat embryos and fetuses with CDH are the consequence of an abnormal development in terms of delay and neural damage.

3. The bronchopulmonary innervation is deficient both in rats and in infants with CDH because of a delayed development with persistence of the enteric neuron precursors, that is compensated by a certain increase of the supporting glial tissue. The latter has been interpreted as a response to neural damage and compensation for the defective neuronal tissue.

4. Both in animals and in infants with CDH the lung ipsilateral and contralateral to the hernia are equally affected, supporting the concept that lung hypoplasia associated with CDH is a primary developmental defect.

5. In cultured, nitrofen-exposed lung explants in which the frequency of peristaltic waves is decreased, the bronchial neural tissue is deficient as well.

6. The deficient bronchial neural tissue in the explanted rat hypoplastic lungs is rescued, together with airway peristalsis and lung growth, by retinoic acid.

7. Amniotic fluid stem cells rescue lung growth, airway peristalsis and bronchial neural tissue when co-cultured with nitrofen-induced hypoplastic rat lungs.

8. When co-cultured with nitrofen-induced hypoplastic lungs, amniotic fluid stem cells secrete increased amounts of FGF10 and VEGFα.

9. Lung growth and motility are rescued when AFS cells are injected intra-amniotically to nitrofen-exposed pregnant rats.

1. La inervación traqueal de los fetos pretérmino con hernia diafragmática congénita, causada mediante administración de nitrofen a la madre, es deficiente en términos de una menor densidad de estructuras nerviosas y de una disminución de la superficie de los ganglios.

2. Los defectos de la inervación traqueal en embriones y fetos con hernia diafragmática congénita son el resultado de un retraso en el desarrollo y de daño del tejido nervioso.

3. La inervación broncopulmonar es deficiente tanto en ratas como en niños recién nacidos con hernia diafragmática congénita debido a un retraso en el desarrollo con persistencia de los precursores de las neuronas entéricas, que se compensa con un cierto aumento del tejido glial de soporte. Este último ha sido interpretado como una respuesta al daño neuronal y una compensación del defecto de estructuras nerviosas.

4. Tanto en animales como en recién nacidos con hernia diafragmática congénita el pulmón ipsilateral y el contralateral a la hernia se ven igualmente afectados, apoyando el concepto de que la hipoplasia pulmonar asociada con la hernia diafragmática congénita es un defecto primario de desarrollo.

5. En los explantes expuestos al nitrofen cultivados, en los cuales la frecuencia de las ondas peristálticas está disminuida, también el tejido neural bronquial es deficiente.

6. La deficiencia del tejido nervioso bronquial en los pulmones hipoplásicos de rata explantados es rescatado, junto con la peristalsis de las vías aereas y el crecimiento del pulmón, por el ácido retinoico.

7. Las células madre de origen amniótico son capaces de rescatar el crecimiento del pulmón, la peristalsis de las vías aereas y el tejido nervioso bronquial cuando se co-cultivan con los pulmones hipoplasicos de ratas expuestas al nitrofen.

8. Cuando se co-cultivan con los pulmones hipoplasicos expuestos al nitrofen, las células madre de origen amniótico secretan una mayor cantidad de FGF10 y de VEGFα.

9. El crecimiento y la peristalsis de los pulmones hipoplásicos son rescatados cuando se inyectan células madre de origen amniótico en la cavidad amniótica de ratas preñadas expuestas al nitrofen.

References

1. Lally KP. Congenital diaphragmatic hernia. Curr Opin Pediatr 2002;14:486-90.
2. Stege G, Fenton A, Jaffray B. Nihilism in the 1990s: the true mortality of congenital diaphragmatic hernia. Pediatrics 2003;112:532-5.
3. Levison J, Halliday R, Holland AJ, et al. A population-based study of congenital diaphragmatic hernia outcome in New South Wales and the Australian Capital Territory, Australia, 1992-2001. J Pediatr Surg 2006;41:1049-53.
4. Clark RH, Hardin WD, Jr., Hirschl RB, et al. Current surgical management of congenital diaphragmatic hernia: a report from the Congenital Diaphragmatic Hernia Study Group. J Pediatr Surg 1998;33:1004-9.
5. Smith NP, Jesudason EC, Featherstone NC, Corbett HJ, Losty PD. Recent advances in congenital diaphragmatic hernia. Arch Dis Child 2005;90:426-8.
6. Xu C, Liu W, Wang Y, Chen Z, Ji Y. Depressed exocytosis and endocytosis of type II alveolar epithelial cells are responsible for the surfactant deficiency in the lung of newborn with congenital diaphragmatic hernia. Med Hypotheses 2009;72:160-2.
7. Beals DA, Schloo BL, Vacanti JP, Reid LM, Wilson JM. Pulmonary growth and remodeling in infants with high-risk congenital diaphragmatic hernia. J Pediatr Surg 1992;27:997-1001; discussion -2.
8. Hislop A, Reid L. Persistent hypoplasia of the lung after repair of congenital diaphragmatic hernia. Thorax 1976;31:450-5.
9. Geggel RL, Murphy JD, Langleben D, Crone RK, Vacanti JP, Reid LM. Congenital diaphragmatic hernia: arterial structural changes and persistent pulmonary hypertension after surgical repair. J Pediatr 1985;107:457-64.
10. Wischermann A, Holschneider AM, Hubner U. Long-term follow-up of children with diaphragmatic hernia. Eur J Pediatr Surg 1995;5:13-8.
11. Vanamo K, Rintala R, Sovijarvi A, et al. Long-term pulmonary sequelae in survivors of congenital diaphragmatic defects. J Pediatr Surg 1996;31:1096-9; discussion 9-100.
12. Trachsel D, Selvadurai H, Bohn D, Langer JC, Coates AL. Long-term pulmonary morbidity in survivors of congenital diaphragmatic hernia. Pediatr Pulmonol 2005;39:433-9.
13. Trachsel D, Selvadurai H, Adatia I, et al. Resting and exercise cardiorespiratory function in survivors of congenital diaphragmatic hernia. Pediatr Pulmonol 2006;41:522-9.
14. Cortes RA, Keller RL, Townsend T, et al. Survival of severe congenital diaphragmatic hernia has morbid consequences. J Pediatr Surg 2005;40:36-45; discussion -6.
15. Naik S, Greenough A, Zhang YX, Davenport M. Prediction of morbidity during infancy after repair of congenital diaphragmatic hernia. J Pediatr Surg 1996;31:1651-4.
16. Falconer AR, Brown RA, Helms P, Gordon I, Baron JA. Pulmonary sequelae in survivors of congenital diaphragmatic hernia. Thorax 1990;45:126-9.

17. Nagaya M, Akatsuka H, Kato J, Niimi N, Ishiguro Y. Development in lung function of the affected side after repair of congenital diaphragmatic hernia. J Pediatr Surg 1996;31:349-56.
18. Ijsselstijn H, Tibboel D, Hop WJ, Molenaar JC, de Jongste JC. Long-term pulmonary sequelae in children with congenital diaphragmatic hernia. Am J Respir Crit Care Med 1997;155:174-80.
19. Marven SS, Smith CM, Claxton D, et al. Pulmonary function, exercise performance, and growth in survivors of congenital diaphragmatic hernia. Arch Dis Child 1998;78:137-42.
20. Peetsold MG, Heij HA, Kneepkens CM, Nagelkerke AF, Huisman J, Gemke RJ. The long-term follow-up of patients with a congenital diaphragmatic hernia: a broad spectrum of morbidity. Pediatr Surg Int 2009;25:1-17.
21. Thurlbeck WM, Kida K, Langston C, et al. Postnatal lung growth after repair of diaphragmatic hernia. Thorax 1979;34:338-43.
22. Ten Have-Opbroek AA. The development of the lung in mammals: an analysis of concepts and findings. Am J Anat 1981;162:201-19.
23. Sutliff KS, Hutchins GM. Septation of the respiratory and digestive tracts in human embryos: crucial role of the tracheoesophageal sulcus. Anat Rec 1994;238:237-47.
24. Spooner BS, Wessells NK. Mammalian lung development: interactions in primordium formation and bronchial morphogenesis. J Exp Zool 1970;175:445-54.
25. Zoetis T, Hurtt ME. Species comparison of lung development. Birth Defects Res B Dev Reprod Toxicol 2003;68:121-4.
26. Warburton D, Schwarz M, Tefft D, Flores-Delgado G, Anderson KD, Cardoso WV. The molecular basis of lung morphogenesis. Mech Dev 2000;92:55-81.
27. Tollet J, Everett AW, Sparrow MP. Spatial and temporal distribution of nerves, ganglia, and smooth muscle during the early pseudoglandular stage of fetal mouse lung development. Dev Dyn 2001;221:48-60.
28. Burns AJ, Delalande JM. Neural crest cell origin for intrinsic ganglia of the developing chicken lung. Dev Biol 2005;277:63-79.
29. Freem LJ, Escot S, Tannahill D, Druckenbrod NR, Thapar N, Burns AJ. The intrinsic innervation of the lung is derived from neural crest cells as shown by optical projection tomography in Wnt1-Cre;YFP reporter mice. J Anat 2010;217:651-64.
30. Durbec P, Marcos-Gutierrez CV, Kilkenny C, et al. GDNF signalling through the Ret receptor tyrosine kinase. Nature 1996;381:789-93.
31. Tollet J, Everett AW, Sparrow MP. Development of neural tissue and airway smooth muscle in fetal mouse lung explants: a role for glial-derived neurotrophic factor in lung innervation. Am J Respir Cell Mol Biol 2002;26:420-9.
32. Sparrow MP, Warwick SP, Mitchell HW. Foetal airway motor tone in prenatal lung development of the pig. Eur Respir J 1994;7:1416-24.

33. Sparrow MP, Warwick SP, Everett AW. Innervation and function of the distal airways in the developing bronchial tree of fetal pig lung. Am J Respir Cell Mol Biol 1995;13:518-25.
34. McCray PB, Jr. Spontaneous contractility of human fetal airway smooth muscle. Am J Respir Cell Mol Biol 1993;8:573-80.
35. Roman J. Effects of calcium channel blockade on mammalian lung branching morphogenesis. Exp Lung Res 1995;21:489-502.
36. Schittny JC, Miserocchi G, Sparrow MP. Spontaneous peristaltic airway contractions propel lung liquid through the bronchial tree of intact and fetal lung explants. Am J Respir Cell Mol Biol 2000;23:11-8.
37. Harding R, Hooper SB. Regulation of lung expansion and lung growth before birth. J Appl Physiol 1996;81:209-24.
38. Kitano Y, Flake AW, Quinn TM, et al. Lung growth induced by tracheal occlusion in the sheep is augmented by airway pressurization. J Pediatr Surg 2000;35:216-21; discussion 21-2.
39. Cilley RE, Zgleszewski SE, Chinoy MR. Fetal lung development: airway pressure enhances the expression of developmental genes. J Pediatr Surg 2000;35:113-8; discussion 9.
40. Sparrow MP, Weichselbaum M, McCray PB. Development of the innervation and airway smooth muscle in human fetal lung. Am J Respir Cell Mol Biol 1999;20:550-60.
41. Weichselbaum M, Sparrow MP. A confocal microscopic study of the formation of ganglia in the airways of fetal pig lung. Am J Respir Cell Mol Biol 1999;21:607-20.
42. Cadieux A, Springall DR, Mulderry PK, et al. Occurrence, distribution and ontogeny of CGRP immunoreactivity in the rat lower respiratory tract: effect of capsaicin treatment and surgical denervations. Neuroscience 1986;19:605-27.
43. Sparrow MP, Lamb JP. Ontogeny of airway smooth muscle: structure, innervation, myogenesis and function in the fetal lung. Respir Physiol Neurobiol 2003;137:361-72.
44. Towers PR, Woolf AS, Hardman P. Glial cell line-derived neurotrophic factor stimulates ureteric bud outgrowth and enhances survival of ureteric bud cells in vitro. Exp Nephrol 1998;6:337-51.
45. Widenfalk J, Nosrat C, Tomac A, Westphal H, Hoffer B, Olson L. Neurturin and glial cell line-derived neurotrophic factor receptor-beta (GDNFR-beta), novel proteins related to GDNF and GDNFR-alpha with specific cellular patterns of expression suggesting roles in the developing and adult nervous system and in peripheral organs. J Neurosci 1997;17:8506-19.
46. Jesudason EC, Connell MG, Fernig DG, Lloyd DA, Losty PD. Early lung malformations in congenital diaphragmatic hernia. J Pediatr Surg 2000;35:124-7; discussion 8.

47. Jesudason EC, Smith NP, Connell MG, et al. Peristalsis of airway smooth muscle is developmentally regulated and uncoupled from hypoplastic lung growth. Am J Physiol Lung Cell Mol Physiol 2006;291:L559-65.
48. Greer JJ, Babiuk RP, Thebaud B. Etiology of congenital diaphragmatic hernia: the retinoid hypothesis. Pediatr Res 2003;53:726-30.
49. Kawaguchi R, Yu J, Honda J, et al. A membrane receptor for retinol binding protein mediates cellular uptake of vitamin A. Science 2007;315:820-5.
50. Pasutto F, Sticht H, Hammersen G, et al. Mutations in STRA6 cause a broad spectrum of malformations including anophthalmia, congenital heart defects, diaphragmatic hernia, alveolar capillary dysplasia, lung hypoplasia, and mental retardation. Am J Hum Genet 2007;80:550-60.
51. Smith SM, Dickman ED, Power SC, Lancman J. Retinoids and their receptors in vertebrate embryogenesis. J Nutr 1998;128:467S-70S.
52. Zile MH. Function of vitamin A in vertebrate embryonic development. J Nutr 2001;131:705-8.
53. Zile MH. Vitamin A and embryonic development: an overview. J Nutr 1998;128:455S-8S.
54. Wilson JG, Roth CB, Warkany J. An analysis of the syndrome of malformations induced by maternal vitamin A deficiency. Effects of restoration of vitamin A at various times during gestation. Am J Anat 1953;92:189-217.
55. Mendelsohn C, Lohnes D, Decimo D, et al. Function of the retinoic acid receptors (RARs) during development (II). Multiple abnormalities at various stages of organogenesis in RAR double mutants. Development 1994;120:2749-71.
56. Babiuk RP, Thebaud B, Greer JJ. Reductions in the incidence of nitrofen-induced diaphragmatic hernia by vitamin A and retinoic acid. Am J Physiol Lung Cell Mol Physiol 2004;286:L970-3.
57. Thebaud B, Tibboel D, Rambaud C, et al. Vitamin A decreases the incidence and severity of nitrofen-induced congenital diaphragmatic hernia in rats. Am J Physiol 1999;277:L423-9.
58. Chen MH, MacGowan A, Ward S, Bavik C, Greer JJ. The activation of the retinoic acid response element is inhibited in an animal model of congenital diaphragmatic hernia. Biol Neonate 2003;83:157-61.
59. Mey J, Babiuk RP, Clugston R, Zhang W, Greer JJ. Retinal dehydrogenase-2 is inhibited by compounds that induce congenital diaphragmatic hernias in rodents. Am J Pathol 2003;162:673-9.
60. Baptista MJ, Melo-Rocha G, Pedrosa C, et al. Antenatal vitamin A administration attenuates lung hypoplasia by interfering with early instead of late determinants of lung underdevelopment in congenital diaphragmatic hernia. J Pediatr Surg 2005;40:658-65.

61. Montedonico S, Nakazawa N, Puri P. Retinoic acid rescues lung hypoplasia in nitrofen-induced hypoplastic foetal rat lung explants. Pediatr Surg Int 2006;22:2-8.
62. Montedonico S, Sugimoto K, Felle P, Bannigan J, Puri P. Prenatal treatment with retinoic acid promotes pulmonary alveologenesis in the nitrofen model of congenital diaphragmatic hernia. J Pediatr Surg 2008;43:500-7.
63. Nakazawa N, Montedonico S, Takayasu H, Paradisi F, Puri P. Disturbance of retinol transportation causes nitrofen-induced hypoplastic lung. J Pediatr Surg 2007;42:345-9.
64. Nakazawa N, Takayasu H, Montedonico S, Puri P. Altered regulation of retinoic acid synthesis in nitrofen-induced hypoplastic lung. Pediatr Surg Int 2007;23:391-6.
65. Sugimoto K, Takayasu H, Nakazawa N, Montedonico S, Puri P. Prenatal treatment with retinoic acid accelerates type 1 alveolar cell proliferation of the hypoplastic lung in the nitrofen model of congenital diaphragmatic hernia. J Pediatr Surg 2008;43:367-72.
66. De Coppi P, Bartsch G, Jr., Siddiqui MM, et al. Isolation of amniotic stem cell lines with potential for therapy. Nat Biotechnol 2007;25:100-6.
67. Ditadi A, de Coppi P, Picone O, et al. Human and murine amniotic fluid c-Kit+Lin- cells display hematopoietic activity. Blood 2009;113:3953-60.
68. Perin L, Da Sacco S, De Filippo RE. Regenerative medicine of the kidney. Adv Drug Deliv Rev 2011;63:379-87.
69. Bollini S, Cheung KK, Riegler J, et al. Amniotic Fluid Stem Cells Are Cardioprotective Following Acute Myocardial Infarction. Stem Cells Dev 2011.
70. Warburton D, Perin L, Defilippo R, Bellusci S, Shi W, Driscoll B. Stem/progenitor cells in lung development, injury repair, and regeneration. Proc Am Thorac Soc 2008;5:703-6.
71. Carraro G, Perin L, Sedrakyan S, et al. Human amniotic fluid stem cells can integrate and differentiate into epithelial lung lineages. Stem Cells 2008;26:2902-11.
72. Crisostomo PR, Markel TA, Wang Y, Meldrum DR. Surgically relevant aspects of stem cell paracrine effects. Surgery 2008;143:577-81.
73. Rocha GM, Bianchi RF, Severo M, et al. Congenital Diaphragmatic Hernia - The Neonatal Period (Part I). Eur J Pediatr Surg 2008.
74. van den Hout L, Reiss I, Felix JF, et al. Risk factors for chronic lung disease and mortality in newborns with congenital diaphragmatic hernia. Neonatology 2010;98:370-80.
75. Kamata S, Usui N, Kamiyama M, et al. Long-term follow-up of patients with high-risk congenital diaphragmatic hernia. J Pediatr Surg 2005;40:1833-8.
76. Iritani I. Experimental study on embryogenesis of congenital diaphragmatic hernia. Anat Embryol (Berl) 1984;169:133-9.

77. Greer JJ, Allan DW, Babiuk RP, Lemke RP. Recent advances in understanding the pathogenesis of nitrofen-induced congenital diaphragmatic hernia. Pediatr Pulmonol 2000;29:394-9.
78. Kluth D, Kangah R, Reich P, Tenbrinck R, Tibboel D, Lambrecht W. Nitrofen-induced diaphragmatic hernias in rats: an animal model. J Pediatr Surg 1990;25:850-4.
79. Collins MD, Mao GE. Teratology of retinoids. Annu Rev Pharmacol Toxicol 1999;39:399-430.
80. Tzimas G, Nau H. The role of metabolism and toxicokinetics in retinoid teratogenesis. Curr Pharm Des 2001;7:803-31.
81. Bollini S, Pozzobon M, Nobles M, et al. In vitro and in vivo cardiomyogenic differentiation of amniotic fluid stem cells. Stem Cell Rev 2011;7:364-80.
82. Pederiva F, Martinez L, Tovar JA. Retinoic acid rescues deficient airway innervation and peristalsis of hypoplastic rat lung explants. Neonatology 2011;in press.
83. Jesudason EC, Smith NP, Connell MG, et al. Developing rat lung has a sided pacemaker region for morphogenesis-related airway peristalsis. Am J Respir Cell Mol Biol 2005;32:118-27.
84. Togel F, Weiss K, Yang Y, Hu Z, Zhang P, Westenfelder C. Vasculotropic, paracrine actions of infused mesenchymal stem cells are important to the recovery from acute kidney injury. Am J Physiol Renal Physiol 2007;292:F1626-35.
85. Gnecchi M, He H, Liang OD, et al. Paracrine action accounts for marked protection of ischemic heart by Akt-modified mesenchymal stem cells. Nat Med 2005;11:367-8.
86. Caplan AI, Dennis JE. Mesenchymal stem cells as trophic mediators. J Cell Biochem 2006;98:1076-84.
87. Rabb H. Paracrine and differentiation mechanisms underlying stem cell therapy for the damaged kidney. Am J Physiol Renal Physiol 2005;289:F29-30.
88. Tang YL, Zhao Q, Qin X, et al. Paracrine action enhances the effects of autologous mesenchymal stem cell transplantation on vascular regeneration in rat model of myocardial infarction. Ann Thorac Surg 2005;80:229-36; discussion 36-7.
89. Maeda S, Suzuki S, Suzuki T, et al. Analysis of intrapulmonary vessels and epithelial-endothelial interactions in the human developing lung. Lab Invest 2002;82:293-301.
90. Warburton D, Bellusci S. The molecular genetics of lung morphogenesis and injury repair. Paediatr Respir Rev 2004;5 Suppl A:S283-7.
91. Desai TJ, Cardoso WV. Growth factors in lung development and disease: friends or foe? Respir Res 2002;3:2.
92. Cardoso WV. Molecular regulation of lung development. Annu Rev Physiol 2001;63:471-94.
93. Warburton D, Bellusci S, De Langhe S, et al. Molecular mechanisms of early lung specification and branching morphogenesis. Pediatr Res 2005;57:26R-37R.

94. Acosta JM, Thebaud B, Castillo C, et al. Novel mechanisms in murine nitrofen-induced pulmonary hypoplasia: FGF-10 rescue in culture. Am J Physiol Lung Cell Mol Physiol 2001;281:L250-7.
95. Desai TJ, Malpel S, Flentke GR, Smith SM, Cardoso WV. Retinoic acid selectively regulates Fgf10 expression and maintains cell identity in the prospective lung field of the developing foregut. Dev Biol 2004;273:402-15.
96. Wang M, Crisostomo PR, Herring C, Meldrum KK, Meldrum DR. Human progenitor cells from bone marrow or adipose tissue produce VEGF, HGF, and IGF-I in response to TNF by a p38 MAPK-dependent mechanism. Am J Physiol Regul Integr Comp Physiol 2006;291:R880-4.
97. Xia H, Migliazza L, Diez-Pardo JA, Tovar JA. The tracheobronchial tree is abnormal in experimental congenital diaphragmatic hernia. Pediatr Surg Int 1999;15:184-7.
98. Nose K, Kamata S, Sawai T, et al. Airway anomalies in patients with congenital diaphragmatic hernia. J Pediatr Surg 2000;35:1562-5.
99. Muratore CS, Kharasch V, Lund DP, et al. Pulmonary morbidity in 100 survivors of congenital diaphragmatic hernia monitored in a multidisciplinary clinic. J Pediatr Surg 2001;36:133-40.
100. Eber E. Adult outcome of congenital lower respiratory tract malformations. Swiss Med Wkly 2006;136:233-40.
101. Reid IS, Hutcherson RJ. Long-term follow-up of patients with congenital diaphragmatic hernia. J Pediatr Surg 1976;11:939-42.
102. Kusindarta DL, Atoji Y, Yamamoto Y. Nerve plexuses in the trachea and extrapulmonary bronchi of the rat. Arch Histol Cytol 2004;67:41-55.
103. Wilkinson KD, Lee KM, Deshpande S, Duerksen-Hughes P, Boss JM, Pohl J. The neuron-specific protein PGP 9.5 is a ubiquitin carboxyl-terminal hydrolase. Science 1989;246:670-3.
104. Wilson PO, Barber PC, Hamid QA, et al. The immunolocalization of protein gene product 9.5 using rabbit polyclonal and mouse monoclonal antibodies. Br J Exp Pathol 1988;69:91-104.
105. Kajimoto Y, Hashimoto T, Shirai Y, Nishino N, Kuno T, Tanaka C. cDNA cloning and tissue distribution of a rat ubiquitin carboxyl-terminal hydrolase PGP9.5. J Biochem 1992;112:28-32.
106. Stefansson K, Wollmann RL, Moore BW. Distribution of S-100 protein outside the central nervous system. Brain Res 1982;234:309-17.
107. Sheppard MN, Kurian SS, Henzen-Logmans SC, et al. Neurone-specific enolase and S-100: new markers for delineating the innervation of the respiratory tract in man and other mammals. Thorax 1983;38:333-40.

108. Boleken M, Demirbilek S, Kirimiloglu H, et al. Reduced neuronal innervation in the distal end of the proximal esophageal atretic segment in cases of esophageal atresia with distal tracheoesophageal fistula. World J Surg 2007;31:1512-7.
109. Manie S, Santoro M, Fusco A, Billaud M. The RET receptor: function in development and dysfunction in congenital malformation. Trends Genet 2001;17:580-9.
110. Sebald M, Friedlich P, Burns C, et al. Risk of need for extracorporeal membrane oxygenation support in neonates with congenital diaphragmatic hernia treated with inhaled nitric oxide. J Perinatol 2004;24:143-6.
111. Pachnis V, Mankoo B, Costantini F. Expression of the c-ret proto-oncogene during mouse embryogenesis. Development 1993;119:1005-17.
112. Trupp M, Ryden M, Jornvall H, et al. Peripheral expression and biological activities of GDNF, a new neurotrophic factor for avian and mammalian peripheral neurons. J Cell Biol 1995;130:137-48.
113. Yamamoto M, Sobue G, Yamamoto K, Terao S, Mitsuma T. Expression of mRNAs for neurotrophic factors (NGF, BDNF, NT-3, and GDNF) and their receptors (p75NGFR, trkA, trkB, and trkC) in the adult human peripheral nervous system and nonneural tissues. Neurochem Res 1996;21:929-38.
114. Natarajan D, Marcos-Gutierrez C, Pachnis V, de Graaff E. Requirement of signalling by receptor tyrosine kinase RET for the directed migration of enteric nervous system progenitor cells during mammalian embryogenesis. Development 2002;129:5151-60.
115. Young HM, Hearn CJ, Farlie PG, Canty AJ, Thomas PQ, Newgreen DF. GDNF is a chemoattractant for enteric neural cells. Dev Biol 2001;229:503-16.
116. Taraviras S, Marcos-Gutierrez CV, Durbec P, et al. Signalling by the RET receptor tyrosine kinase and its role in the development of the mammalian enteric nervous system. Development 1999;126:2785-97.
117. Yu T, Scully S, Yu Y, Fox GM, Jing S, Zhou R. Expression of GDNF family receptor components during development: implications in the mechanisms of interaction. J Neurosci 1998;18:4684-96.
118. Knox WF, Barson AJ. Pulmonary hypoplasia in a regional perinatal unit. Early Hum Dev 1986;14:33-42.
119. Knox SM, Lombaert IM, Reed X, Vitale-Cross L, Gutkind JS, Hoffman MP. Parasympathetic innervation maintains epithelial progenitor cells during salivary organogenesis. Science 2010;329:1645-7.
120. Rock JR, Hogan BL. Developmental biology. Branching takes nerve. Science 2010;329:1610-1.
121. Rock JR, Onaitis MW, Rawlins EL, et al. Basal cells as stem cells of the mouse trachea and human airway epithelium. Proc Natl Acad Sci U S A 2009;106:12771-5.

122. Thebaud B, Barlier-Mur AM, Chailley-Heu B, et al. Restoring effects of vitamin A on surfactant synthesis in nitrofen-induced congenital diaphragmatic hernia in rats. Am J Respir Crit Care Med 2001;164:1083-9.
123. Noble BR, Babiuk RP, Clugston RD, et al. Mechanisms of action of the congenital diaphragmatic hernia-inducing teratogen nitrofen. Am J Physiol Lung Cell Mol Physiol 2007;293:L1079-87.
124. Beurskens LW, Tibboel D, Lindemans J, et al. Retinol status of newborn infants is associated with congenital diaphragmatic hernia. Pediatrics 2010;126:712-20.
125. Major D, Cadenas M, Fournier L, Leclerc S, Lefebvre M, Cloutier R. Retinol status of newborn infants with congenital diaphragmatic hernia. Pediatr Surg Int 1998;13:547-9.
126. Bellusci S, Grindley J, Emoto H, Itoh N, Hogan BL. Fibroblast growth factor 10 (FGF10) and branching morphogenesis in the embryonic mouse lung. Development 1997;124:4867-78.
127. Mailleux AA, Kelly R, Veltmaat JM, et al. Fgf10 expression identifies parabronchial smooth muscle cell progenitors and is required for their entry into the smooth muscle cell lineage. Development 2005;132:2157-66.
128. So PL, Yip PK, Bunting S, et al. Interactions between retinoic acid, nerve growth factor and sonic hedgehog signalling pathways in neurite outgrowth. Dev Biol 2006;298:167-75.